

ORIGIN OF MAGNESITE IN TURKEY, A STABLE ISOTOPE STUDY

A thesis submitted for the degree of Doctor of Philosophy

by VEYSEL ZEDEF

B.Sc., M.Sc., Selcuk University (Konya, Turkey)

Department of Geology & Applied Geology

University of Glasgow

July, 1994

© Veysel ZEDEF

ProQuest Number: 13833769

All rights reserved

INFORMATION TO ALL USERS

The quality of this reproduction is dependent upon the quality of the copy submitted.

In the unlikely event that the author did not send a complete manuscript and there are missing pages, these will be noted. Also, if material had to be removed, a note will indicate the deletion.



ProQuest 13833769

Published by ProQuest LLC (2019). Copyright of the Dissertation is held by the Author.

All rights reserved.

This work is protected against unauthorized copying under Title 17, United States Code
Microform Edition © ProQuest LLC.

ProQuest LLC.
789 East Eisenhower Parkway
P.O. Box 1346
Ann Arbor, MI 48106 – 1346

Thesis
9848

Copy 1



THESIS DECLARATION

The material presented in this study is the result of research carried out between April 1991 and May 1994 in the Department of Geology & Applied Geology, University of Glasgow, UK., under the supervision of Prof. M. J. RUSSELL and with the help of Dr. C. J. R. BRAITHWAITE.

This thesis is based on my own independent research and any published and unpublished material used by me has been given full acknowledgement in the text.

Veysel ZEDEF

1994

I certify that Veysel ZEDEF has undertaken the bulk of the work involved in this thesis. Specifically; background geology, sample preparation, examinations and analyses, and their interpretation. I have assisted with advice and help of a general, technical, conceptual nature, as would be expected in the course of normal PhD supervision and advice. Veysel ZEDEF has written the thesis himself, and is responsible for its content.

Prof. M. J. RUSSELL

8th July '94

ACKNOWLEDGEMENTS

Firstly, I wish to give my thanks to my supervisor, Prof. Michael Russell, for giving me the opportunity undertake this study. He gave me the much needed direction and encouragement that did much to bring this research to fruition.

I particularly wish to thank one other person who helped me considerably; Dr. Tony Fallick who, by taking such an interest in my research, helped me to see many of the complexities of the problem with which I was faced.

I wish to express my gratitude to Prof. Ahmet Ayhan for introducing me the magnesite problem and his supervision throughout my research in Turkey.

I am also indebted to the academic staff in the Glasgow University, Geology & Applied Geology Department for all their assistance: Dr. C. Braithwaite, Dr. A. Hall, Dr. S. Hazeldine and Dr. C. Farrow. My thanks also go to Dr. P. Dominy, Glasgow University Botany Department, for analysing bacteria in the stromatolite samples.

Thanks to R. Morrison for logistic support, to D. Turner and M. MacLeod and B. Higgison for their assistance in the geochemistry laboratory, to P. Ainsworth for his assistance in the scanning electron microscope, to D. McLean for his help in printing plates, to J. Gillece, A. Jones and A. Monaghan supplied polished section and thin sections, to J. Kavanagh for his assistance in computing, to Tracy and Kate for analysing REE samples on ICP-MS, and Chris for his assistance in the isotope geology unit laboratories at SURRC.

The departmental janitors Edward, John and Jim and secreteries Jenette and Mary are also thanked.

Thanks also to all postgrads, Mehmet (for drawing figures and helping friendly), Huseyin, Bulent, Paul, Kerim, Campbell, Colin, Chris, Susan, Orla, Mark, Ali, Abdulhamid, Rona, Richard, Esam at the geology department, and Kamil Alakus at the university of Strathclyde and to the Turkish Students' society for social support during my stay in Glasgow.

Turkish tax-payers are specially acknowledged, without their financial support, this study probably never have been undertaken.

Last but not least, I wish to express my particular appreciation to my wife for understanding me and for her unlimited patience.

CONTENTS

	Page No
THESIS DECLARATION	I
ACKNOWLEDGEMENTS.....	II
CONTENTS	III
LIST OF FIGURES.....	VI
LIST OF TABLES.....	VIII
LIST OF PLATES	VIII
ABSTRACT	X
 CHAPTER ONE	 1
<i>REGIONAL GEOLOGY OF TURKEY AND A REVIEW OF TURKISH MAGNESITE DEPOSITS</i>	 1
INTRODUCTION	1
HYPOTHESIS.....	2
1.1. REGIONAL GEOLOGY OF TURKEY.....	4
1.2. PREVIOUS STUDIES OF TURKISH MAGNESITES.....	10
1.2.1. Cryptocrystalline vein-stockwork type magnesites.....	16
1.2.2. Sedimentary magnesites.....	20
1.2.3. Stable isotope studies.....	23
 CHAPTER TWO	 24
<i>LOCAL GEOLOGY OF THE DEPOSITS AND THEIR GEOLOGICAL FEATURES</i>	 24
INTRODUCTION	24
2.1. GEOLOGICAL SETTING OF THE KONYA MAGNESITE DEPOSITS.....	24
Ardicli formation	26
Loras limestone	29
Midos formation	29
Cayirbagi ophiolites	30
Neogene dolomitic marls, limestones and alluvium.....	31
2.1.1. Economic significance of the Konya magnesite deposits	35

2.1.2. Mineralogy of the magnesite deposits	35
2.1.3. Description of the deposits	36
2.2. SEYDISEHIR SHALES	36
2.3. ARAPOMER DERESI MAGNESITE DEPOSIT	37
2.4. HIRSIZDERE MAGNESITE DEPOSIT	38
2.5. SALDA LAKE	38
2.5.1. Geological environment of Salda lake.....	38
2.5.2. Climate and hydrogeological conditions.....	40
2.5.3. Biological conditions.....	42
2.5.4. Hydromagnesite deposits	44
2.5.5. Stromatolites	46
CHAPTER THREE.....	57
<i>SAMPLING AND ANALYTICAL TECHNIQUES.....</i>	<i>57</i>
3.1. SAMPLING.....	57
3.2. ANALYTICAL TECHNIQUES.....	59
3.2.1. Laboratory preparation of rock powders for analyses	59
3.2.2. X-Ray diffraction (XRD) analyses	61
3.2.4. Scanning electron microscope (SEM) analyses	61
3.2.5. Atomic absorption spectrometry (AAS) analyses	62
3.2.6. Absorbance spectrometry (AS) analyses.....	62
3.2.7. Inductively coupled plasma-mass spectrometry (ICP-MS) analyses	63
3.2.8. Stable isotope analyses on mass spectrometry (MS).....	63
CHAPTER FOUR.....	66
<i>CARBON and OXYGEN ISOTOPES, REE, XRD, AAS, AS and SEM STUDIES: RESULTS</i>	<i>66</i>
4.1. CARBON and OXYGEN STABLE ISOTOPE RESULTS	66
4.1.1. Sedimentary-hydrothermal deposits.....	67
Salda lake's present-day hydromagnesite deposits	67
Pamukkale Present-day hot-spring travertines.....	68
Hirsizdere magnesite deposits.....	68
Helvacibaba detrital magnesite and bedded dolomites.....	69
Tsakasimta (Chad Basin, Nigeria) magnesites	69

Summary of isotope results	70
4.1.2. Stockwork magnesite deposits	70
Arapomer Deresi	70
Helvacibaba magnesite deposits	70
Helvacibaba silica cap.....	71
Kavakarasi magnesite deposits	71
Yunak and Kozagac magnesite deposits	72
4.1.3. Vein deposits.....	72
Koyakci Tepe and Sodur	72
4.1.4. Palaeozoic and Mesozoic limestones.....	72
4.2. REE RESULTS	93
4.3. XRD RESULTS	93
4.4. AAS RESULTS.....	94
4.5. AS RESULTS.....	96
4.6. SEM RESULTS.....	97
 CHAPTER FIVE	 101
<i>DISCUSSION AND GENETIC MODELS</i>	101
 INTRODUCTION	 101
5.1. SOURCE OF CARBON DIOXIDE.....	103
5.1.1. Cryptocrystalline vein-stockwork magnesites.....	103
5.1.2. Sedimentary-hydrothermal deposits.....	113
Hirsizdere and Tsakasimta magnesite deposits	113
Helvacibaba detrital magnesites and bedded dolomites	115
Salda lake hydromagnesites	116
Pamukkale hot-spring travertine deposits.....	118
5.1.3. Marine limestones	120
5.2. ISOTOPIC COMPOSITION OF THE FLUIDS AND THEIR TEMPERATURE.....	122
5.3. VARIATIONS OF THE REE's	124
5.4. SOURCE OF MAGNESIUM and OTHER ELEMENTS IN THE SALDA LAKE WATERS and ITS SURROUNDS	126
5.5. GENETIC MODEL	127
5.6. FURTHER RESEARCH.....	132

CHAPTER SIX.....	134
6. CONCLUSIONS	134
REFERENCES.....	141
APPENDIX-1 Evaporation rates around Salda lake.....	155
APPENDIX-2 Average monthly rainfall around Salda lake.....	156
APPENDIX-3 Chemical composition of culture BG-11+.....	157
APPENDIX-4 REE contents of magnesite, hydromagnesite, ultramafic rocks and water	158
APPENDIX-5 Chondrite normalised REE concentrations	159

LIST OF FIGURES

CHAPTER ONE

Figure 1.1. $\delta^{13}\text{C}$ and $\delta^{18}\text{O}$ values of Serbian and Bosnian magnesites.....	3
Figure 1.2. The position of Turkey, from the plate-tectonic point of view.....	5
Figure 1.3. Major geological features of Turkey.....	7
Figure 1.4. Discontinuous ophiolitic belts with related magnesite deposits in Turkey.....	11
Figure 1.5. The stability diagram of the $\text{MgO-CO}_2\text{-H}_2\text{O}$	18
Figure 1.6. The four types of magnesite development in Salda lake	22

CHAPTER TWO

Figure 2.1. General geological map of south-western Turkey	25
Figure 2.2. Geological map of Meram-Cayirbagi area, Konya.....	27
Figure 2.3. Stratigraphic section of Ardicli formation.....	28
Figure 2.4. Sketch of relationship between ultramafic rocks at Konya.....	32
Figure 2.5. The stratigraphic relation between rock units in Konya district.....	33
Figure 2.6. Geological cross-sections of the Meram-Cayirbagi area	34
Figure 2.7. Geological map of southern part of Salda lake.....	39
Figure 2.8. Average monthly evaporation rates around Salda lake.....	41
Figure 2.9. Average monthly rainfall around Salda lake.....	43
Figure 2.10. Geological cross section of the Salda lake area	45

CHAPTER THREE

Figure 3.1. Location of sample areas in this study.....	58
---	----

Figure 3.2. Frequency histogram of analytical tools and number of samples analysed in this study	60
Figure 3.3. Simplified CO ₂ extraction line	65

CHAPTER FOUR

Figure 4.1.1. The plot of $\delta^{13}\text{C}$ v $\delta^{18}\text{O}$ of the Turkish carbonate deposits.....	82
Figure 4.1.1-A. Plot of D v $\delta^{18}\text{O}$ of two water samples from Salda lake.....	83
Figure 4.1.2. Frequency histograms of $\delta^{13}\text{C}$ and $\delta^{18}\text{O}$ values of Salda lake's hydromagnesites	84
Figure 4.1.3. Frequency histograms of $\delta^{13}\text{C}$ and $\delta^{18}\text{O}$ values of Hirsizdere magnesite deposits.....	85
Figure 4.1.4. Systematically collected sample places at Hirsizdere.....	86
Figure 4.1.5. Relationship between $\delta^{13}\text{C}$ with depth at top and bottom beds in the Hirsizdere sedimentary magnesite deposits	87
Figure 4.1.6. $\delta^{18}\text{O}$ v depth at top and bottom magnesite beds at Hirsizdere magnesite deposits.....	88
Figure 4.1.7. The histograms of frequency v $\delta^{13}\text{C}$ and $\delta^{18}\text{O}$ of 52 samples from sedimentary-hydrothermal carbonates.....	89
Figure 4.1.8. The sample sites in the Helvacibaba open pit mine.....	90
Figure 4.1.8-A. Sample sites of silica samples from Helvacibaba silica cap.....	91
Figure 4.1.9. The variations of $\delta^{13}\text{C}$ and $\delta^{18}\text{O}$ values at Helvacibaba.....	92
Figure 4.4.1. Sample sites at Salda lake and its surrounds	<i>following</i> 94
Figure 4.5.1. Absorbance spectrum of cyanobacteria of Salda lake.....	96

CHAPTER FIVE

Figure 5.1. Proposed genetic model for western Turkish carbonate deposits	<i>following</i> 132
---	----------------------

CHAPTER SIX

Figure 6.1. A comparison of the Miocene sedimentary magnesite deposits with the presently forming hydromagnesite deposits	138
Figure 6.2. Idealised three end-member of Turkish carbonate deposits, based on stable isotopes	140

LIST OF TABLES

CHAPTER ONE

Table 1.1. Turkish magnesite deposit reserves (by Provinces)	12
Table 1.2. Published results of stable isotope analyses of Turkish magnesites	23

CHAPTER TWO

Table 2.1. Reserve of the hydromagnesite deposits in Salda.....	44
---	----

CHAPTER THREE

Table 3.1. Sample distribution for each area in this study.....	58
Table 3.2. Number of samples analysed using the particular analytical tools ..	59

CHAPTER FOUR

Table 4.1.1. Stable isotope results of Turkish carbonate deposits.....	74
Table 4.3.1. The mineralogical composition of hydromagnesite v temperatures	94
Table 4.4.1. AAS results of the Salda lake and surrounding areas' water	95
Table 4.4.2. Average concentration of Mg, Ca, Na and Si (in ppm) and pH of the water samples from Salda lake	95

CHAPTER FIVE

Table 5.1.1. $\delta^{13}\text{C}$ and $\delta^{18}\text{O}$ values of calcite samples of the limestone formations from the western Turkey and their age	121
Table 5.2.1. Used values of constant A and B to calculate the isotopic composition of the fluids responsible mineralisation.....	123
Table 5.2.2. The isotopic composition of the fluids responsible mineralisation of the western Turkish carbonate deposits.....	125

LIST OF PLATES

CHAPTER TWO

Plate 2.1. Thin magnesite veins (white) in the serpentinitised peridotites	47
Plate 2.2. Carbonated serpentinites at Helvacibaba open pit mine.....	47
Plate 2.3. Silicified serpentinites over the stockwork magnesites at Helvacibaba	48
Plate 2.4. Helvacibaba open pit mine, looking NE	48

Plate 2.5. Brecciated, porous and vuggy silicified texture at Helvacibaba.....	49
Plate 2.6. Shrinkage structure on the magnesite vein interior surface.....	49
Plate 2.7. Caltepe limestones and organic-rich meta-argillites, Caltepe.....	50
Plate 2.8. Silicified serpentinite at Arapomer Deresi	50
Plate 2.9. Extensively altered loose magnesite at Arapomer Deresi	51
Plate 2.10. Hirsizdere faulted sedimentary magnesite beds	51
Plate 2.11. Conglomeratic level at the bottom of magnesite bed at Hirsizdere	52
Plate 2.12. The town of Yesilova (Burdur), the Yesilova delta, the Salda lake and the Cretaceous limestones	52
Plate 2.13. Completely dried lake Akgol, 8 miles north-east of Salda lake.....	53
Plate 2.14. Salda delta in the south of Salda village.....	53
Plate 2.15. Hydromagnesite deposit at Kocaadalar burnu, south-west Salda lake	54
Plate 2.16. Stromatolite on a marram-like grass.....	54
Plate 2.17. Stromatolitic hydromagnesite island, north-west of the Salda lake	55
Plate 2.18. Porous, cauliflower-like structure of stromatolite	55
Plate 2.19. Internally laminated structure of the stromatolite.....	56

CHAPTER FOUR

Plate 4.6.1. Cyanobacterial filaments, mucilage, hydromagnesite crystals and diatoms in the newly formed stromatolites from Salda lake.....	98
Plate 4.6.2. Rose-like hydromagnesite crystals "desert roses", Salda lake.....	98
Plate 4.6.3. Orientation of hydromagnesite rosetts, Salda lake.....	99
Plate 4.6.4. Blade-like, flatty individual hydromagnesite crystals of Salda lake stromatolites	99
Plate 4.6.5. Scattered and different sized diatoms from Salda lake.....	100
Plate 4.6.6. Surface dissolving of diatom.....	100

ABSTRACT

This thesis is concerned with the problem of the genesis of the various types of cryptocrystalline magnesite deposits found in western Turkey. Veins and stockworks of cryptocrystalline magnesite deposits are found within the discontinuous ultramafic belts of western Turkey. Sedimentary-hydrothermal lacustrine magnesites and presently forming hydromagnesite deposits lie above these ultramafic rocks. A hot-spring calcite deposit at the northern edge of a Menderes graben is also considered.

From the stable carbon and oxygen isotopic signatures of the magnesite, hydromagnesite and calcite formations of western Turkey, three end-members can be distinguished:-

End-member-1 : represents the cryptocrystalline, vein-type of magnesite deposits. Decarboxylation of organic-rich sediments may have provided about two thirds of the carbonate in the vein-type of Koyakci Tepe magnesite deposits, Konya, which have ~ -13 and $\sim +27$ ‰ of $\delta^{13}\text{C}$ and $\delta^{18}\text{O}$ respectively. Stockwork deposits at Helvacibaba, Yunak and Kozagac, all in Konya, have slightly heavier $\delta^{13}\text{C}$ and $\delta^{18}\text{O}$ values indicating more involvement of atmospheric carbon dioxide (as bicarbonate in the circulating meteoric water) compared to those of Koyakci Tepe.

End-member-2 : represents carbon dioxide of atmospheric origin. Presently forming hydromagnesite deposits at Salda lake, Yesilova, Burdur reflect such a carbon dioxide origin with $\delta^{13}\text{C}$ of $\sim +4$ ‰PDB and $\delta^{18}\text{O}$ of $\sim +36$ ‰SMOW.

End-member-3 : represents the carbon dioxide of metamorphic origin. Present-day, hot-spring travertine (calcite) deposits at Pamukkale, Denizli, have the heaviest $\delta^{13}\text{C}$ ($\sim +6$ ‰,PDB) and extremely light $\delta^{18}\text{O}$ ($\sim +20$ ‰,SMOW) values and these values are probably the result of decarbonation and/or dissolution of limestone formations beneath travertines. Sedimentary magnesite deposits at Hirsizdere, Denizli and stockwork magnesite deposit at Arapomer Deresi have unexpectedly heavy $\delta^{13}\text{C}$ ($\sim +2$ and 0 ‰,PDB respectively), and these deposits probably gained their carbonates from decarbonation and/or dissolution of limestones.

The extremely low REE contents of magnesite, hydromagnesite and ultramafic host-rocks indicate that the magnesium is derived from the ultramafic rocks.

The Salda lake hydromagnesite deposits are being formed by a microbial community in the lake itself. In terms of isotopic signatures, physical features and geological environment, Salda's hydromagnesite deposits are comparable with the Miocene, lacustrine, sedimentary magnesite deposits elsewhere, perhaps especially to Bela-Stena in Serbia. Therefore Salda's hydromagnesites may be a precursor of magnesite.

CHAPTER ONE

REGIONAL GEOLOGY OF TURKEY AND A REVIEW OF TURKISH MAGNESITE DEPOSITS

INTRODUCTION

The genesis of cryptocrystalline magnesite deposits related to Alpine-Type ultramafic rocks has been extensively discussed (see for example Kralik et al., 1989). In these discussions a controversial issue has been the source of the carbon dioxide required for their formation. Various authors have suggested that it might be derived from atmospheric carbon dioxide (O'Neil and Barnes, 1971), from metamorphic rocks (by decarbonation of limestone and dolomite) (Abu-Jaber and Kimberley, 1992), from volcanic (including mantle-derived) sources (Ilich, 1968), from soils (by the decomposition of organic matter) (Zachmann and Johannes, 1989), by decarboxylation of organic matter (or other forms of oxidation of organics) in sediments (Fallick et. al., 1991; Brydie et. al., 1993), or by a combination of these possibilities.

The aim of this thesis has been to examine magnesite deposits in western Turkey, to better understand their origin, and to offer a solution to this problem in the situations they represent. Presently forming hydromagnesite and potentially related hot-spring calcite deposits have been examined, as well as cryptocrystalline sedimentary magnesite and vein-stockwork deposits in four principal areas from which samples have been collected. Stable isotopes have been the principal tool used during this study, backed by Inductively Coupled Plasma-Mass Spectroscopy (ICP-MS),

Scanning Electron Microscopy (SEM), and Atomic Absorption Spectrometry (AAS).

HYPOTHESIS

Fallick et al (1991) in discussion of the Serbian cryptocrystalline magnesite deposits, argued that one source of the carbonate was probably the carbon dioxide being released during decarboxylation. Such carbonate has light $\delta^{13}\text{C}$ ($<-10\%$) and $\delta^{18}\text{O}$ ($<26\%$) values, representing the end-member. The other carbon source derives from atmospheric carbon dioxide, which is comprised of heavy $\delta^{13}\text{C}$ and $\delta^{18}\text{O}$, as in certain sedimentary-exhalative magnesites. The stockwork and detrital magnesite straddle these "end members" and were assumed to be the result of mixing. Therefore on the basis of distinctive $\delta^{13}\text{C}$ and $\delta^{18}\text{O}$ values the two main types ie. vein and sedimentary the end members can be explained by mixing of atmospheric carbon dioxide and decarboxylation generated carbon dioxide (Figure 1.1). The Oshve vein magnesite deposit in Bosnia is an exception, having heavy $\delta^{13}\text{C}$ and yet light $\delta^{18}\text{O}$ values, which according to Fallick et al. (1991), indicate that the carbon dioxide was generated during contact metamorphism of local limestones.

The magnesite deposits in Turkey offer a testing ground of Fallick et al's hypothesis. These authors predict that organic-rich sediments should underlie the ultramafic host to the magnesite deposits, and that they should have lighter $\delta^{13}\text{C}$ and $\delta^{18}\text{O}$ values than the consequent magnesite deposits. Furthermore, the sedimentary magnesite deposits are expected to be represented by heavy $\delta^{13}\text{C}$ and $\delta^{18}\text{O}$ values. During field work we found a candidate for this organic-rich source of carbonate, a lower Palaeozoic meta-argillite, containing carbonate veinlets, which extrapolates beneath the

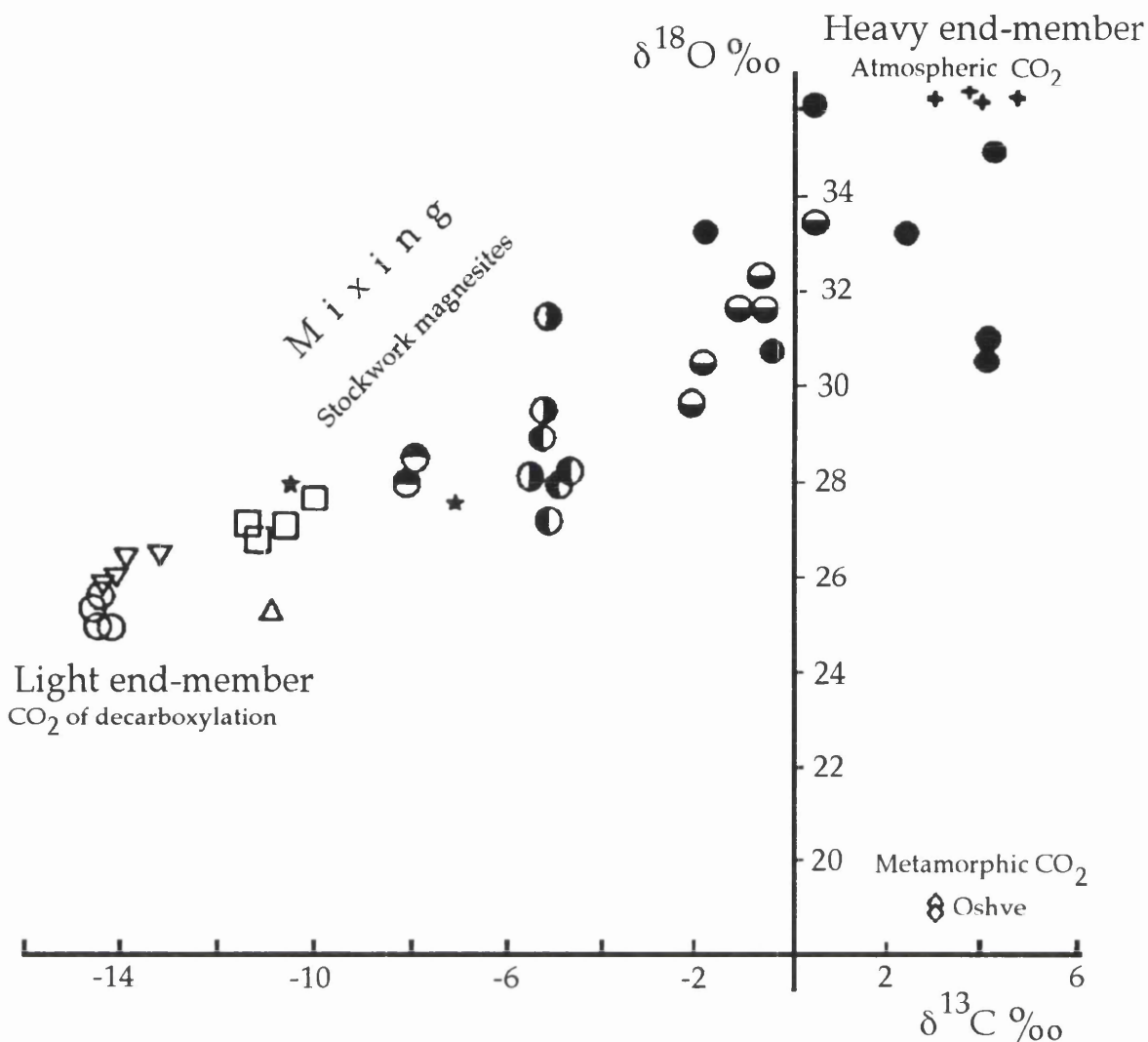


Figure 1.1. $\delta^{13}\text{C}$ and $\delta^{18}\text{O}$ values of Serbian and Bosnian magnesite deposits which generated Fallick et al (1991)'s hypothesis of two end-members as an explanation of the broad positive trend.

ultramafic thrust slice hosting the Konya magnesite deposits. Moreover we also discovered an actualistic example of the exhalative-sedimentary, lacustrine (hydro)magnesite genetic process, which involves microbialite controlled deposition over a groundwater seepage or warm spring. These giant hydromagnesite microbialites might be expected, by comparison with Bela-Stena in Serbia, to reveal an atmospheric source of carbon dioxide and meteoric derived groundwater (Figure 1.1). I also considered the hot spring travertine deposits at Pamukkale as being of contact metamorphic origin as

are the veins at Oshve in Bosnia. If so it should have light $\delta^{18}\text{O}$ and heavy $\delta^{13}\text{C}$ values.

1.1. REGIONAL GEOLOGY OF TURKEY

There is a close relationship between ore deposits of all kinds and regional geological features. For cryptocrystalline magnesite deposits, there is an association with ultramafic rocks which occur in areas in Serbia, Greece and Turkey where extensional tectonic regimes have been dominant since the Oligocene.

The geological history of Turkey essentially begins with the deposition of marine sediments (some of which are Palaeozoic) in the Tethyan ocean, and with the subsequent collision (in the early Mesozoic) of Laurasia and Gondwanaland (Africa). Turkey is a land squeezed between these two continental plates (Figure 1.2). Ketin (1966) divided Turkey into four major tectonic units:

1. the Pontides (in the north)
2. the Anatolides (in the centre)
3. the Taurides (in the south)
4. the Border folds (in the south-east)

The Anatolides, Taurides and Border folds are made up of sedimentary packages affiliated to Gondwanaland whereas the Pontides belong to Laurasia. The boundary between Gondwanaland and Laurasia is formed by the "Izmir-Ankara-Erzincan suture zone", also known as "the Tethyan suture". Turkey's tectonic subdivisions and this suture zone are

shown in figure 1.3. Ultramafic rocks are widespread but those associated with magnesite deposits occur principally in the western parts of the Anatolides and Taurides.

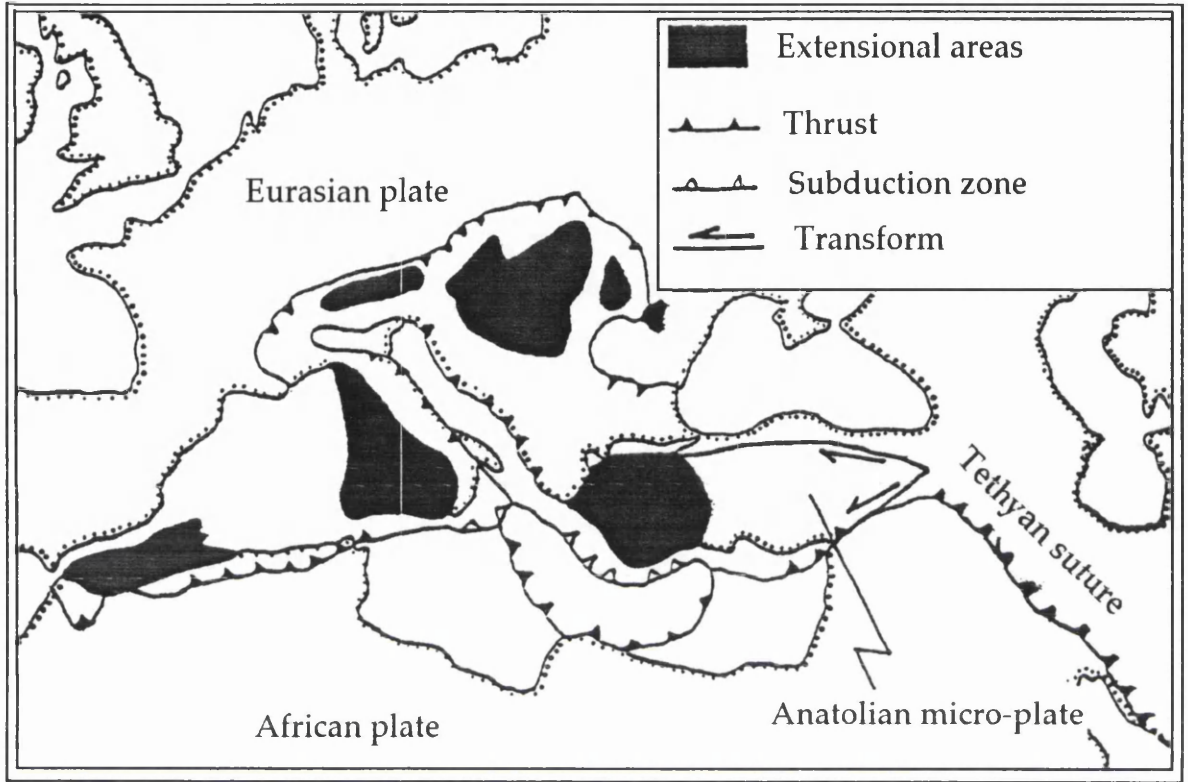


Figure 1.2. The position of Turkey (the Anatolian micro-plate) in relation to the Eurasian and African plates. Modified from Kastens (1991).

The effects of Alpine deformation (from the late Mesozoic onwards) are seen in the Anatolides, Taurides and the Border folds. There is little folding and no evidence of any post-Jurassic regional metamorphism in the Pontides. The Anatolides reflect both strong Alpine deformation and regional metamorphism while the Taurides, although deformed, show little metamorphism. The "Border folds", representing the northern edge of the Arabian platform, again include few metamorphic rocks. The major difference between the Turkish and European Alps appears to be the absence

within the Turkish orogen of any Hercynian deformation and metamorphism. Okay (1986) suggested that the Pontides can be correlated with the southern Austro-Alpine zone, the Anatolides with the Penninic zone; the Taurides with the Helvetic zone; while the Border folds are equivalent to the Jura Mountains.

Sengor (1979) and Sengor and Kidd (1979), indicated that the Anatolides and Taurides formed as an extensive Tethyan platform during the Mesozoic and earlier. The continuations of this platform are seen in the Hellenides and Dinarides to the west. The closure of the Tethys seaway, subduction of the oceanic crust (including ophiolitic sequences), and the subsequent collision of the two continents, Gondwanaland and Laurasia, caused the uplift of ultramafic rocks along the collision zone. These are seen in Bosnia, Serbia, Albania, Macedonia, Greece, Turkey and Cyprus, and perhaps further east. However, the closure of Tethys was more complex than this suggests because there are also notable ophiolitic rocks in the Pontides, north of the suture. These indicate that there were probably a series of short-lived small oceans and subduction zones on the north side of Tethys.

The Pontides, Anatolides and Taurides can be subdivided into several sub-zones, separated by minor and often controversial sutures (Figure 1.3).

The Pontides: There are three major sub-zones in the Pontides: (i) the Istranca massif, made up of Palaeozoic and early Mesozoic sediments and metamorphics, (ii) the Istanbul zone, equivalent to the Istanbul nappe of

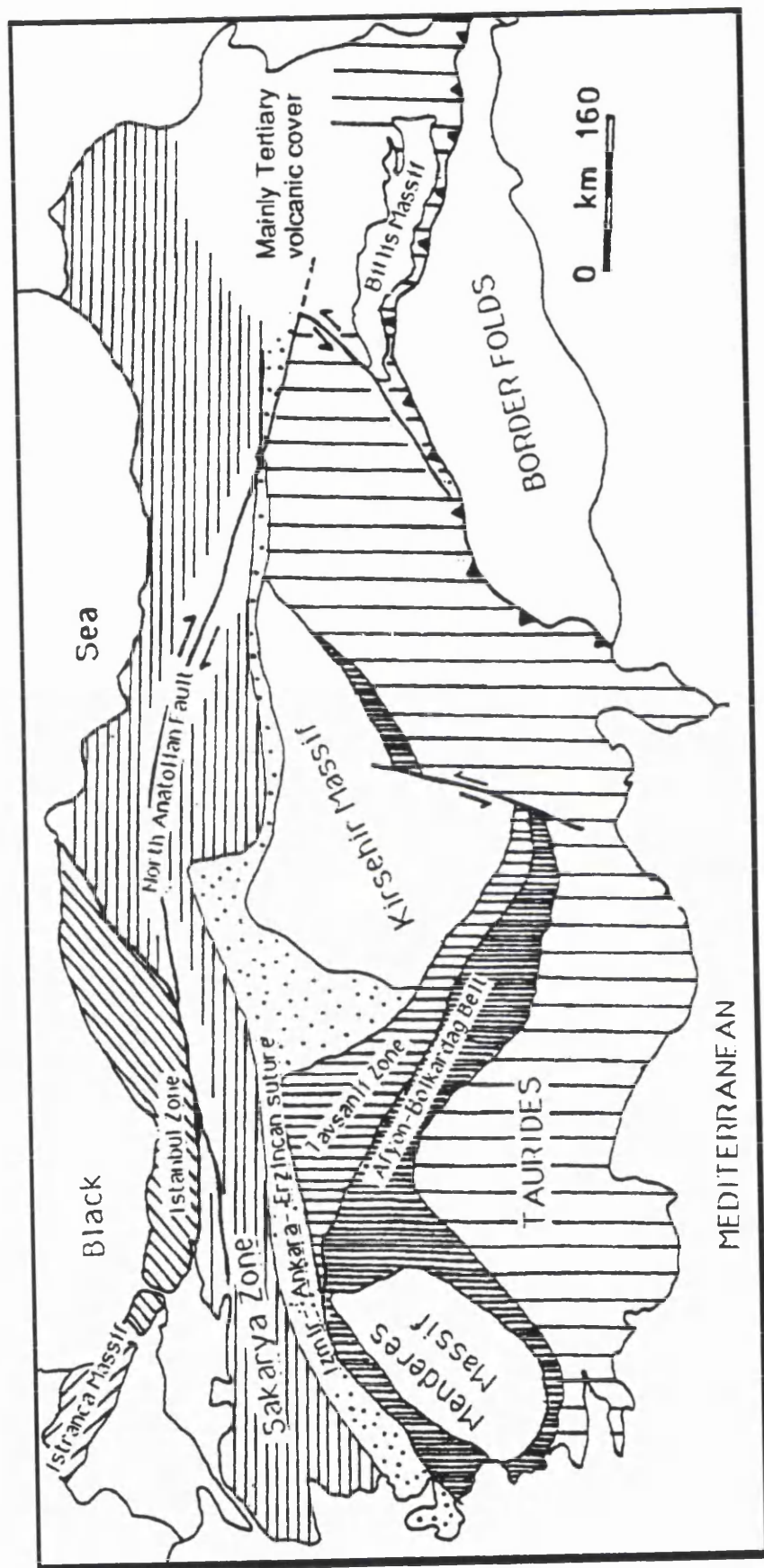


Figure 1.3. Major geological features of Turkey. The Taurides are not subdivided. Major faults are indicated by heavy lines. Modified from Okay (1986) and Kocyigit (1991).

Sengor et al. (1984), with a basement of Precambrian amphibolite, metadiorite and mica-schist, and (iii) the Sakarya zone (also called 'the Sakarya continent' by Sengor and Yilmaz, 1981; and 'the Karakaya complex' by Bingol et al., 1975), characterised by Permo-Triassic metamorphic rocks.

The Anatolides: The Anatolides comprise four major units: (i) the Menderes massif, in the extreme west of Turkey, contains extensive areas of Precambrian gneisses but also includes some younger schists and marbles, (ii) the Afyon-Bolkardag belt (also called the Afyon zone), consists of a thick sequence of basic metaclastic Palaeozoic rocks overlain by a thick section of Mesozoic marbles, reddish limestones and flysch. Serpentinities are also present in this zone. The stratigraphy and metamorphism of the Afyon-Bolkardag belt show some similarities with the northern part of the Menderes massif, (iii) the Tavsanlı zone, north of the Menderes massif, is composed of Cretaceous metavolcanic and metasedimentary rocks of blueschist facies which are partly thrust over the Afyon-Bolkardag belt, (iv) the Kirsehir massif (also known as the Central Anatolian massif) is made up high temperature/low pressure metamorphic rocks and contains extensive granite intrusions (Tolluoglu, 1989; Bayhan and Tolluoglu, 1987).

The Taurides: The Taurides cover much of the southern part of Turkey. They consist of a series of superimposed nappes comprising mostly sedimentary rocks representing platform and continental margin products. The rock sequences in the Taurides range in age from Early Palaeozoic to Early Tertiary. In the central Taurides Ozgul (1976, 1984) differentiated a number of tectono-stratigraphic units with distinctive stratigraphic, metamorphic and tectonic features. The Aladag unit is a complex of thrust sheets of platform type sediments which spans the Devonian to the Late

Cretaceous. It is partly covered by the Bozkir unit which comprises ultramafic and Mesozoic volcano-sedimentary rocks. The Antalya unit (also known as the Antalya nappes) lies to the south of the Aladag and Bozkir units, and records the rifting of a Permian carbonate platform and the subsequent development of a continental margin (Robertson and Woodcock, 1982). The Lycian nappes, found in the west of Antalya, comprise a complex of thrust sheets made up mostly of Mesozoic sedimentary and volcanic rocks with one major ultramafic nappe.

In simple terms, the Menderes massif, the Afyon-Bolkardag belt and the major part of the Taurides, represent a dismembered carbonate platform (perhaps comparable to the modern Bahamian carbonate platform) developed upon continental crust. This was bordered to the north by the Tethys ocean, and separated from Gondwanaland by a rifted pelagic basin where rocks of the Antalya unit were being deposited and where oceanic crust developed during the Late Mesozoic. The consumption of the Tethys ocean by northward dipping subduction zones perhaps caused the creation of a magmatic arc in the Pontides, and the formation of ultramafic belts elsewhere in Turkey. In south-eastern Turkey a distinct unit, the Bitlis massif, apparently lying on the southern margin of the Taurides and comprising gneisses, phyllites, metaquartzites, marbles and metabasites with low-grade Alpine metamorphism (Boray, 1975), was overthrust from the north. It is separated by an ophiolite, together with an ophiolitic melange and flysch, from the Palaeozoic to Mesozoic shelf sequences of the Arabian platform beneath (Hall, 1976). From the Late Tertiary onward the Bitlis massif and the ophiolite continued moving southward, driven by the convergence of Eurasia and Arabia.

In western Turkey, Greece and Yugoslavia, however, there has been a relaxation and an extension which began in the Oligocene and which has resulted (in Turkey) in the formation of normal faults and grabens. Sancar (1982) suggested that the hydrothermal circulation associated with many of the magnesite deposits began at this time.

1.2. PREVIOUS STUDIES OF TURKISH MAGNESITES

Magnesite is widespread in Turkey. Most deposits are related to ultramafic rocks, generally serpentinite and peridotite, of Lower Mesozoic age (Figure 1.4). According to Erdem (1974) and Sengor and Yilmaz (1983), these rocks were tectonically emplaced during the Upper Cretaceous but Okay (1986) considers that in some areas, for example south-eastern Turkey, the emplacement of ultramafic rocks is still taking place .

Over one hundred magnesite deposits occur within, or directly overlying, these ultramafic rocks. The major deposits are concentrated in Konya, Kutahya, and Eskisehir Provinces. Demirhan (1986) provided a list indicating that, in 1984, 93 % of Turkish reserves were in these three provinces (Table 1.1). He did not, however, include the extensive Yunak deposits (also in Konya Province) in his calculations so the proportion is even higher. Erzincan, Cankiri and Denizli Provinces also contain notable reserves.

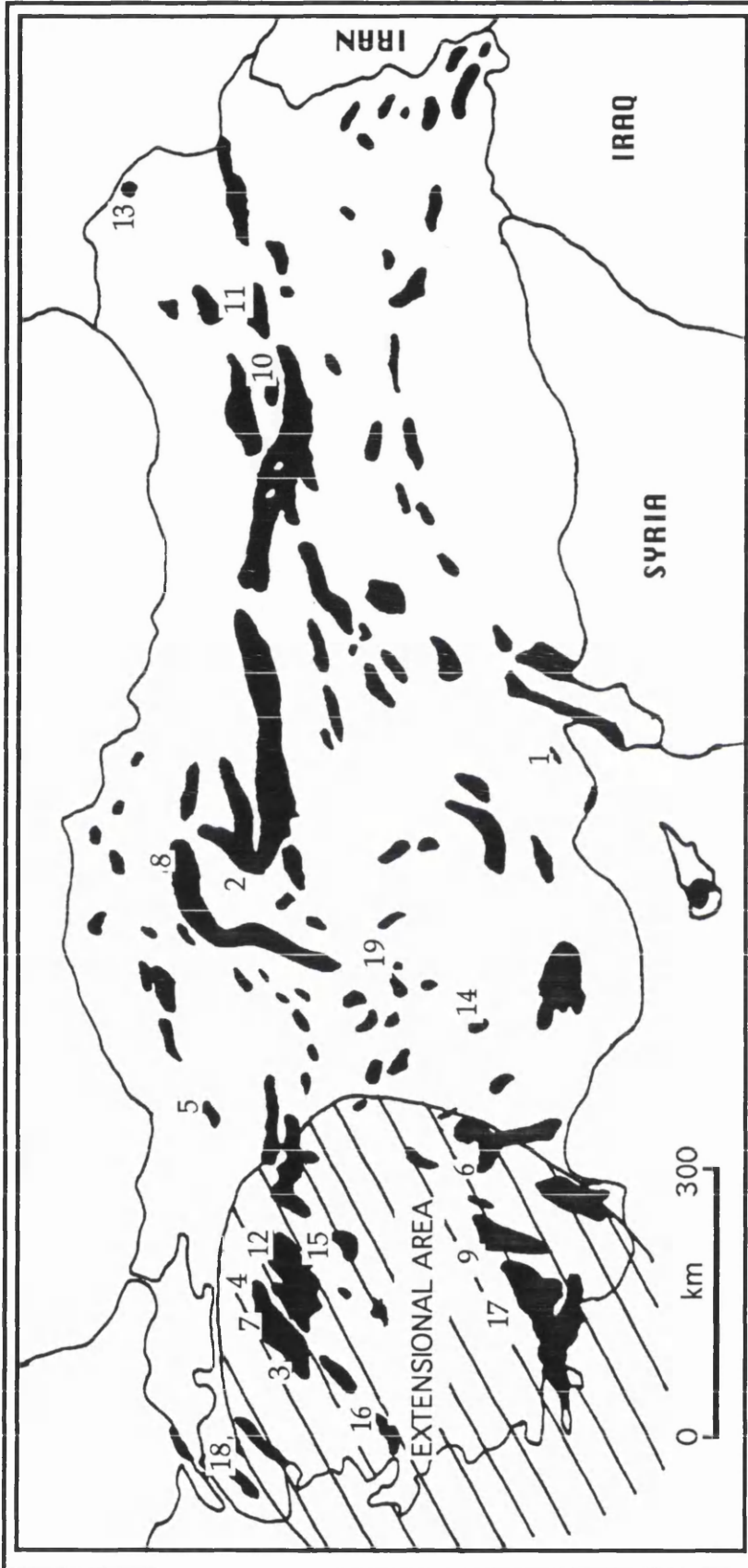


Figure 1.4. Discontinuous ophiolitic belts with related magnesite deposits in Turkey. The deposits are:- 1. Adana, 2. Ankara, 3. Balıkesir, 4. Bilecik, 5. Bolu, 6. Burdur, 7. Bursa, 8. Cankiri, 9. Denizli, 10. Erzurum, 11. Erzincan, 12. Eskisehir, 13. Kars, 14. Konya, 15. Kutahya, 16. Manisa, 17. Mugla, 18. Canakkale, 19. Tuz Golu (Salt lake); modified from Erdem (1974) and Sancar (1982).

Table 1.1. Turkish magnesite deposit reserves (by Provinces)
after Sancar, 1982).

<u>PROVINCE</u>	<u>TOTAL MAGNESITE RESERVES (TONNES)</u>
Adana	4,000
Ankara	97,000
Balikesir	551,000
Bilecik	225,750
Bolu	20,000
Burdur	85,000
Bursa	630,000
Cankiri	2,048,000
Denizli	1,100,000
Erzincan	5,879,500
Erzurum	730,000
Eskisehir	38,873,000
Kars	465,000
Konya (Helvacibaba)	50,000,000
(Others)	33,091,600
Kutahya	34,649,000
Manisa	18,000
Mugla	+ 150,000
Total	168,616,850

Although most of the Turkish magnesite deposits are in western areas ultrabasic rocks are much more widespread. There are two possible reasons for this. First, the magnesite deposits are mostly concentrated in extensional zones which, as indicated, are only present in the west (Figure 1.4). The faults in these probably provided channelways for exploitation by hydrothermal systems. The second reason is less theoretical. Eastern Anatolia is still largely unexplored and it remains to be seen if there are other, as yet undiscovered, magnesite deposits in this area. But one purpose of this thesis is to ascertain whether the development of magnesite deposits in western Turkey is sufficiently explained by faulting or whether there are other factors.

The great majority of Turkish deposits are of the cryptocrystalline vein-stockwork type, only seven are sedimentary. The last include a present-day freshwater hydromagnesite body (described in Chapter-2) discovered in Salda Lake (Burdur, southwest Turkey) by Schmid (1987) and also a minor continental sabkha-type magnesite in Tuz Gölü (Salt Lake) in Central Anatolia (Pohl, 1989). One metamorphic occurrence of magnesite has been reported at Yunak (Konya) by Yenyol (1982). There are no reported sparry-type deposits in Turkey.

There is a major controversy regarding the genesis of cryptocrystalline magnesites. The main contention is whether they originate as a result of weathering (O'Neil and Barnes, 1971; Möller, 1989; Zachmann and Johannes, 1989) or by hydrothermal processes (Ilich, 1968; Fallick et al., 1991; Abu-Jaber and Kimberley, 1992) .

Weathering: Meteoric waters containing carbon dioxide (dissolved from the atmosphere) may be expected to react with ultramafic rocks and to take magnesium and silicon into solution, leaving iron behind. As these percolate downwards they leach more and more Mg and Si and thus become supersaturated. The precipitation of magnesite takes place when the solutions lose carbon dioxide and thus change pH as they approach the surface again. O'Neil and Barnes (1971) described a variety of magnesium and calcium carbonate deposits in California, thought to have formed as a result of surficial weathering. In these the interaction between ultramafic rocks and ground water drives near surface carbonate precipitation at temperatures of 15-25°C. Barnes and O'Neil (1969) distinguished two types of water. 1) $\text{Ca}^{2+}\text{OH}^{-1}$ -type water (formed as a result of the reaction between pyroxenes relatively rich in calcium, and groundwater) is held to be

responsible for the deposition of travertine (calcite), and 2) $\text{Mg}^{2+}\text{HCO}_3^{-1}$ -type water (formed by the reaction between serpentinites and groundwater) is argued to be responsible for nesquehonite precipitation. Hydromagnesite in this area is precipitated from $\text{Mg}(\text{HCO}_3)_2$ -saturated solutions (O'Neil and Barnes, *ibid.*).

Hydrothermal: According to Ilich (1968), the formation of both lacustrine-sedimentary and ultramafic-hosted vein-stockwork-type magnesites results from CO_2 -rich volcanogenic exhalations. Fractured ultramafic rocks are leached by these CO_2 -bearing hydrothermal solutions, becoming rich in Mg^{2+} . Magnesite is precipitated by the release of CO_2 as a result of rapidly falling pressure as the solutions move towards the surface. This precipitation mechanism has been accepted by Fallick et al. (1991), Abu-Jaber and Kimberley (1992) and others. Ilich (1968) also suggested, that similarities in Hg concentration in lacustrine-sedimentary and ultramafic-hosted vein-stockwork magnesites indicates that both formed from hydrothermal sources. In Serbia, vein-stockwork and lacustrine magnesites, both have high Hg (700 ppb) concentrations whilst ultramafic rocks in the area have only 9 ppb (Abu-Jaber and Kimberley, 1992). In areas where mercury is present, hydrothermal solutions at depth are rich in both mercury and magnesium. When these solutions find a suitable fractured-faulted zone, which may emerge at the base of a lake, the pressure drop leads to a release of CO_2 from the solution and to the precipitation of mercury (as cinnabar) as well as magnesite.

In both weathering and hydrothermal processes there are four general requirements. 1) there must be a magnesium source, 2) there must be a suitable water supply, 3) a pump to drive the system, and 4) there must

be a carbon dioxide source. In addition, for carbonates to precipitate, carbon dioxide must be lost. This loss probably controls the pH of the solution, both the falling temperature and carbon dioxide pressure drop cause lowering of the pH (Krauskopf, 1979). In order that mineralization can occur, all these necessities must come together.

The magnesium source : It is generally accepted that the magnesium in magnesite was originally derived from olivine or serpentine in ultramafic rocks. Alteration of these minerals is possible even at temperatures as low as 15°C (Barnes and O'Neil, 1969).

The water source : Meteoric water is an attractive fluid source since it potentially provides large volumes near surface. Fallick et al. (1991) suggested that generally the large amount of water needed for magnesite mineralisation can only be satisfied by meteoric water recharge.

The pumping of fluid : The source of energy to pump the fluid is hydrostatic flow driven by the topography (Artesian drive system).

The carbon dioxide source: One of the most disputed subjects in the study of cryptocrystalline magnesite deposits is the source of the carbon dioxide (carbonate). The possibilities are: 1) atmospheric carbon dioxide (O'Neil and Barnes, 1971), 2) metamorphic carbon dioxide released during decarbonation of limestones or dolomites (Abu-Jaber and Kimberley, 1992), 3) volcanogenic carbon dioxide (Ilich, 1968), 4) soil-generated carbon dioxide (produced during decomposition of plant material in the soil) (Zachmann and Johannes, 1989), 5) carbon dioxide produced by decarboxylation of

organic sediments (Fallick et al., *ibid.*; Brydie et al., 1993)) or 6) any combination of the above possibilities.

Despite the fact that Turkish magnesite deposits such as that at Helvacibaba (Konya, see location 14 on figure 1.4) have been mined since before the first World War, scientific studies did not begin until 1962 (Demirhan, 1986). The Turkish Mineral Research and Exploration Institute (MTA) prepared an inventory in 1986 in which 114 sedimentary and cryptocrystalline magnesite deposits were reported with estimates of reserves and quality. A variety of origins have been suggested for these. The following section will review and critically examine previous work.

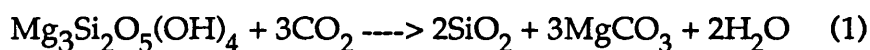
1.2.1. Cryptocrystalline vein-stockwork type magnesites

As indicated, most Turkish magnesite deposits are of the cryptocrystalline, vein-stockwork type. Three have been relatively well studied. The Turkmentokat-Karatepe (Eskisehir) deposits have been described by Sariiz (1990) (see location 12 on figure 1.4), the Burdur deposits by Fisekci (1989) (see location 6), and the Yunak-Konya deposits by Yeniyol (1982) (see location 14).

The Tukmentokat-Karatepe deposits: The Tukmentokat-Karatepe (Eskisehir) deposits (location 12, Fig. 1.4) appear to result from two magnesite-forming processes: present-day infiltration and hydrothermal processes (Sariiz, 1990). Sariiz (*ibid.*) argued that botryoidal, cauliflower-like structures and concretions are characteristic of low temperature (25°C) infiltration and that meteoric waters in this area cannot have been heated to more than 60°C. Sariiz (*ibid.*) described the occurrence of a limonitic cap on

top of the magnesite deposits and argued that this formed as a result of surficial weathering of the ultramafic rocks beneath. However, this seems to imply that the magnesite formed between the source rocks and the weathered cap. Sariiz (ibid.) did not reveal how weathering of the ultramafic rocks takes place, beyond suggesting that Mg^{2+} and Si^{4+} were 'taken from the environment' so that the remaining ultramafics were relatively rich in iron. Oxidation of this iron results in the formation of a limonitic cap (Sariiz, 1990).

Sariiz (1990) also argued that hydrothermal magnesite and quartz preceded calcite and dolomite during mineralisation. He suggested that the vein-stockwork magnesite at Turkmentokat-Karatepe formed hydrothermally by the reaction;



Sariiz (ibid.) used the Langmuir diagram (Figure 1.5), to argue that magnesite cannot form below 60°C and a partial pressure of carbon dioxide of 1 bar. In view of this he suggested that under surface conditions, hydromagnesite is normally the first product of a near surface mineralisation process. He concluded that the vein-stockwork magnesites at Turkmentokat-Karatepe might have been precipitated from hydrothermal fluids at about 150°C by comparison with the Delaro deposit in Canada as described by Griffis (1972). Griffis (ibid.) suggested that the magnesite-talc-quartz paragenesis in the centre of the deposit indicates a high temperature (as high as 650°C) since it involves talc. In contrast, a magnesite-quartz assemblage in the outer margins probably reflects a lower temperature (150-300°C). Sariiz (1990) compared the Delaro and

Turkmentokat-Karatepe deposits, and found many common geological, mineralogical and petrographic features. He suggested that the magnesite-quartz assemblage in particular indicates a hydrothermal mineralisation for Turkmentokat-Karatepe.

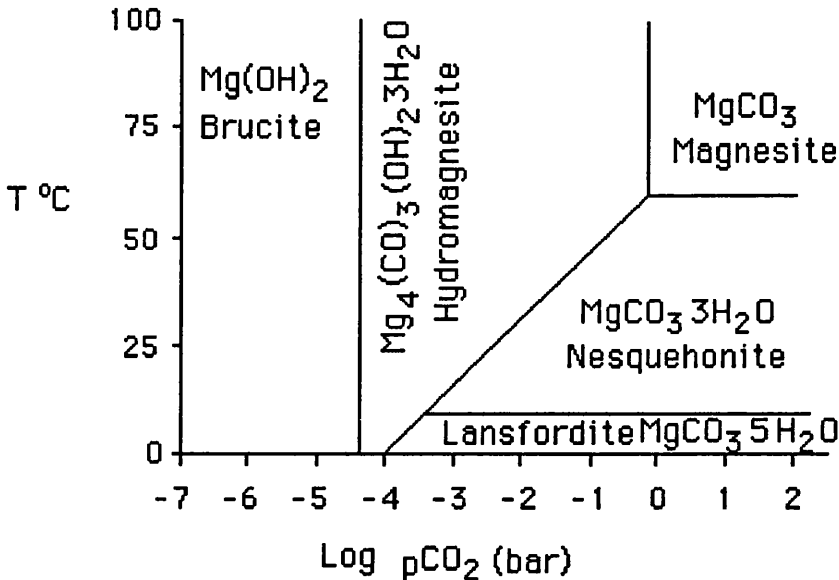


Figure 1.5. The stability diagram of the MgO-CO₂-H₂O system relative to Temperature and CO₂ pressure (Sariiz, 1990, after Langmuir, 1965).

The existence of talc in the mineral paragenesis, however, does not always indicate high temperature (650°C or so) mineralisation. It has been reported that talc may be formed by the interaction of silica-bearing hydrothermal fluid with hot ocean water (Costa et al., 1980 and 1983). Costa et al. (1983) stated that the talc and carbonates (calcite, dolomite, ankerite, siderite) are the most abundant minerals in the Mattagami lake mine, Quebec, Canada. They indicate that the ultimate source of Mg, Fe, Mn, Si and Ca in the hydrothermal fluids is the hydrothermal alteration of rhyolite and chlorite. The occurrence of talc and carbonates as well as metal sulphides and oxides has been attributed to the mixing of hydrothermal

fluids with ocean water in the sea-bed (Costa et al., 1983). Fluid inclusion studies and $\delta^{18}\text{O}$ values of carbonates and quartz all indicate that when the mineralisation was taking place the temperature at Mattagami lake mine was between 90°C (ocean water) and 300°C (hydrothermal fluid) (Costa et al., 1983). Thus, the presence of talc in the mineral paragenesis is not always the result of high temperature mineralisation.

Griffis (1972) suggested that the carbon dioxide for magnesite formation in the Delaro deposits was metamorphically generated by the decarbonation of limestone and dolomite. Sariiz (1990) gave no clear source(s) for carbon dioxide. His suggested equation (1), for the formation of cryptocrystalline vein-stockwork magnesite is not consistent with a hydrothermal reaction since, if there is a hydrothermal process, water (in many cases meteoric water) will inevitably be involved, especially where large amounts of magnesite are being precipitated (Fallick et al., 1991). His suggested formation temperature for the hydrothermal magnesite at Turkmentokat-Karatepe is probably too high, since the oxygen isotopic composition of the magnesite (~27.5 ‰SMOW, Zachmann, 1989; Kralik et al., 1989) indicates a temperature of about 80°C (for further information see Chapter-5, The isotopic composition of the fluids and their temperature). Finally, there is some argument to suggest that the limonitic cap referred to by Sariiz (1990) may have formed as a result of hydrothermal alteration of olivine-fayalite (Fe_2SiO_4), rather than by the surficial alteration of olivine. Hydrothermal limonitic caps have been reported from ultramafic-hosted magnesite deposits in Venezuela (Abu-Jaber and Kimberley, 1992) and Serbia (Fallick et al., 1991).

The Konya Deposits: In Konya, (location 14, Fig. 1.3) stockwork and vein magnesite occurs in altered serpentinites. There are two main opinions regarding the genesis of the deposits. That magnesite was formed from (a) descending meteoric waters (Kaaden, 1965) or (b) from ascending hydrothermal fluids (Petraschek, 1971). Kaaden (1965) and Petraschek (1971) both worked in cooperation with the MTA (Mineral Research and Exploration Institute of Turkey). Neither was concerned primarily with the origins of the magnesite and their explanations were simply delivered *en passant*. I have examined these deposits in detail and their genesis will be considered in Chapters 2, 4 and 5.

The Yesilova-Burdur Deposits: The Yesilova-Burdur magnesite deposits (location 6 on Fig. 1.4) have been preliminarily investigated by Fisekci (1989) for the MTA. This province contains both cryptocrystalline vein-stockwork and sedimentary magnesite deposits, including presently-forming hydromagnesites (Brennich 1959, Cayirli and Yavas 1975, Schmid 1987). The cryptocrystalline vein-stockwork type magnesites in Yesilova-Burdur are generally massive, but sometimes exhibit cauliflower-like structures. They have been emplaced in faults and fractures within the ophiolitic rocks and are sometimes overlain by silicified serpentinite, as in Cokrakcukuru Sirti, Otluburun Tepe and Mesdinegolu Tepe (Fisekci, 1989). The Arap Omer Deresi deposits, 13 km north-west of Salda Lake, are also of the vein-stockwork type and will be discussed in Chapters 2, 4 and 5.

1.2.2. Sedimentary magnesites

So far, seven sedimentary magnesite deposits have been reported in Turkey (Sancar 1982; Gundogdu and Ataman 1976). These are: 1) Cayirli (at

Erzincan, locality 10, Fig. 1.4), 2) Karantina Koyu (at Canakkale, locality 18), 3) Tavsanlı (at Kutahya, locality 15), 4) Hirsizdere-Cambasikoy (at Denizli, locality 9, see chapters 2, 4 and 5), 5) Torunlar-Yunak (at Konya, locality 14), 6) Salda Lake (at Yesilova-Burdur, locality 6, see chapters 2, 4 and 5), 7) Tuz Gölü (salt lake) in Central Turkey (locality 19). Only Salda and Hirsizdere-Cambasikoy will be described in detail.

Salda Lake: The hydromagnesite deposits at Salda Lake have been investigated by the MTA but as the Lake and surrounding area has been declared a historical and cultural area, they are no longer important for the mining industry (Fisekci, 1989). The exploration emphasis was on reserves and quality (grade) of the deposits rather than origins. Schmid (1987) was the first to suggest that magnesite mineralisation is still taking place in Salda Lake. He regarded the deposits as providing a model for larger sedimentary magnesite occurrences in Australia. Four types of magnesite were recognised : 1) Cryptocrystalline magnesite (in veins and stockwork in the hills to the northwest at Arap Omer Deresi), 2) Detrital magnesite, 3) Magnesite-rich mud, 4) Secondary, cryptocrystalline magnesite. Schmid (1987) indicated that the cryptocrystalline vein-stockwork magnesite (position 1 on Fig 1.6) occurs within the serpentinites in the manner described in the section above. These are weathered and eroded, so that detrital magnesites are formed (position 2 on Fig. 1.6). Detrital grains are then transported and eventually deposited in the lacustrine environment. At this stage, complete chemical and physical alteration of the magnesite takes place in the lake water resulting in the formation of magnesite-rich mud (position 3 on Fig. 1.6). Mud is then re-deposited on the shore and, after leaching and physical separation of contaminants, forms nodular concretions relatively enriched in magnesite (Schmid, 1987). These

supposed stages are summarised in figure 1.5. However, the sequence of events and supposed products were apparently based only on speculation. Detailed observations lead to quite different conclusions (see chapters 2, 4 and 5).

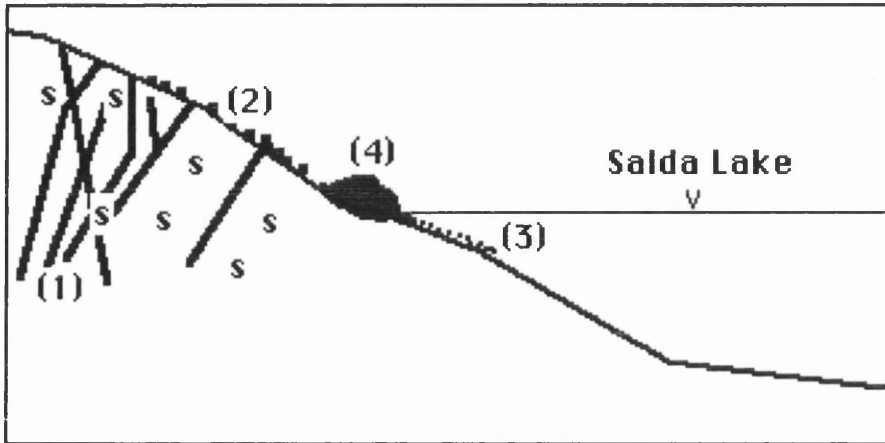


Figure 1.6. The four types of magnesite developed in Salda Lake and the surrounding area according to Schmid (1987). Note: 1-Vein-stockwork, 2-Detrital, 3-Magnesite-rich mud, 4-Secondary magnesite (redeposited), s-Serpentine.

An alternative view of the magnesite concentration process in lakes has been proposed for Tuz Gölü, the largest salt lake in Central Anatolia (Ergun, 1988; Pohl, 1989). Here, according to Pohl (ibid.), present-day magnesite mineralisation is taking place along with the deposition of gypsum, celestite, polyhalite and halite forming greyish-white muds. Lake waters are saturated with Cl^- , SO_4^{2-} , Mg^{2+} , Na^+ and K^+ . The levels of Ca^{2+} are relatively low and Pohl (1989) suggested that Ca^{2+} is consumed in the precipitation of gypsum in summer. Thus the $\text{Mg}^{2+}/\text{Ca}^{2+}$ ratio increases and huntite and magnesite are deposited in response to evaporation in the central area of the lake.

There are thus two general explanations for the deposition of magnesite in the lakes, either it is essentially detrital, or it is a chemical precipitate formed in response to evaporation. These alternatives will be discussed in the light of evidence presented in Chapters 2, 4 and 5.

1.2.3. Stable isotope studies

Few isotope studies have been undertaken on Turkish magnesites. The results of analyses of the Kumbet magnesite deposit (which may be in either the Kutahya, locality 15, or Eskisehir, locality 12 in Fig. 1.4) have been reported by Zachmann and Johannes (1989). Zachmann (1989) has also reported one result for the Eskisehir magnesite deposit. These results are shown in Table 1.2. Neither of these papers gives any interpretation of the results, although Zachmann and Johannes (1989) argued that the CO₂ for magnesite mineralisation is derived from meteoric water.

Table 1.2. Published results of stable isotope analyses of Turkish magnesite deposits (from Zachmann and Johannes, 1989 and Zachmann, 1989).

Location	$\delta^{13}\text{C}$ ‰, PDB	$\delta^{18}\text{O}$ ‰, SMOW
Kumbet	-8.2	28.2
Eskisehir	-10.9	27.2

The following Chapters are concerned with the Geology of the deposits examined (Chapter 2), Analytical methods (Chapter 3) and Results of Analyses (Chapter 4). Chapter 5 will consist of a discussion of these results and Chapter 6 Conclusions.

CHAPTER TWO

LOCAL GEOLOGY OF THE DEPOSITS AND THEIR GEOLOGICAL FEATURES

INTRODUCTION

In western Turkey magnesite deposits are concentrated in the Tavsanlı zone (Konya-14d, figure 3.1), in the Kutahya-Bolkardag belt (Konya-14a,b,c) and in the Western Taurides (Konya-14e; Burdur-6a,b; Denizli-9a,b and Mugla-17). The sites of the deposits Konya-14d,f and Denizli-9a,b appear to be in the boundaries of the tectonic units. The sites of the deposits and their geological relationships with surrounding rocks have been shown in figure 2.1.

Extensive field work has only been undertaken at Konya (Helvacibaba and Koyakci Tepe magnesite deposits) and Burdur (Salda lake hydromagnesite deposits) during the summers of 1989, 1992 and 1993. Some places for example Denizli and Mugla have been visited for a short time only, usually one or two days' excursions. Here I intend to explain the general geological environments of the deposits studied during my research.

2.1. GEOLOGICAL SETTING OF THE KONYA MAGNESITE DEPOSITS

The Konya province is located in the south-western part of the Central Turkish Region. Geologically the magnesite deposits at Konya (location 14 a,b,c,e on figure 3.1) are situated within the Kutahya-Bolkardag belt which in a broad sense lies between the Menderes and Kirsehir massifs. Western Turkey comprises one of the structural elements of the Alpine-Mediterranean Zone.

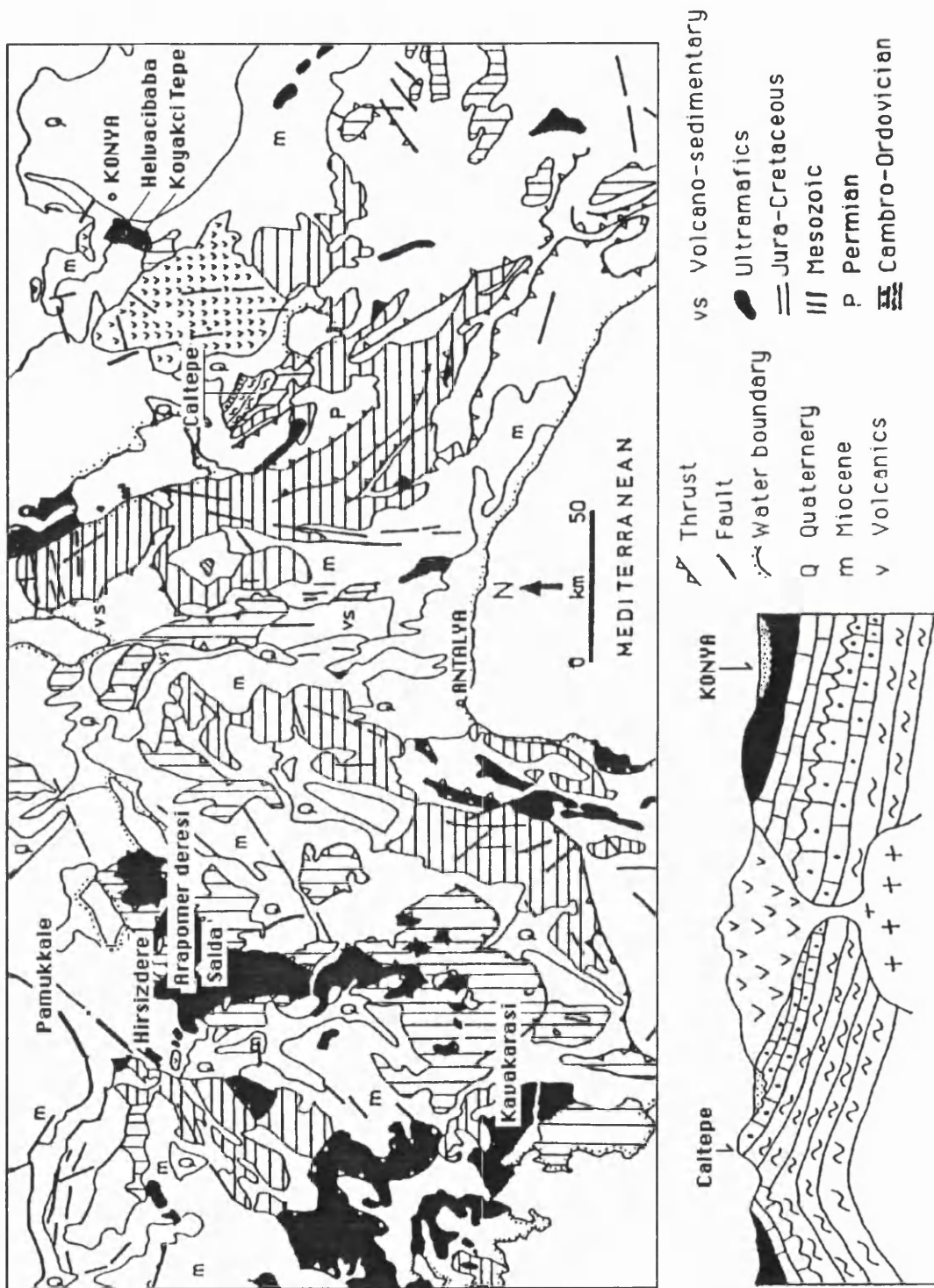


Figure 2.1. General geological map of southwestern Turkey. The locations of carbonate deposits are also marked where possible. The geological cross-section is between Konya and Caltepe where organic-rich meta-argillites crop out within the Seydisehir formation.

According to Gulec (1991) two major palaeotectonic units are present in Western Turkey, the Menderes-Taurus Block (The Tavsanlı zone is also included by some authors) in the south, and the Sakarya Continent to the north. These units are separated from each other by the Izmir-Ankara-Erzincan branch of the Neo-Tethyan Suture Zone. The Konya district is about 80 kilometres south of this zone.

Various lithologies are represented in the Kutahya-Bolkardag Belt, such as limestone, chert, shale, siltstone, greywacke, dolomite, quartzite and various magmatic rocks including diabase dikes and ultramafics (Ozcan et al. 1988). Limestone, quartzite, dolomite, ultramafic rocks, dolomitic marls and alluvium occur in the Konya province (Figure 2.2).

Rock units have been classified into five major categories, from youngest to oldest:

- Neogene dolomitic marls, limestones and alluvium
- Cayirbagi ophiolitic complex (Upper Cretaceous)
- Midos formation (Upper Cretaceous)
- Loras limestone (Upper Jurassic-Upper Cretaceous)
- Ardicli formation (Permian-Lower Jurassic)

Ardicli formation

The oldest formation in the field consists of dolomite, limestone and dolomitic limestone. In general dolomites are common in the lower levels of the formation whereas limestones dominate the upper levels. The middle section of the formation comprises alternations of dolomite, dolomitic limestone and

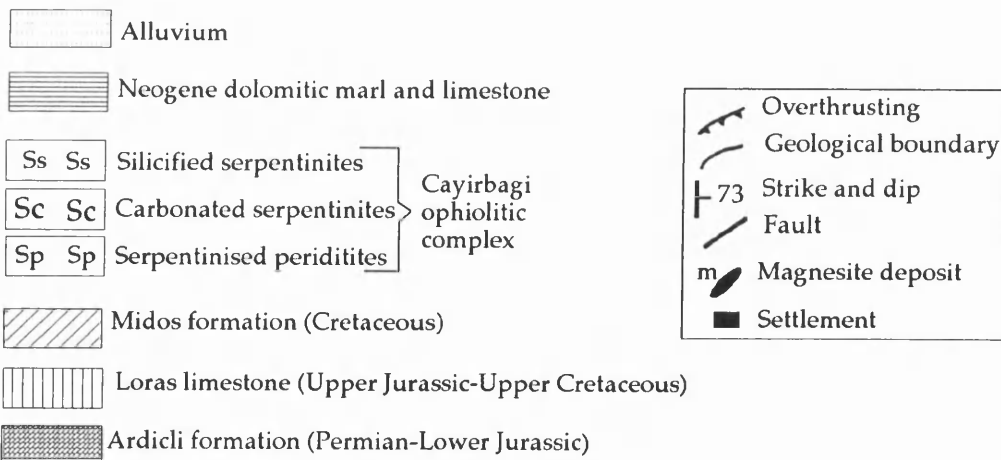
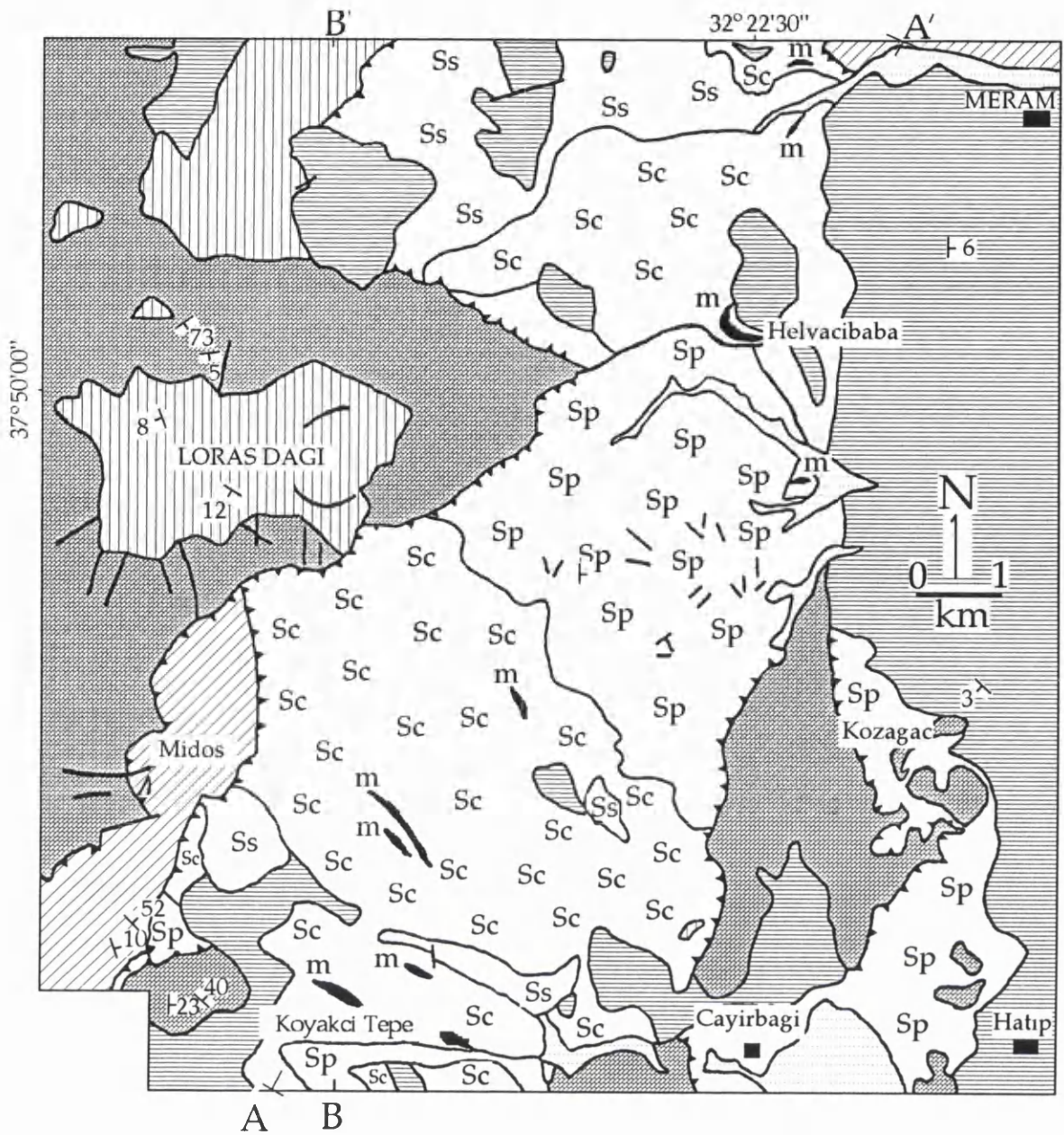


Figure 2.2. Geological map of the Meram-Cayirbagi area, Konya, Turkey, made by the author and based on 1:25,000 Ilgin-Konya sheet. Note A-A' and B-B' are the sections and shown in figure 2.5.

limestone (Figure 2.3). The limestones are dark grey and are laminated. Calcite veins 1-5 cm wide are common and may be up to one metre long.

In thin section, microsparite, sparite, micrite, ooliths, fossils, intraclasts and pellets are observed. These constituents are present in the following quantities: Pellets 65-70%, micrite 10-15%, ooliths 10-15% and fossil remains 8-10%. The ooliths have silicic seeds. According to Folk's (1962) classification this rock is an oopelmicrite. Stylolites are often well developed in these rocks.

The formation is around 600 m thick and is thin to medium bedded. No characteristic fossils could be found in the formation from microscopic examination or field study but several have been reported by Gormus (1984), i.e. *Hemigordius sp.*, *Fronicularia sp.*, *Thaumatoporella sp.*, *Favreina sp.* Gormus (1984) using this data, estimates the age of this formation as spanning the Permian to the Lower Jurassic. Gormus has also indicated that the oldest strata in the formation were deposited in reef facies, but later sequences were laid down in a gradually deepening basin.

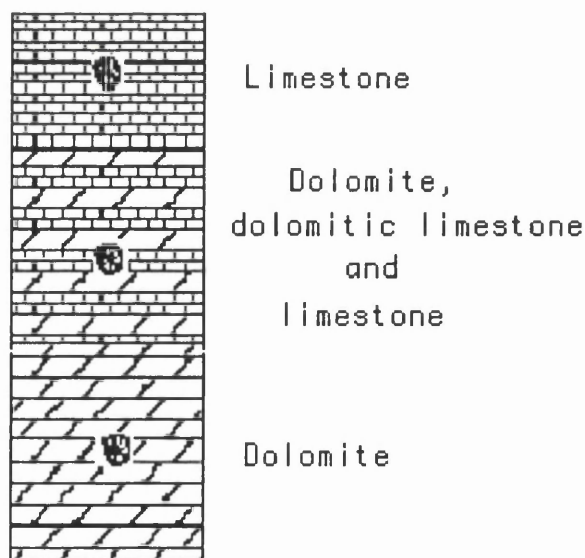


Figure 2.3. Stratigraphic section portraying the relationship between the lithologies of the Ardicli formation.

Loras limestone

The limestone, which is about 100 metres thick, is lighter in colour than the Ardicli formation. Limestones at the base of the Loras are gray coloured but get progressively lighter towards the top. The formation is marked on the surface by karstic features such as dolines which are 1-2 m deep and 5-6 m wide. The limestones are flat lying and medium to thick bedded.

Pellets, ooliths and intraclasts are observed in thin section. According to Folk (1962) such rock types may be termed peloointrasparrite, whereas according to Gormus (1984), the rock is a globotruncana-rich biomicrite.

Gormus (1984) has found the following fossils i.e.: *Fronidularia sp.*, *Thaumatoporella sp.*, *Globotruncana tricarinate*, *Globotruncana cf. elevata*, *Globotruncana cf. arca*, *Globotruncana linneiana*, *Globotruncana sp.*, and estimated an Upper Jurassic-Upper Cretaceous age for the Loras Limestone.

Midos formation

The rocks belonging to this formation within the study area are slightly recrystallised limestones, calc-schists, reddish limestones and reddish-grey quartzite. These rocks have been slightly metamorphosed (low temperature/low pressure).

In some places up to 44 % wt haematite occurs within the quartzites. These high levels of iron oxide have caused the red colour seen on the plain. Iron oxide values decrease towards the top of the formation perhaps indicating a deepening of the sedimentary basin. Some of the oxidation may be of

framboidal pyrite which usually develops in anaerobic deep marine environments.

Cayirbagi ophiolites

The Cayirbagi ophiolites take their name from Cayirbagi Village where there are extensive outcrops of the ophiolite (Figure 2.2). These ophiolites overlie the Mesozoic and Palaeozoic carbonates as a result of overthrusting events which took place over much of Turkey during the Upper Cretaceous. It is very probable that these overthrusting events caused the development of suitable tectonic conditions for the formation of cryptocrystalline magnesite deposits seen in much of Turkey. These ophiolites contain olistoliths which are usually composed of limestone blocks 200 m long, 200 m wide and perhaps not more than 100 m thick. They show sharp boundaries with the surrounding serpentinite.

The ophiolites in the area can be divided into three types as follows:-

Serpentinised peridotites, carbonated serpentinites and silicified serpentinites.

Serpentinised peridotites : Serpentinised peridotites are present at the base of the series. These serpentinites range from black, through dark green, green, grey to light green. The rocks are strongly fractured in a variety of trends. The main minerals present in the rocks are; chrysotile, lizardite, quartz, clay, calcite, forsterite and chlorite. In places thin magnesite veins are found within the serpentinised peridotites (Plate 2.1).

Carbonated serpentinites : These serpentinites, which occur in the middle and upper parts of the sequence, are host to the vein and stockwork magnesites (Plate 2.2). The carbonated serpentinites comprise approximately 20% of the

outcrops. The carbonated serpentinites are usually yellow and very soft and friable. The contacts between the carbonated serpentinites and serpentinitised peridotites are transitional. On the other hand, the contacts between magnesite veins and host-rock serpentinites are usually sharp. Chrysotile and lizardite are the common minerals in the host-rock. Chromite veins (2 metres long, 0.5 metres wide) are found within the rock in one locality, ~2km northwest of Koyakci Tepe magnesite deposits. These chromites may contain up to ~50% Cr_2O_3 .

Silicified serpentinites : This rock type often occurs at the top of the serpentinite sequences (Plate 2.3). For instance, the Helvacibaba magnesite deposit occupies silicified serpentinite as well as serpentinitised peridotite and carbonated serpentinite. However, silicified serpentinite is absent at the Koyakci Tepe open cast magnesite deposit although there is a silica cap over the smaller vein type deposit close to the Koyakci Tepe.

These "silica cap" rocks range from light green to light brown and are up to 3 metres thick. The predominant mineral found is quartz with minor occurrences of jasper.

The relationship between the three types of serpentinite is shown in figure 2.4.

Neogene dolomitic marls, limestones and alluvium

The marls are known as limestone by the local geologists, but XRD determinations reveal that dolomite is the predominant mineral in the rock at the top of the Helvacibaba opencast. We therefore refer to these rocks as Neogene dolomitic marl. It is probably these lacustrine sediments have been

influenced by magnesium-rich fluids. However, the Neogene is generally represented by flat lying limestones in the region. Between the serpentinites and the overlying Neogene there are some conglomeratic layers (up to 3 metres thickness) containing detrital magnesite pebbles. The alluvium is mainly made of fragments of the surrounding rocks such as ultramafics, limestone, dolomite and quartzite.

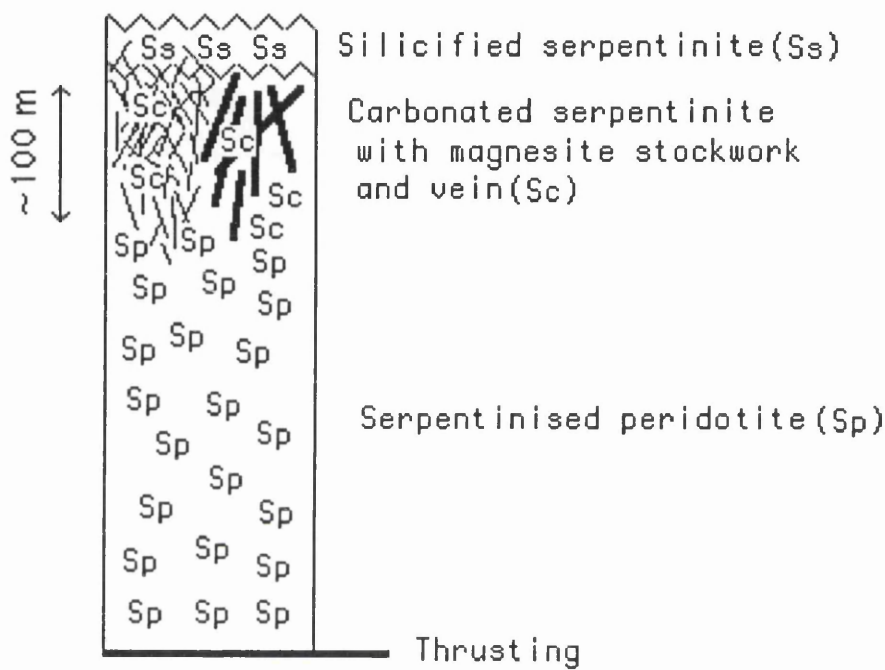


Figure 2.4. Sketch of relationship between serpentinitised peridotite, carbonated serpentinite and silicified serpentinite (Silica cap) at Konya (Turkey).

The overall stratigraphic relationships between the rock units seen in the Cayirbagi-Meram (Konya) area are shown in figures 2.5 and figure 2.6.

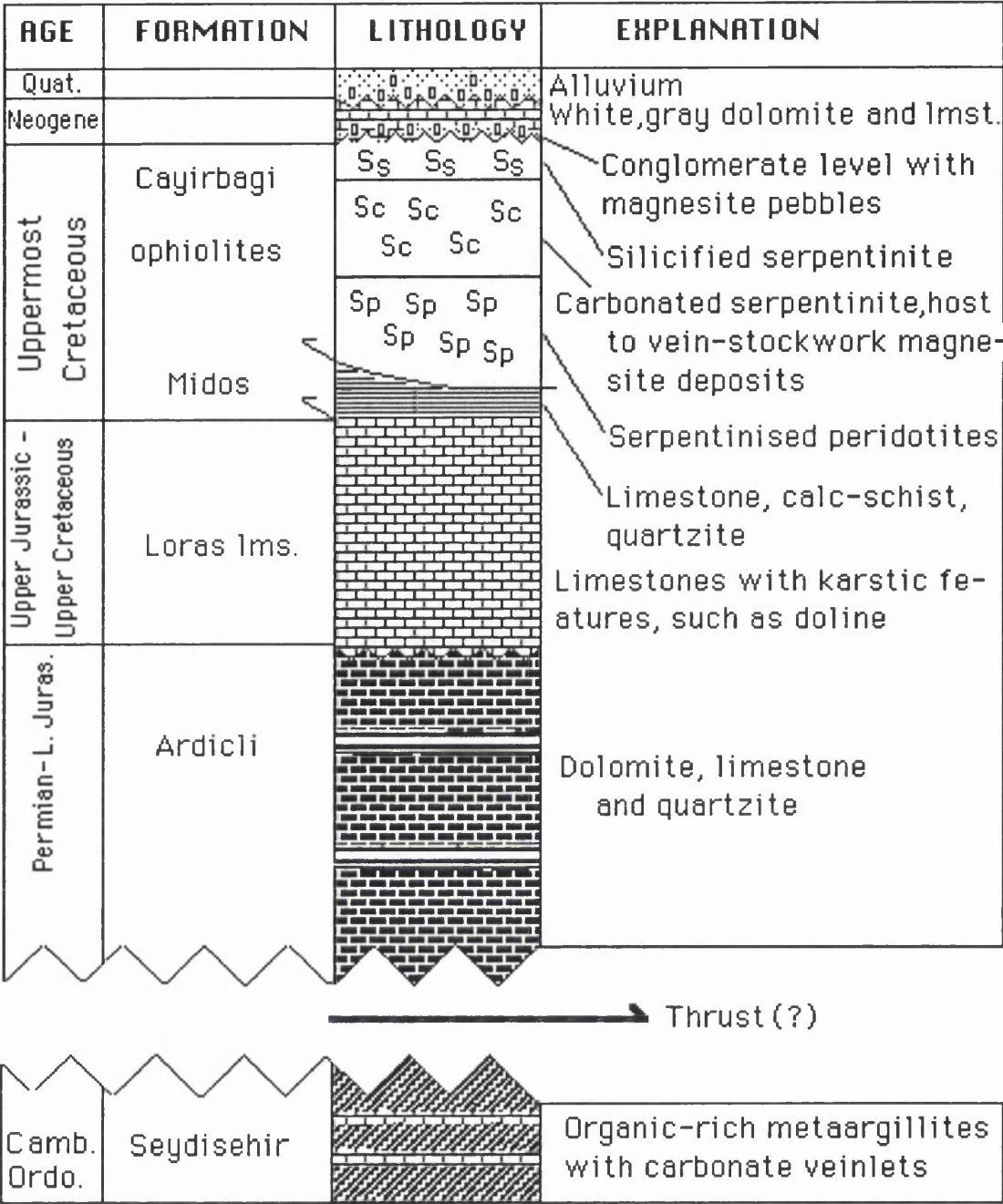


Figure 2.5. The stratigraphic relationships between rock units in the Konya district.

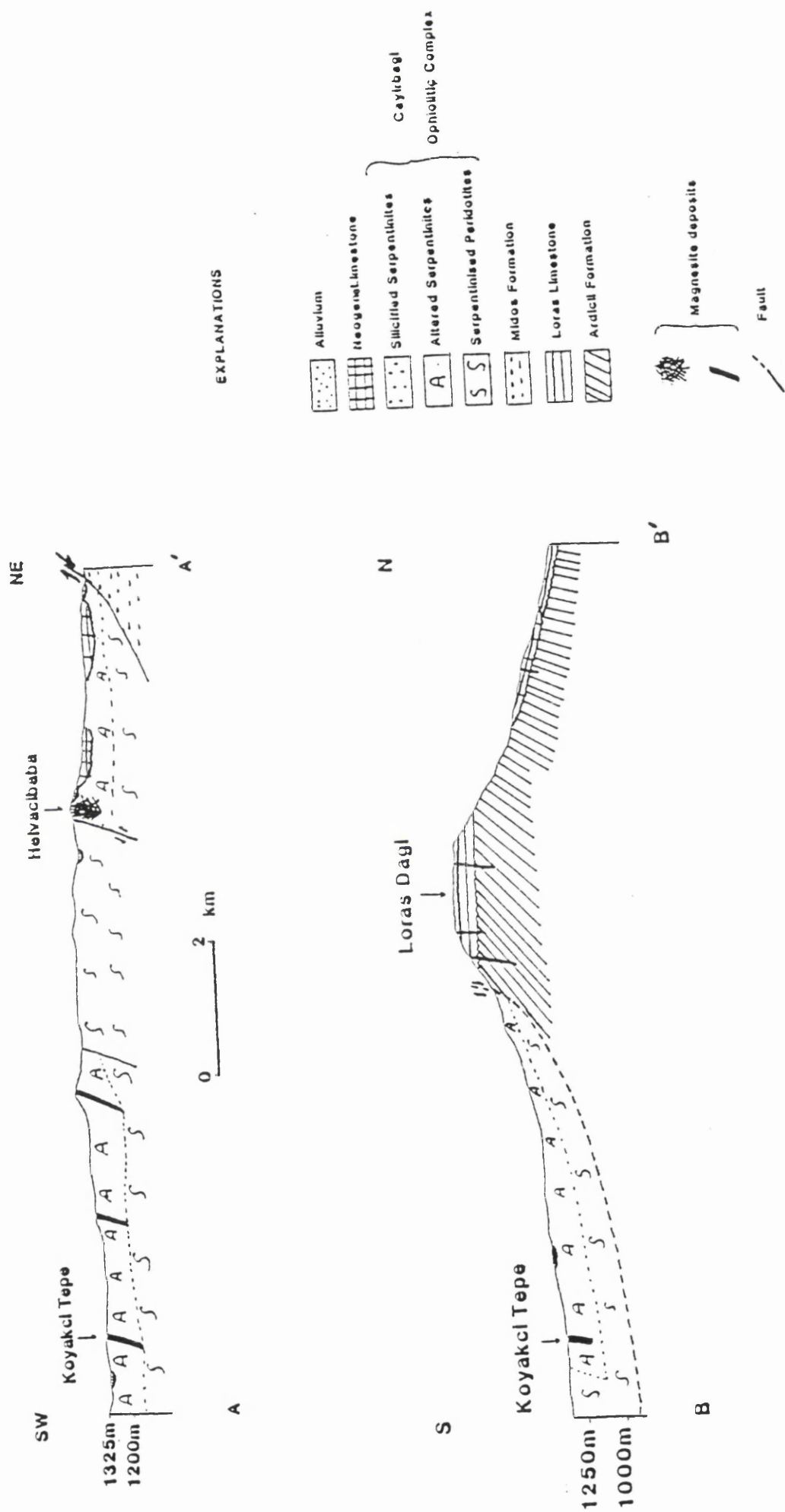


Figure 2.5. Geological cross-sections of the Meram-Cayirbagi area, Konya (Refer to fig. 2.2).

2.1.2. ECONOMIC SIGNIFICANCE OF THE KONYA MAGNESITE DEPOSITS

In Konya there are five major cryptocrystalline, vein-stockwork type magnesite deposits. Helvacibaba (Figure 3.1, location 14a), Koyakci Tepe (14b), Kozagac (14c), Sodur (14f) and Yunak (14d). Helvacibaba and Koyakci Tepe magnesite deposits are especially important because they are the largest orebodies. Although the magnesite market has been depressed by cheap Chinese and Indian exports over the last two or three years, after borax magnesite is the second most important ore exported from Turkey (Kendall, 1993).

2.1.3. MINERALOGY OF THE MAGNESITE DEPOSITS

Magnesite is the predominant mineral in these deposits, accompanied by small amounts of cryptocrystalline quartz (up to 6%). Such levels of quartz give rise to problems during factory processing and as a result of this, the deposit in Helvacibaba is no longer worked. The economic threshold is 5% SiO₂.

The magnesite is generally snowy white with rare light yellow developments. It is massive with a porcellaneous lustre and conchoidal fracture. The cryptocrystalline magnesites occur as veins (Koyakci Tepe, Sodur) and stockworks (Helvacibaba, Kozagac, Yunak), in the serpentinites. Small amounts of calcium, iron and manganese may also be present in the magnesites. The Helvacibaba silica cap is especially notable in terms of iron. Iron is represented as haematite in the silica cap which overlies the stockwork magnesite deposits at Meram-Cayirbagi area, Konya.

2.1.4. DESCRIPTION OF THE DEPOSITS

There are two open pits in the Meram-Cayirbagi magnesite field; Helvacibaba (Figure 3.1, location 14a), a giant (Plate 2.4) is in the north-east and the smaller Koyakci Tepe (14b) is in the south-west. The Kozagac (14c) magnesite deposits just a few hundred metres from the Helvacibaba pit have yet to be worked. Magnesite veins at Helvacibaba are usually between 20 and 50 centimetres wide whereas the veins at Koyakci Tepe could reach a thickness of up to 4 metres. As mentioned previously, carbonated serpentinite is the main host rock. Serpentinised peridotites below the magnesite deposits contain small unworkable amounts of magnesite (Plate 2.1). Silicified serpentinites, which comprise brecciated, porous, vuggy silica, are found above the Helvacibaba deposit (Plate 2.5).

The exposed magnesite veins and stockworks show little sign of having been faulted. Contacts between magnesite veins and the host rock are sharp but irregular, so making complete recovery of the ore difficult. Individual veins may be over 600m long. On some of the magnesite surfaces, shrinkage structures occur as a result of desiccation implying that some of the initial precipitate was a hydrated colloid (Plate 2.6). The magnesite orebodies of both Helvacibaba and Koyakci Tepe extend to approximately 110 m depth.

2.2. SEYDISEHIR SHALES

The shales are described in detail by Termier and Monod (1978). According to these authors the formation is best exposed at Caltepe and surrounding area, between Seydisehir and Beysehir. We visited this place in the summer of 1992. Our intention was to investigate a possible carboxyl source for

carbon dioxide for the cryptocrystalline, stockwork-vein type of Konya magnesite deposits.

Termier and Monod (1978) demonstrated that the formation consists of a 50 m thick sequence of yellow shales containing *Paradoxides* (Middle Cambrian) and a more than 1000 m thick shale sequence which yields the Lower Ordovician trilobites, *Neseuretus*, *Colpocoryphe*, *Thaihungshania* and *Geragnostus*. They also indicated that small limestone lenses in the lower parts of this thick sequence contain a fauna of Lower Ordovician aspect including *Euloma cf. laticeps*, *Nileus sp.* and *Conotreta sp.*, although they stated that the first two fossils have already been identified by Dean (1971).

In our observations ~1 km south of Caltepe (Plate 2.7) we have seen that the Caltepe limestone of Cambrian age is overthrust or overturned upon the younger Ordovician Seydisehir shales (A cross-section inserted in figure 2.1) which contain organic-rich metaargillites.

2.3. ARAPOMER DERESI MAGNESITE DEPOSIT

This cryptocrystalline, stockwork type deposit is situated ~13 km north-west of Salda lake. The magnesite stockwork stands proud of the surrounding carbonated serpentinites and its top is extensively silicified (Plate 2.8). Even the magnesite is intensively altered (Plate 2.9). With the guidance of Ahmet Koc of Duden village, it was established that the area is certainly in a different watershed from Salda lake. This is why, despite some detrital magnesite transportation in the streams around the deposit, this cannot, in spite of the views of Schmid (1987), reach Salda lake.

The deposit was mined between 1984 and 1986; 100 tons of ore were taken. The deposit is ~200m long, ~150m wide and at least ~30m deep, and therefore contains more than a million tons of magnesite. Mining has been discontinued owing to the high cost of transportation.

2.4. HIRSIZDERE MAGNESITE DEPOSIT

We interpret this deposit as located on the western margin of a former lake in the Acigol basin. The lake still survives in the deeper part of this basin.

At least five magnesite beds occur over carbonated serpentinites. Neogene lacustrine sediments (marl, dolomite, limestone, conglomerate) alternate with magnesite beds (Plate 2.10). The grade of magnesite gradually decreases upwards and the contact between the magnesite beds and the lacustrine sediment is occupied by conglomerate mainly made of serpentinite sand and pebbles (Plate 2.11). The magnesite beds are up to 4 metres thick, and can be traced 3 km broadly from west to east. The beds usually dip 15° north-east. According to Sancar (1982), the lake sediments are Pliocene and contain a minimum of some 450,000 tons reserves.

2.5. SALDA LAKE

2.5.1. Geological environment of Salda lake

An intermontane deep (~200 metres) lake, Salda lake is situated northwest of the small town of Yesilova (Plate 2.12) in the Turkish Lake District. The surface area of the lake is ~45 km². Most of the coast is ringed by ultramafic

rocks, but Cretaceous limestones outcrop south-east of the lake. Alluvium covers significant portions of the low-lying ground around the lake (Figure 2.7).

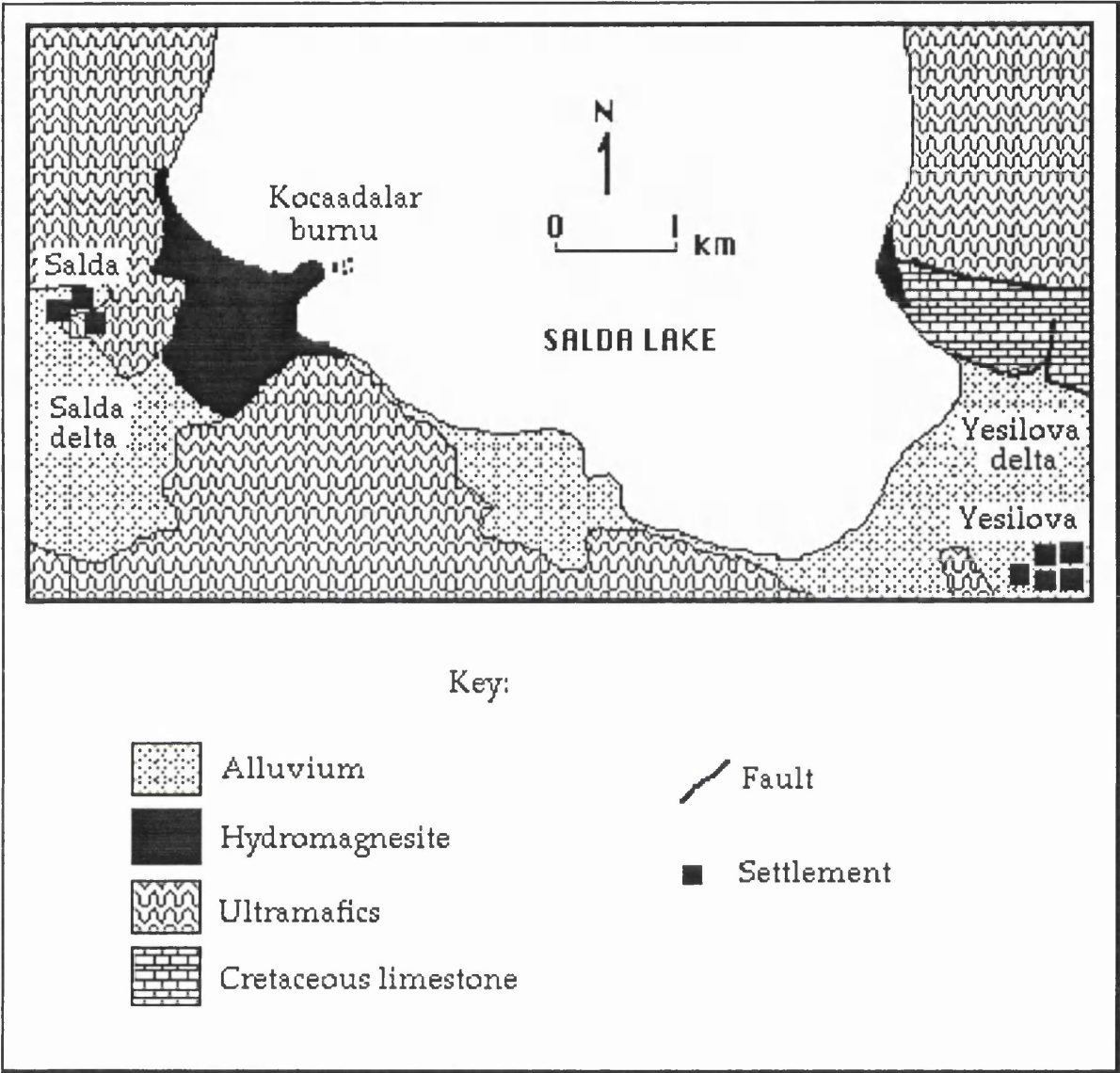


Figure 2.7. General geological map of south of Salda lake and surrounding area.

No detailed mapping of the area has been undertaken in this study. Doyen (pers. commun.) has subdivided the ultramafic rocks in Tefenni close to Yesilova into several rock types. He has recognised tectonites, cumulates, an ophiolitic melange, and volcanics. Tectonites and cumulates are composed of

harzburgite, dunite, gabbro, and troctolite, with a considerable volume of chromite deposits. In places, some listwaenitisation has been reported at the contacts of between olistolithic limestones and tectonite and/or cumulate (Karaman, 1987). Karaman (ibid.) has pointed out serpentine, radiolarite, mudstone, sandstone and limestone as components of the ophiolitic melange. He also suggested that the volcanics have been affected by low P/T metamorphism (green-schist and zeolite facies).

The area is tectonically and hydrothermally active. South-western Turkey has seen several recent earthquakes the whole of the western part of the country is often shown as a seismologically active area on maps (for example, Jackson and McKenzie, 1984; Bolt, 1993). The biggest geothermal energy areas of Turkey are also in this region at Kizildere-Denizli, Aydin and Izmir. The temperature of water-steam in these emissions varies from 90-200°C with a pH of about 9.5 (Ayhan, pers. commun.).

The presently forming hydromagnesite $Mg_4(CO_3)_3(OH)_2 \cdot 3H_2O$ deposits in Salda lake and along its shore present us with the best opportunity since the study of sedimentary magnesite deposits began to ascertain their origin. Because of this I would like to emphasise its climatic, hydrogeological and biological as well as its geological characteristics.

2.5.2. Climate and hydrogeological conditions

Salda lake is geographically situated in a district which includes about 20 natural and artificial water bodies. The climate is predominantly Mediterranean although it is a fraction cooler than the Mediterranean coastal areas. According to data at hand evaporation rates gradually increase from July

to October (Appendix-1 and figure 2.8). The most rainfall is in the winter months (December, January, February) (Appendix-2 and figure 2.9). The temperature of the lake water varies between 22-36°C on the surface but is generally about 24-25°C in August. High temperatures (36°C) were recorded in relatively shallow areas such as the margins of Yesilova delta, while the lower values (22°C) were measured 2-3 metres deep in the water. However, the temperature drops abruptly (from ~25 to ~22°C) within a few metres of the surface.

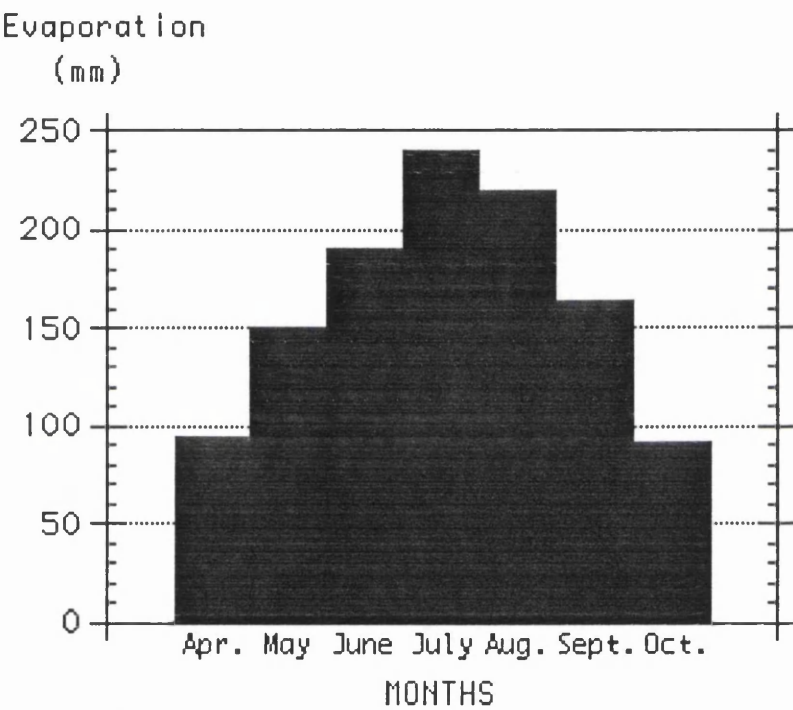


Figure 2.8. Histogram of average monthly (From 1971 to 1988) evaporation rates of Salda lake and surrounding area. Note date base: Turkish Meteorology Office.

Many of the lakes close to Salda have dried up in the past 10-20 years. Akgol is a good example of these (Plate 2.13), and Kurugol and Acigol are among the others. The possible reason for this could be global warming (the Greenhouse effect) and there is apparently no irrigation around these dried lakes. However, Salda lake survives despite intensive irrigation from ground

water. There are at least 200 irrigation wells in the ground south-east of the lake alone and this has resulted in a visible fall of lake level. There is no significant surface inflow to Salda lake except for a relatively large spring in the south. Discharge of this spring is about 8 l/s. There is no outflow. The lake is apparently being recharged by hydrothermal and/or ground water inflow. The pH of this inflowing water is probably higher than that of the overall lake water. The pH of the lake water is about 9-9.5 in August whilst it reaches about 10-10.5 in early October, since at this time the lake is being fed relatively more by these hydrothermal and/or ground water sources. The water table in the region reaches the lowest level in early October. However, the pH of ground water averages 8.6 (Table 4.4.2) in the region, thus, the pH of the hydrothermal water is very probably more effective than the ground water in increasing the pH values of the lake water.

Our observations indicate at least six deltas around the lake. Three of these are large, greater than about 2x2 km² each. These are: in the south-east (north-west of the town of Yesilova), in the south-west (south of the small town of Salda) (Plate 2.14) and in the north (south of Doganbaba village). Usually rounded serpentinite and gabbro pebbles (up to 10 cm) are the most abundant constituents of these deltas. Intensive surficial weathering can be seen on these pebbles.

2.5.3. Biological conditions

Generally pine trees cover the moderately low hills around lake but the high ground is bare. Some grain and vegetables are grown on the relatively flat areas, for example on the deltas. Small fish (and a few notable large ones) and frogs have been seen in the lake. Some shallow areas are carpeted with an

unidentified spiky green weed. Together these form the macrobiota. Cyanobacteria and diatoms form the microbial biota. Also it is probable that precipitation of stromatolitic hydromagnesite is caused by cyanobacterial growth.

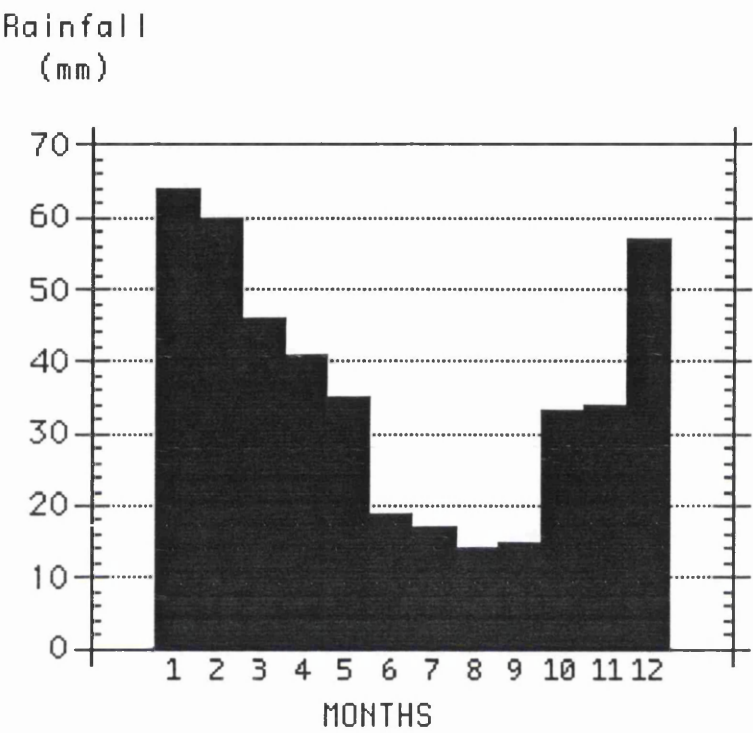


Figure 2.9. Average monthly (From 1971 to 1988) rainfall around Salda lake.

Key:-

1:January	5:May	9:September
2:February	6:June	10:October
3:March	7:July	11:November
4:April	8:August	12:December

Note data base: Turkish Meteorology Office.

2.5.4. Hydromagnesite deposits

Extensive hydromagnesite deposits can be seen in two localities; south-east and south-west of the lake (Figure 2.7), although stromatolitic hydromagnesite occurs all around Salda lake. The locality to the south-west, at Kocaadalar burnu, is about 5 metres thick (Plate 2.15) and is the most important. The deposit at Kocaadalar burnu has a large reserve whilst that to the south-east has a limited reserve (Table 2.1). In both occurrences, the range of deposits is almost identical: living stromatolites (made of hydromagnesite) in the shallow (up to 8 metres deep) lake water with mainly hydromagnesite sands. Older stromatolite boulders are present in the beach and finally the deposits form terraces (Figure 2.10). No inorganic precipitation or discernible magnesite veins as Schmid (1987) previously described for Salda lake hydromagnesite deposits have been identified. Even in small pools (on the beach) 2-3 metres in diameter, and 5-10 centimetres deep and with relatively high temperatures (for example 36°C), in which inorganic precipitation might be expected, there was no sign of abiogenic precipitation.

Table 2.1. Reserves of the two distinguishable hydromagnesite deposits in Salda*.

Deposit	Surface area (m ²)	Thickness (m)	Volume (m ³)	Reserve (Tonnes)
Kocaadalar burnu	1.5 x10 ⁶	5	7.5 x10 ⁶	15 x10 ⁶
SE of Salda lake (No specific name)	5000	7	35,000	70,000

*Numbers are approximate and the relative density of the hydromagnesite assumed to be ~2.

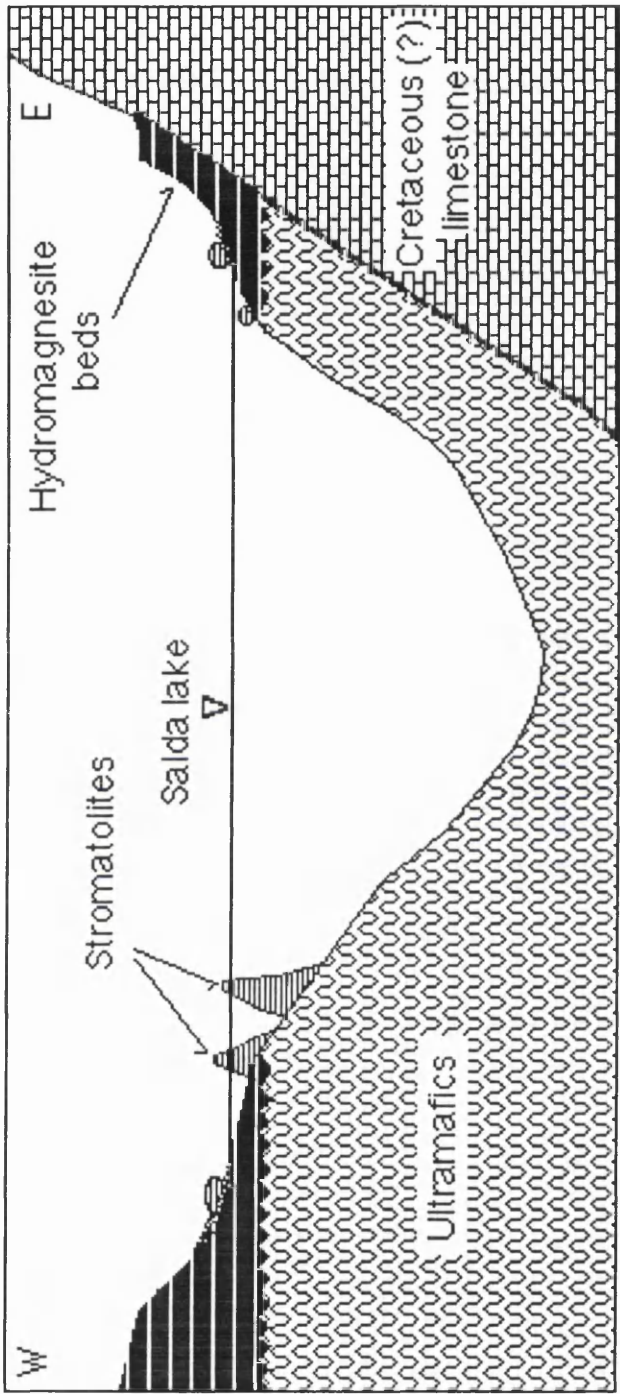


Figure 2.10. Relationships between stromatolites, hydromagnesite beds and hydromagnesite boulders at Saida lake. Note that the vertical scale is exaggerated.

Waves are causing re-distribution of the stromatolitic hydromagnesite. Transportation on the beach is extremely fast. About 5 mm sized particle could be transported 20 cm/min by small wave movements on a calm day. Thus when precipitation and subsequently alteration are established, transportation and (re)deposition could easily occur in topographically suitable places such as Kocaadalar burnu. These processes could destroy any trace of the organic nature of the precipitation. The hydromagnesites in the deposits are generally porous and friable. Layering is obvious with alternating hydromagnesite and blackish ultramafic rock particle dominated laminae in some places .

2.5.5. Stromatolites

As noted, stromatolites can be seen all around the lake, in either shallow or deeper water (between 0 and 8 metres). We could not dive in the deeper water due to lack of equipment. Stromatolites can start to grow on pebbles, boulders, branches of trees or even on root tussocks of a marram-like grass (Plate 2.16). Small islands ~20 metres in diameter in the lake are entirely made of stromatolite. Some five islands have been observed in the south-west of the lake, and one in the north-west (Plate 2.17). These islands are 2-3 metres above the present lake level. According to local people these islands were covered by water only five years ago. If this is true the lake level must have fallen 2-3 metres in recent years. In most parts of the lake there are stromatolite clusters which resemble the "coral gardens" of some reef environment. The largest observed stromatolite rises about 5 metres above the lake floor.

The surface of the stromatolites is cauliflower-like (botryoidal) and porous (Plate 2.18). When it is cut vertically the internal lamination can easily be seen (Plate 2.19). Details of microscopic structure are given in section 4.6.

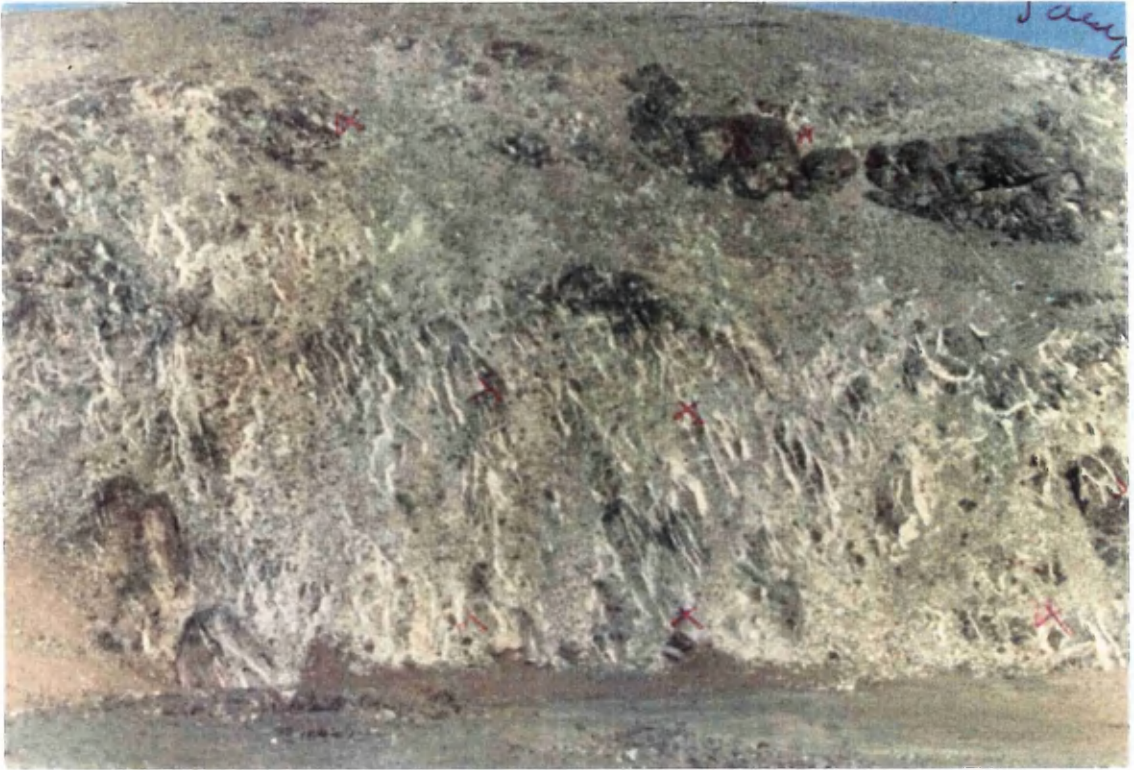


Plate 2.1. Thin magnesite veins (white) in the serpentinised peridotites, south-east Koyakci Tepe: width of picture is ~30 m.



Plate 2.2. Carbonated serpentinites as host rock to the stockwork magnesites at Helvacibaba open pit.

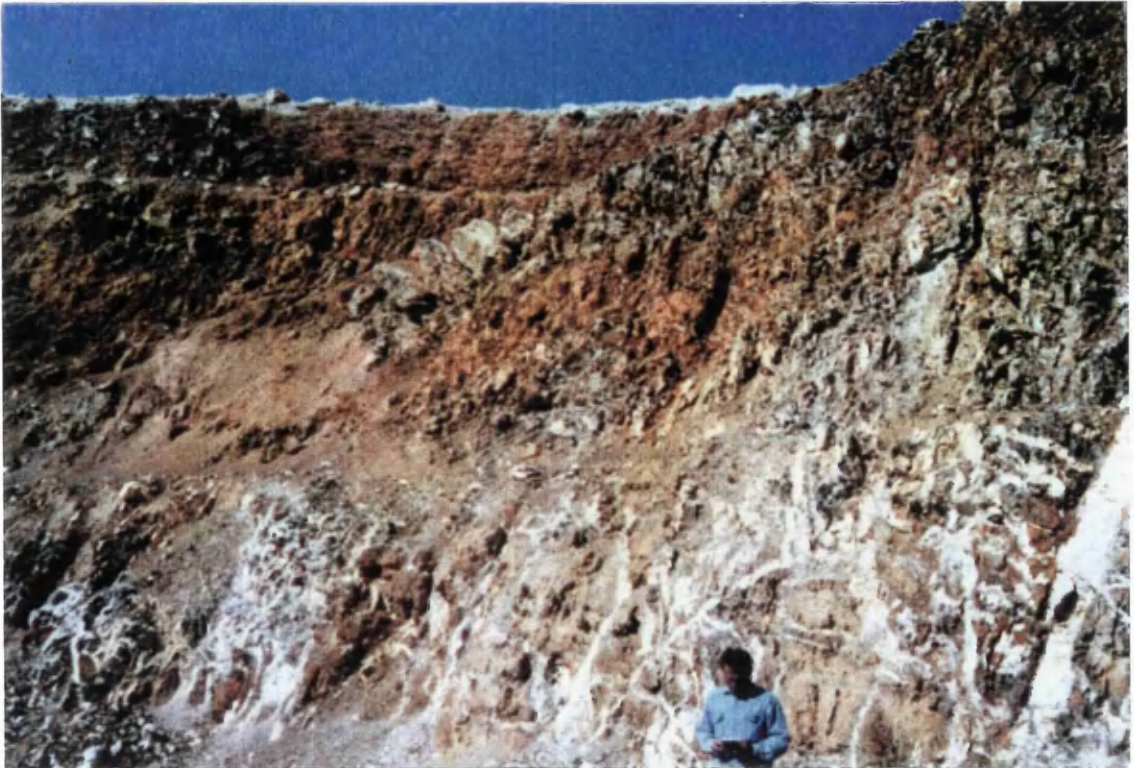


Plate 2.3. Haematite bearing silicified serpentinites (brown parts of the picture) over the stockwork magnesites (white) at Helvacibaba (Konya).

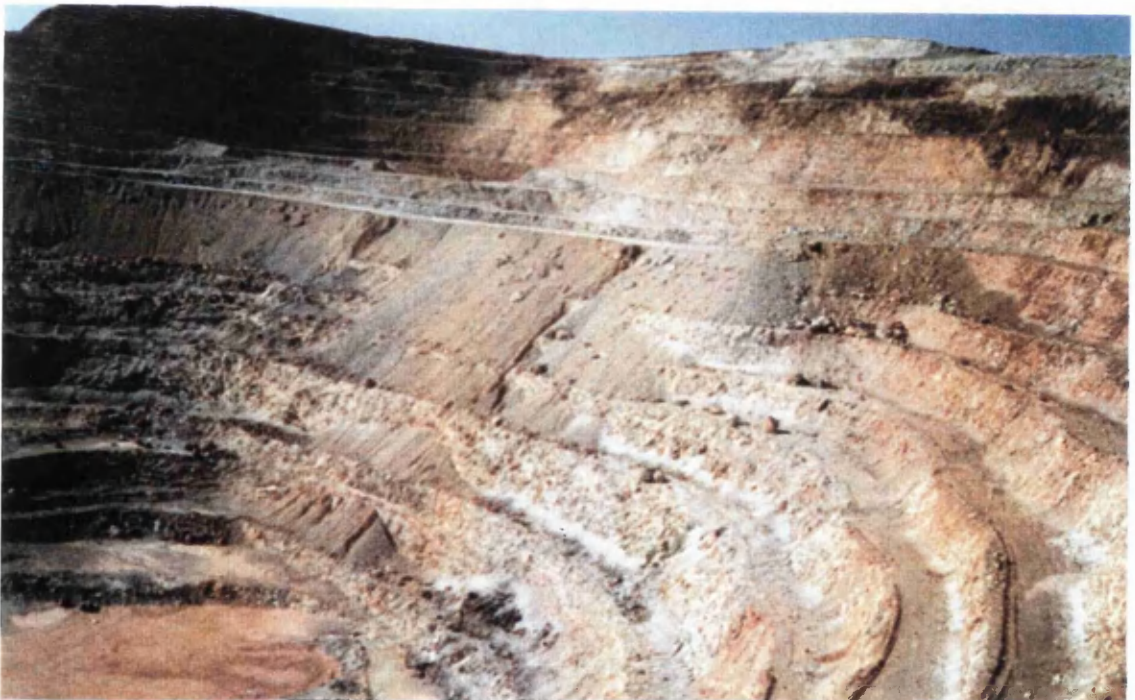


Plate 2.4. Helvacibaba open pit mine. Dark brown portions near the surface of the pit are predominantly silicified serpentinite, (looking NE).



Plate 2.5. Brecciated, porous and vuggy silicified texture at the top of the Helvacibaba stockwork magnesite deposit.



Plate 2.6. Shrinkage structure on the magnesite vein interior surface.



Plate 2.7. Caltepe limestones (white) outcrop on the top of two small hills, with underlying organic-rich meta-argillites (pale green). Photo taken ~1 km south of Caltepe, view looking north.



Plate 2.8. Silicified serpentinite at the top of Arapomer Deresi magnesite deposit.



Plate 2.9. Extensively altered loose magnesite (white) at Arapomer Deresi.
The brown colour at the back of the picture is silicified serpentinite.



Plate 2.10. Hirsizdere sedimentary magnesite beds (white) and alternating lacustrine sediments.



Plate 2.11. Conglomeratic level (pale green, brown serpentinite) at the bottom of magnesite bed (white) at Hirsizdere.



Plate 2.12. The town of Yesilova (Burdur), the Yesilova delta and the Salda lake. Cretaceous limestones (white-gray) exposed at the high ground (right side of the picture) and hydromagnesite in the distance.



Plate 2.13. Completely dried lake Akgol, 8 miles north-east of Salda lake, looking east.



Plate 2.14. Salda delta (plain ground) found in the south of Salda village (middle left side of the picture). The hydromagnesites (in the middle of the picture) are white coloured.



Plate 2.15. Hydromagnesite deposit at Kocaadalar burnu, south-west Salda lake. View from west to east.



Plate 2.16. Stromatolite on a marram-like grass. Scale is 50 cm.



Plate 2.17. Stromatolitic hydromagnesite island in the north-west of the Salda lake.



Plate 2.18. Porous, cauliflower-like structure of stromatolite.



Plate 2.19. Internally laminated structure of the stromatolite.

CHAPTER THREE

SAMPLING AND ANALYTICAL TECHNIQUES

This chapter concerns sample sites in southwestern Turkey as well as the analytical methods. Statistics are also considered.

3.1. SAMPLING

A total of 151 outcrop samples (mainly magnesite, hydromagnesite, calcite, dolomite, quartzite and some ultramafic rocks) and 22 water samples were taken from the eight areas (Figure 3.1 and Table 3.1). Also two sedimentary magnesite samples were contributed from the Chad basin by Emeka Okafor (Nigeria, Africa). Some sampling was undertaken at Helvacibaba and Hirsizdere pits in order to test for any systematic variation of isotopic values with depth. Outcrop samples generally weighing 0.5-1 kg were collected using a ~1 kg hammer, and then stored in individual sealable plastic bags for transport to the laboratory. Water samples of wells, lake or streams were kept in sterilised plastic bottles. Stromatolite samples from Salda lake have been stored in plastic containers and about 20 ml lake water added in an attempt to keep the biota alive. The bottles were carefully sealed with nylon sheets.

Samples were analysed by X-Ray diffractometer (XRD), Scanning electron microscope (SEM), Atomic absorption spectrometry (AAS), Mass spectrometry (MS), Absorbent spectrometry (AS), Inductively coupled plasma-mass spectrometry (ICP-MS), and in thin sections by polarising microscope. The distribution of the samples analysed by each analytical tool has been summarised in table 3.2 and figure 3.2.

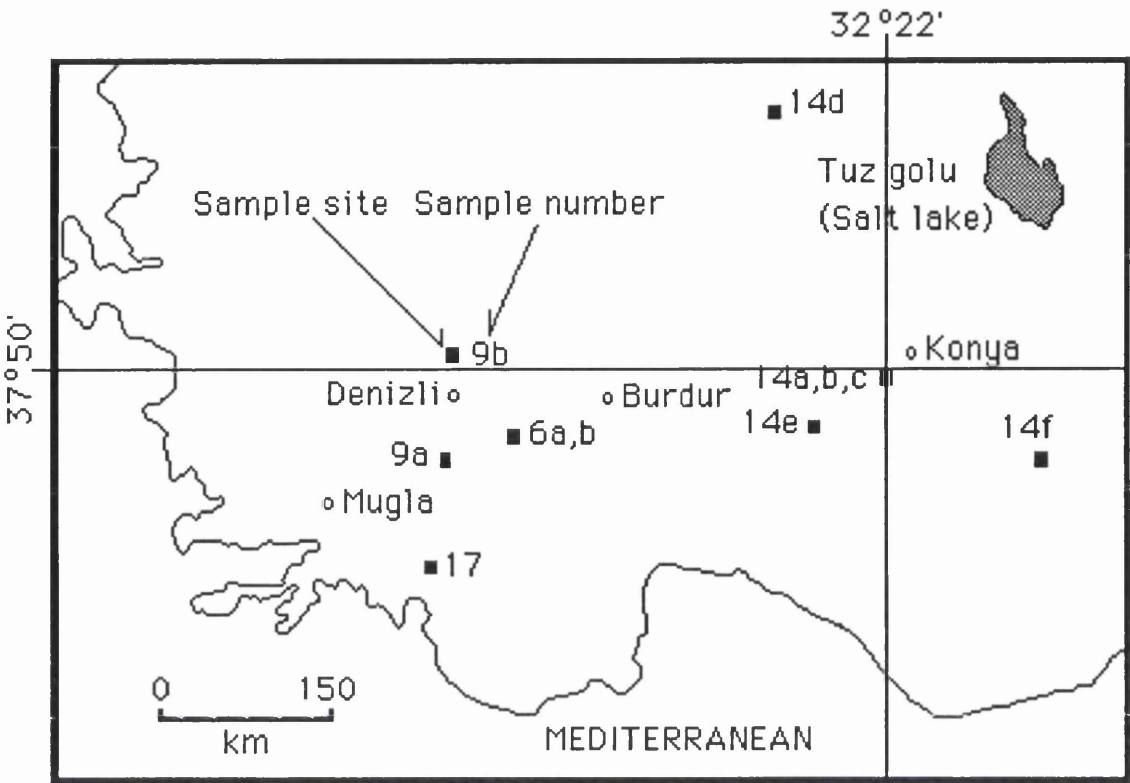


Figure 3.1. Location of sample areas in this study, for Key see table 3.1. Not shown is Tsakasimta, Nigeria.

Table 3.1. Sample distribution for each area in figure 3.1.

<u>Name of deposit</u>	<u>Province</u>	<u>Number of samples</u>
Helvacibaba	Konya (14a)	34
Koyakci Tepe	Konya (14b)	11
Helvacibaba and Koyakci Tepe	Konya	24
Kozagac	Konya (14c)	1
Yunak	Konya (14d)	2
Seydisehir	Konya (14e)	4
Sodur (Karaman)	Konya (14f)	2
Salda	Burdur (6a)	52
Arapomer Deresi	Burdur (6b)	4
Hirsizdere	Denizli (9a)	27
Pamukkale	Denizli (9b)	6
Kavakarasi Koyu	Mugla (17)	4
Tsakasimta	Chad basin (Nigeria)	2
		173

Table 3.2. Number of samples analysed using the particular analytical tools (except polarising microscope).

<u>Analytical tool</u>	<u>Analysed number of samples</u>
XRD	146
SEM	10
AAS	20
MS	139
AS	1
ICP-MS	16

As seen in table 3.2 and figure 3.2, XRD and mass spectrometry have been extensively used during my research.

3.2. ANALYTICAL TECHNIQUES

This section outlines the analytical procedures used in the collection of data from Turkey and Nigeria. All the analyses were carried out at the University of Glasgow excepting the isotopic studies, REE and some mineral separation. These were undertaken at the SURRC (Scottish Universities Research and Reactor Centre, East Kilbride).

3.2.1. Laboratory preparation of rock powders for analyses

Prior to crushing, the rocks were carefully washed in cold running water to avoid unwanted surface impurities such as dust and plant material. The rock was broken with a hydraulic rock splitter to fragments a few centimetres across which were further broken down in a jaw crusher. Then the resultant fragments

were passed through an adjustable roller crusher to produce rock particles less than 2 mm across. These particles were then pulverised in a tema mill to produce 100 mesh powder samples. Grinding by tema disc mill was only done for short lengths of time, usually less than 90 seconds. Long periods of grinding can have a destructive effect on carbonates because of the high temperature that can be realized during a long grinding time (Gray, 1986). Further grinding was continued in a ball mill to achive a 250 mesh sample powder.

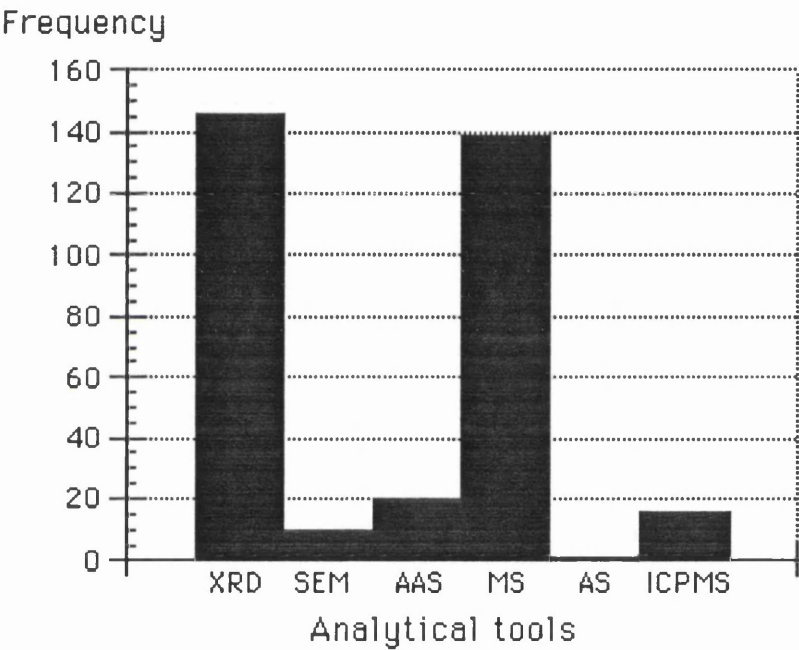


Figure 3.2. Frequency histogram of analytical tools and number of samples analysed in this study.

Cleaning of the jaw crusher and tema mill between crushing of each sample was by use of a stiff brush and warm water and, where necessary, acetone was also used. All of the powdered samples were dried in an oven at 100°C for at least 24 hours before use.

3.2.2. X-Ray diffraction (XRD) analyses

The standard and classical way of determining sample purity is by using a binocular microscope. However, this is not an ideal method as it may not reveal minor impurities which may have been introduced as intergrowths during carbonate mineralisation. The carbon and oxygen isotopic ratio analyses of these samples require at least 90 % purity of any one particular mineral (Fallick, pers. commun.). Some of the silica samples have been treated for one hour at 100°C in 10 % HCl acid to destroy any carbonate(s) in the sample. Thus samples of >95 % purity were produced and checked further by XRD. For XRD analyses about 0.03 g of material were mixed with 0.5 ml acetone and then poured on a glass slide which was dried and then inserted into the machine.

The XRD machine used was a Philips PW 1140 generator which powered a Philips PW 1050/35 goniometer. The generator was run at 36 kv and 20 mA. The goniometer was geared to run at 2 degrees (2θ) per minute. The goniometer was started at 4° and for most analyses was run through to about 60°. The determinations were made under the supervision of A. Hall, D. Turner and M. McLeod.

3.2.4. Scanning electron microscope (SEM) analyses

Some of the samples were prepared as (carbon coated) polished thin sections. Other samples were prepared by cementing a reasonably small sample (1-2 cm in diameter) on a metal stub which was later placed in the SEM analysing chamber. The cement used to fix these samples was silver paint. Once the cement was dry the sample was gold coated. This coating provides an electrically conductive film which allows the sample to be analysed.

The analyses were carried out on a Leica Cambridge Stereoscan 360 with an integrated link analytical AN10855 X-ray microanalyser under the supervision of P. Ainsworth.

3.2.5. Atomic absorption spectrometry (AAS) analyses

Twenty water samples from Salda lake and the surrounding area were analysed by AAS. The elements Mg, Ca, Na, Si, Fe and Ni were determined in order to better understand the relationship between the lake water and ground and surface waters. The water was analysed directly (without prior treatment) on a Thermo Jarrell Ash-Smith Hieftje 12 Atomic Absorption Spectrometry under the supervision of D. Turner.

3.2.6. Absorbance spectrometry (AS) analyses

This was used to determine the presence or otherwise of cyanobacteria in samples brought wet from Salda Lake.

About 0.2 g of sample were scraped from wet stromatolite and encouraged to grow in a culture medium BG-11+. The composition of BG-11+ is given in appendix-3. After about four weeks the growth of adequate bacteria was completed. The absorbance spectrometry of the bacteria was carried out on a Shimadzu uv-2101 PC spectrometer fitted with an Au integrating sphere (IRS-260) under the supervision of P. Dominy, Botany Department, Glasgow University.

3.2.7. Inductively coupled plasma-mass spectrometry (ICP-MS) analyses

Five ml of hydrofluoric acid (40 %) and the same amount of nitric acid (5 %) was added to 0.200g of sample in a clean "digestion bomb". The bomb was then carefully sealed and placed on a hot plate at 80°C for 24 hours. The bomb was then removed from the oven and allowed to cool for a reasonable time. The bomb was then carefully opened and placed on a hot plate (200°C) to evaporate the contents. When dry, 25 ml of 5 % nitric acid was added to the remains and heated (up to 80°C) to dissolve the residue. This solution was filtered (N42 paper) into a 100 ml volumetric flask and diluted to 100 ml with 5 % nitric acid and transferred to clean polypropylene bottles. The samples were analysed on a machine VG-Plasmaquad 2+ under the supervision of K. Sampson and T. Shimmield.

Notes: 1. It is important to ensure that all containers and pipettes used (for example glassware and polypropylene bottles) are very clean. This is achieved by soaking all apparatus in a clean glass vessel and rinsing with pure water before drying.

2. Two blanks were run in each analytical case using the same reagents and procedures but excluding a sample.

3. Some samples were run in duplicate to check method for the replication of the results.

5. Dilution factor= x500 for rock samples

x2 for water samples

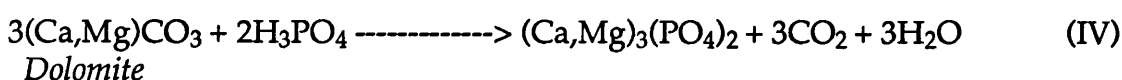
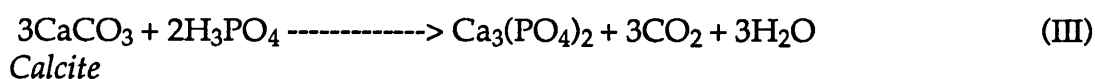
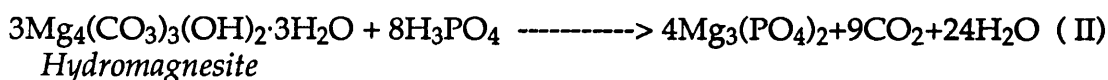
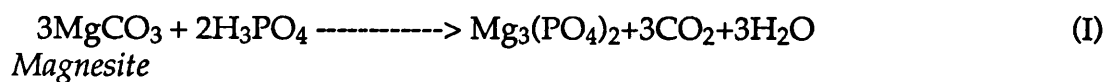
3.2.8. Stable isotope analyses on mass spectrometry (MS)

A sample of carbonate was weighed (10 to 15 mg for magnesite, 15 to 20 mg for calcite, dolomite and aragonite) and placed in a vial with approximately

5 ml of 103 % orthophosphoric acid, which is kept separate from the sample at this stage.

The air is then evacuated from the test tube by both low and high vacuum pumps until a good vacuum is obtained. The glass-tube with sample and acid are now placed in either a "hot bath" at 25°C (calcite and aragonite), or a "hot plate" at 100°C (magnesite, dolomite, hydromagnesite). Once the temperature has equilibrated the acid-carbonate reaction is initiated and left for a suitable amount of time, usually 17-18 hours to allow a reasonable amount of carbon dioxide to be produced. The CO₂ is then purified in the extraction line by McCrea's (1950) standard procedures and the yield was measured by an attached digital manometer. The method of extraction of CO₂ from the sample is shown in Figure 3.3. The ratios of ¹⁸O/¹⁶O and ¹³C/¹²C of the samples were analysed on a mass spectrometer (ISOGAS, SIRA-10 and ISOGAS, SIRA-2). This procedure runs with accuracies of ±0.1 ‰ for both elemental isotopes.

During the acid (H₃PO₄)-carbonate reaction (Reaction I, II, III and IV), the δ¹⁸O value of the released CO₂ is not a precise representation of the original carbonate mineral. For this reason δ¹⁸O values must be obtained by using "oxygen isotopic fractionation factor (10³lnα)" which is specific for each mineral. These factors are 9.29, 10.25, and 11.79 for magnesite, dolomite and calcite respectively (Rosenbaum and Sheppard, 1986). The same factor has been used for hydromagnesite and magnesite.



Oxygen isotopes in silicate minerals were analysed, as follows:

Oxygen was liberated from approximately 10mg samples of purified silicate minerals (quartz) by oxidation reaction with ClF_3 (Borthwick and Harmon, 1982) in nickel reaction vessels at 650°C . The oxygen was cleaned and reduced to CO_2 using a vacuum extraction line similar to that described by Clayton and Mayeda (1963). The oxygen yield was determined by comparing the starting weight of mineral with the number of micromoles of gas produced. A VG-SIRA 10 mass spectrometry was used to analyse the CO_2

The results are reported as delta values (δ) relative to SMOW and PDB standards.

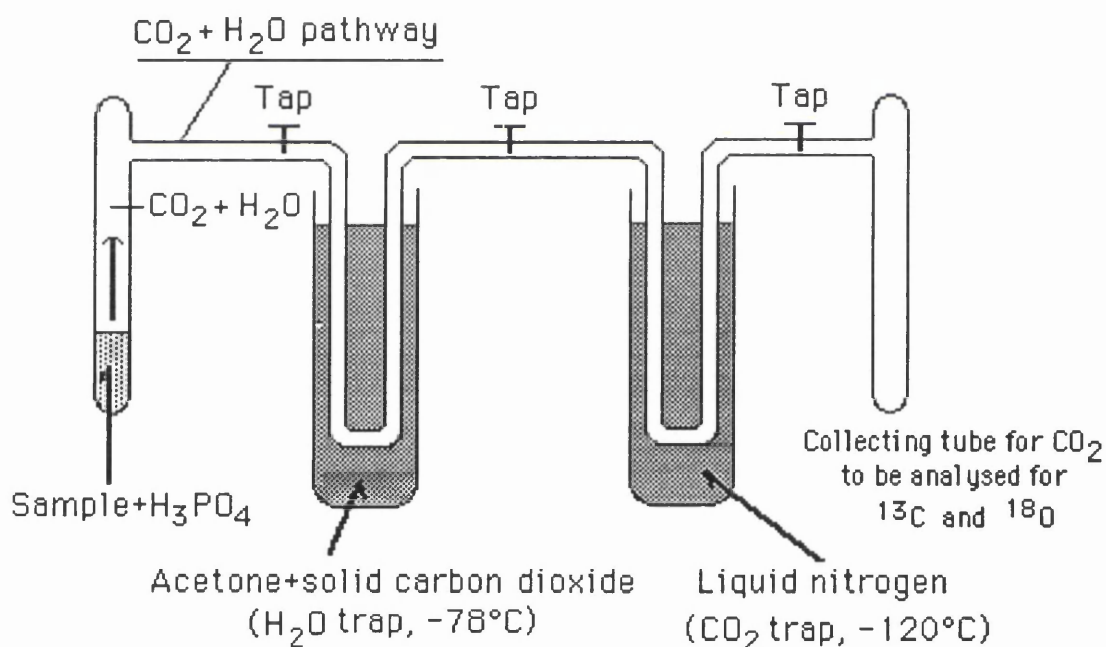


Figure 3.3. Simplified CO_2 extraction line.

CHAPTER FOUR

CARBON and OXYGEN ISOTOPES, REE, XRD, AAS, AS and SEM STUDIES: RESULTS

This chapter concerns the isotopes of carbon (^{13}C), oxygen (^{18}O), and deuterium (D), rare earth elements (REE), X-ray diffractometry (XRD), atomic absorbption spectrometry (AAS), absorbance spectrometry (AS) and scanning electron microscope (SEM) results.

4.1. CARBON and OXYGEN STABLE ISOTOPE RESULTS

Both carbon and oxygen isotope analyses were performed on 123 samples from the magnesites, hydromagnesites, calcites and dolomites from selected western Turkish carbonate deposits. In addition oxygen isotope analyses were done on fourteen quartzes and two water samples. Deuterium analyses have been also undertaken on two water samples.

Experimentally determined isotope data ($\delta^{13}\text{C}$ and $\delta^{18}\text{O}$) of 21 present-day hydromagnesite samples and one present-day aragonite, 6 hot-spring calcites, 27 hydrothermal-sedimentary magnesites, 29 stockwork and 13 vein magnesites and 19 other calcite and 7 dolomite samples, 14 quartzes and two water samples from western Turkey are presented in Table 4.1.1. The deuterium analyses of two water samples are also added on this table. Both $\delta^{13}\text{C}$ and $\delta^{18}\text{O}$ values are plotted on Figure 4.1.1. The results of $\delta^{13}\text{C}$ and $\delta^{18}\text{O}$ are clearly scattered but they do reveal two main trends, the one is a vertical trend roughly representing the sedimentary/hydrothermal stratabound

deposits; the other an oblique trend represents the vein-stockwork through sedimentary deposits. These two trends meet at the Salda lake's values (Figure 4.1.1).

The overall $\delta^{13}\text{C}$ values range from -20.0 to +7.2 ‰ relative to PDB whilst $\delta^{18}\text{O}$ values vary between +17.7 and 38.1 ‰ relative to SMOW. Each carbonate deposit has its own field (Figure 4.1.1) representing different types (or at least geographical areas) of deposition. As we have seen Western Turkey is host to a variety of carbonate deposits including microbially driven present-day hydromagnesite, hot-spring calcite, vein-stockwork, detrital and hydrothermal-sedimentary magnesites as well as dolomites.

Two water samples of Salda lake have been plotted (D v $\delta^{18}\text{O}$) on Figure 4.1.1-A. These are clearly not on the Eastern Mediterranean meteoric water line despite the fact that the lake itself is in the Eastern Mediterranean region.

4.1.1. Sedimentary-hydrothermal deposits

Salda lake's present-day hydromagnesite deposits

In total 21 samples have been taken from the presently forming hydromagnesites in Salda lake. Their $\delta^{13}\text{C}$ values vary between 0.2 and 4.8 ‰ PDB whilst the $\delta^{18}\text{O}$ ranges from 33.0 to 38.1 ‰ SMOW. But most of the values concentrate about 4 to 5 ‰ for $\delta^{13}\text{C}$ and 36 to 37 ‰ for $\delta^{18}\text{O}$ (Figure 4.1.2 A and B). One sample of aragonitic mud from the north coast of the lake has 3.6 and 33.0 ‰ for $\delta^{13}\text{C}$ and $\delta^{18}\text{O}$ respectively. With the exception of the Pamukkale hot-spring travertine deposits, Salda lake hydromagnesites represent the heaviest $\delta^{13}\text{C}$ and $\delta^{18}\text{O}$ in the plot although the $\delta^{13}\text{C}$ values of

travertines are even heavier than the hydromagnesites. However, Salda lake's results are quite different from those of other hydromagnesite deposits (for example New Idria, USA, O'Neil and Barnes, 1971) but are comparable with other sedimentary magnesites.

Two water samples from Salda lake have $\delta^{18}\text{O}$ values of +3.1 and +2.5 ‰ respectively, δD values of these two samples are 5.2 and 1.8 ‰, SMOW (Table 4.1.1).

Pamukkale Present-day hot-spring travertines

With the heaviest $\delta^{13}\text{C}$ but relatively light $\delta^{18}\text{O}$ values these hot-spring travertines occupy a very restricted area on the plot (Figure 4.1.1). The values are within the range of 5.3 to 7.2 ‰ and 19.3 to 23.0 ‰ for $\delta^{13}\text{C}$ and $\delta^{18}\text{O}$ respectively. The average $\delta^{13}\text{C}$ is 6.1 ‰ whilst $\delta^{18}\text{O}$ averages 20.7 ‰. These $\delta^{13}\text{C}$ and $\delta^{18}\text{O}$ isotopic signatures are comparable with other travertine deposits from Italy, Germany and U.S.A. In general most of the $\delta^{13}\text{C}$ values of the travertines from these countries vary between -1 to +10 ‰ (Turi, 1986). On the other hand the $\delta^{18}\text{O}$ is much restricted, with the range of 22 to 27 ‰ with some notable exceptions such as Yellowstone Park, California, U.S.A, which have exceptionally low $\delta^{18}\text{O}$, between 2 and 10 ‰, (Friedman, 1970).

Hirsizdere magnesite deposits

Hirsizdere $\delta^{18}\text{O}$ values are among the lightest isotopic ratios recorded in either the Turkish or other sedimentary magnesite deposits from elsewhere in the world (Kralik et al., 1989; Zachmann, 1989). The $\delta^{18}\text{O}$ values of Hirsizdere magnesites range from 21.6 to 26.5 ‰. The $\delta^{13}\text{C}$ values range from -0.3 to +4.4

‰. The mode of $\delta^{13}\text{C}$ is between 3 and 4 ‰ whilst $\delta^{18}\text{O}$ is between 25 and 26 ‰ (Figure 4.1.3).

There are at least five different magnesite beds alternating with lacustrine sediments at Hirsizdere (Denizli). I systematically sampled the top bed and one of the bottom beds (Figure 4.1.4). With the exception of two samples the $\delta^{13}\text{C}$ values of the top bed gradually increase with depth although this is not the case for the bottom bed (Figure 4.1.5). On the other hand there is no systematic ^{18}O isotope variation with depth in either beds (Figure 4.1.6).

Helvacibaba detrital magnesite and bedded dolomites

Three magnesite pebbles from the conglomeratic level which unconformably overlies the stockwork magnesite deposits at Helvacibaba (Konya) have $\delta^{13}\text{C}$ and $\delta^{18}\text{O}$ ranging from -7.9 to -8.2 ‰ and 24.9 to 25.3 ‰ respectively. Five dolomite samples were collected from the bedded dolomites which overlie the conglomerates (for sample locations for both magnesite pebbles and bedded dolomites see Figure 4.1.8). These dolomites have isotopic values approximating to those of the conglomerate magnesites, from -7.0 to -7.9 ‰ $\delta^{13}\text{C}$ and 25.3 to 27.0 ‰ $\delta^{18}\text{O}$ (Table 4.1.1). The values of $\delta^{13}\text{C}$ for the magnesite pebbles and bedded dolomites are significantly heavier than those for the stockwork magnesites of Helvacibaba but their $\delta^{18}\text{O}$ signatures are slightly lighter.

Tsakasimta (Chad Basin, Nigeria) magnesites

Two magnesite samples from the Chad basin which are interlayered with dolomite and marl beds (Okafor, pers. commun.) have similar values to those of Hirsizdere (Denizli, Turkey) sedimentary-hydrothermal magnesites.

The $\delta^{13}\text{C}$ values of these two samples are identical (2.7 ‰) but their $\delta^{18}\text{O}$ values are 25.8 and 26.7 ‰ respectively.

Summary of isotope results

The values of $\delta^{13}\text{C}$ and $\delta^{18}\text{O}$ of sedimentary-hydrothermal (including hot-spring travertine deposits) carbonates are plotted in figure 4.1.7 as histograms. As can be seen from these figures most of the $\delta^{13}\text{C}$ values lie between 3 and 5 ‰ whilst the $\delta^{18}\text{O}$ values are quite scattered.

4.1.2. Stockwork magnesite deposits

Arapomer deresi

With the value of $\delta^{13}\text{C}$ ranging from -0.4 to 1.4 ‰ and $\delta^{18}\text{O}$ ranging between 27.0 and 27.7 ‰, this stockwork magnesite deposit occupies an anomalous area on the plot (Figure 4.1.1). Their ^{13}C isotopic signatures are considerably heavier than the other stockwork deposits although $\delta^{18}\text{O}$ can be correlated with sedimentary magnesites. However both $\delta^{13}\text{C}$ and $\delta^{18}\text{O}$ are between Hirsizdere sedimentary magnesite deposits and typical marine calcite values.

Helvacibaba magnesite deposits

In total 20 magnesite samples (14 of them were systematically collected) were analysed. The $\delta^{13}\text{C}$ ranges from -13.8 to -10.0 ‰, whilst the $\delta^{18}\text{O}$ ranges from 26.2 ‰ to a maximum of 29.0 ‰. The modes of the $\delta^{13}\text{C}$ and $\delta^{18}\text{O}$ values of these 20 samples are -11.1 and 27.2 ‰ respectively. Fourteen of the samples have been systematically collected from the east and west-side of the open pit

(Figure 4.1.8). The $\delta^{13}\text{C}$ values of the east-side of the open pit gradually increase with depth although a similar isotopic profile cannot be seen on the west-side of the pit (Figure 4.1.9-A). On the other hand, there is no visible $\delta^{18}\text{O}$ trend with depth on either side of the open pit (Figure 4.1.9-B).

Helvacibaba silica cap

One quartz sample from the surface (taken from ~100 m north of the open pit) of the silica cap over the Helvacibaba stockwork magnesite has a $\delta^{18}\text{O}$ value of 26.2 ‰. The other eleven samples have been systematically collected from the silica cap (Figure 4.1.8-A) which is over the magnesite deposit and the $\delta^{18}\text{O}$ values of these silica (SiO_2) samples range from 22.7 to 26.3 ‰ (Table 4.1.1). The mean value of $\delta^{18}\text{O}$ is 24.8 ‰ which is about 2.4 ‰ lighter than the overall magnesite values of Helvacibaba.

Kavakarasi magnesite deposits

We were misinformed as to the presence here of in-situ magnesite deposits; however, four isolated samples were taken from the surface, three of which were magnesite while the other one was dolomite. The $\delta^{13}\text{C}$ values of these four samples are extremely scattered with a range of -5.5 to -11.5 ‰. Their $\delta^{18}\text{O}$ values are much more uniform and vary between 26.8 and 29.2 ‰. The type of the deposit is unknown, but Sancar (1982) mentioned the existence of 5-25 cm thick magnesite veins within the fractured serpentinites in the region, probably a stockwork.

Yunak and Kozagac magnesite deposits

The $\delta^{13}\text{C}$ values of two samples from Yunak are -8.8 and -8.9 ‰ and the $\delta^{18}\text{O}$ isotopic signatures are 27.7 and 28.0 ‰. One sample of Kozagac has -10.0 and 27.0 ‰ for $\delta^{13}\text{C}$ and $\delta^{18}\text{O}$ respectively. The $\delta^{13}\text{C}$ and $\delta^{18}\text{O}$ values of both deposits are quite similar to those of the Helvacibaba stockwork deposits.

4.1.3. Vein deposits

Koyakci Tepe and Sodur

With a mean of -13.1 ‰ the $\delta^{13}\text{C}$ values of the Koyakci Tepe magnesite deposits have the lightest values of all the Turkish magnesite deposits examined, although the mean value of $\delta^{18}\text{O}$ (26.6 ‰) can be compared to other magnesite deposits, including sedimentary-hydrothermal types.

The eleven magnesite samples collected from Koyakci Tepe have $\delta^{13}\text{C}$ values ranging from -14.3 to -11.8 ‰. The $\delta^{18}\text{O}$ values of this deposit vary between 25.9 and 27.7 ‰. The $\delta^{18}\text{O}$ values of two quartz samples from the same area are similar (26.3 ‰). Two magnesite samples of Sodur (Karaman) have similar $\delta^{13}\text{C}$ value (-12.4 and -12.3 ‰) to samples from Koyakci Tepe, but the $\delta^{18}\text{O}$ values are rather lighter (25.9 and 25.7 ‰) compared to those at Koyakci Tepe.

4.1.4. Palaeozoic and Mesozoic limestones

Two calcium carbonate (limestone) samples of probable Cretaceous age were collected from the Salda lake shoreline. Their $\delta^{13}\text{C}$ values are 1.6 and 2.4

‰ and their $\delta^{18}\text{O}$ values are 30.9 and 29.8 ‰. Four calcite (limestone) samples from a quarry in Konya (Midos formation) occupy a very restricted area on the plot (Figure 4.1.1). The isotopic signatures of these calcites are similar (1.1 to 1.9 ‰ for $\delta^{13}\text{C}$ and 28.7 to 29.3 for $\delta^{18}\text{O}$ ‰) to those of Salda calcites. In contrast two calcium carbonate samples have been taken from an olistolitic limestone probably derived from the Loras limestone (Jurassic-Upper Cretaceous) within the ultramafics of Konya. These have $\delta^{13}\text{C}$ values of -4.6 and -3.9 ‰ and relatively light $\delta^{18}\text{O}$ values of 20.7 ‰. Two samples of Jurassic age from Bozkir (Konya) have $\delta^{13}\text{C}$ of 3.6 and 3.5 ‰ and $\delta^{18}\text{O}$ of 24.5 and 25.1 ‰.

Two calcium carbonate samples from the oldest formation of Meram-Konya (Ardicli formation, Permian-Lower Jurassic) have $\delta^{13}\text{C}$ values of 2.3 and 1.8 ‰, and $\delta^{18}\text{O}$ values of 24.7 and 23.4 ‰. Four calcium carbonate samples from the organic-rich carbonate veinlets of the Seydisehir formation (Cambro-Ordovician) range from -19.3 to -20.0 ‰ and 21.3 to 22.2 ‰ for $\delta^{13}\text{C}$ and $\delta^{18}\text{O}$ respectively (Table 4.1.1). These values are the lightest isotopic values of all the analysed carbonates from western Turkey.

Table 4.1.1. Isotopic composition of hydromagnesite, magnesite, calcite, dolomite, quartz, aragonite and water from Turkey.

Type and location	Sample no (**)	$\delta^{13}\text{C}$ (‰)PDB	$\delta^{18}\text{O}$ (‰)SMOW	Mineralogy (*)
Present-day, Salda Lake	18	4.5	36.3	H
	19	4.2	36.1	H
	20	4.4	36.8	H
	21	4.7	35.6	H
	22-A	4.5	36.0	H
	22-B	3.9	34.5	H
	24	4.3	36.2	H
	27	4.3	36.5	H
	70	4.2	36.2	H
	93-2	3.6	33.0	H
	93-5	3.7	36.2	H
	93-7	4.7	35.3	A
	93-8	4.3	34.9	H
	93-9	3.8	36.1	H
	93-10	0.2	35.3	H
	93-15	4.4	37.3	H
	93-21	4.1	35.9	H
	93-22	3.9	35.2	H
	93-24-1	3.4	35.8	H
	93-24-2	4.3	36.6	H
	93-24-3	4.8	38.1	H
	93-30	4.4	36.0	H
	(n=22)	4.0±0.9	35.9±1.0	

Table 4.1.1. continued

Type and location	Sample no (**)	D (‰)SMOW	$\delta^{18}\text{O}$ (‰)SMOW	
Water, Salda lake	92-23	5.2	3.1	
	92-25	1.8	2.5	
	(n=2)	3.5±2.4	2.8±0.4	
		$\delta^{13}\text{C}$ (‰)PDB		
Present-day	92-56-A	5.8	19.7	C
Hot-spring, Pamukkale	92-56	6.2	20.7	C
	92-58	5.6	19.3	C
	92-60	5.3	19.9	C
	93-P-A	7.2	21.3	C
	93-P-B	6.2	23.0	C
	(n=6)	6.1±0.7	20.7±1.4	
Sedimentary, Hirsizdere	<u>30</u>	0.9	25.3	M(D,Q,Cl)
	<u>31</u>	2.0	25.2	M(D,Q,Cl)
	<u>32</u>	1.5	26.0	M(D,Q)
	<u>33</u>	1.9	22.8	M(D)
	<u>34</u>	3.1	26.5	M(D,Q)
	<u>35</u>	2.8	25.2	M(D,Q)
	<u>36</u>	4.3	24.6	M(D)
	<u>37</u>	3.8	25.2	M(D)
	<u>38</u>	3.8	25.8	M(D)
	<u>39</u>	2.2	25.3	M(Q,D)
	<u>40</u>	3.7	25.3	M(D,Cl,Q)
	<u>42</u>	1.6	24.2	D(Cl,Q)
	<u>43</u>	4.4	26.0	M(S,D)
	<u>44</u>	0.9	24.9	M(D)
	<u>45</u>	3.4	25.3	M(D)
	<u>46</u>	0.8	25.3	M(D)
	<u>48</u>	-0.3	21.6	M(D)
	<u>49</u>	3.8	25.3	M(D,Cl)
	<u>50</u>	2.8	25.8	M(D)
	<u>51</u>	1.2	26.1	M(D,Cl,Q)
	<u>52</u>	3.2	25.9	M(D)
	<u>53</u>	3.9	26.1	M(D,S)
	<u>54</u>	3.4	25.5	M(D)
	(n=23)	2.6±1.3	25.2±1.1	

Table 4.1.1. continued

Type and location	Sample no (**)	$\delta^{13}\text{C}$ (‰)PDB	$\delta^{18}\text{O}$ (‰)SMOW	Mineralogy (*)
Detrital, Helvacibaba	13-A	-7.5	24.9	M
	13-B	-8.0	25.3	M
	13-C	-8.2	25.2	M
	(n=3)	-7.9±0.4	25.1±0.2	
Bedded dolomite, Helvacibaba	12-N	-7.0	25.3	D
	12-N-B	-7.6	25.8	D
	14-C	-7.9	27.0	D
	H-12-2	-7.0	25.3	D
	H-12-2-B	-7.6	25.8	D
	(n=5)	-7.4±0.4	25.8±0.7	
Sedimentary, Tsakasimta (Nigeria)	92-64-A	2.7	26.7	M
	92-64-B	2.7	25.8	M
	(n=2)	2.7±0.0	26.3±0.6	
Stockwork, Arap Omer Deresi	15-A	1.4	27.5	M
	15-B	0.1	27.0	M
	15-C	-0.4	27.7	M
	15-D	0.2	27.7	M
	(n=4)	0.3±0.8	27.5±0.3	

Table 4.1.1. continued

Type and location	Sample no (**)	$\delta^{13}\text{C}$ (‰)PDB	$\delta^{18}\text{O}$ (‰)SMOW	Mineralogy (*)
Stockwork, West side of open pit, Helvacibaba	<u>13-W-Top</u>	-11.9	26.8	M
	<u>11-W</u>	-11.6	26.5	M
	<u>9-W</u>	-11.4	27.3	M
	<u>7-W</u>	-10.1	26.7	M
	<u>5-W</u>	-11.3	27.2	M
	<u>3-W</u>	-10.5	26.8	M
	<u>1-W-Base</u>	-11.2	26.4	M
	(n=7)	-11.1±0.6	26.8±0.3	
Stockwork East side of open pit, Helvacibaba	<u>11-E-Top</u>	-13.8	27.2	M
	<u>9-E</u>	-13.2	27.3	M
	<u>8-E</u>	-11.1	27.3	M
	<u>7-E</u>	-11.7	26.9	M
	<u>5-E</u>	-11.9	26.6	M
	<u>3-E</u>	-10.3	27.1	M
	<u>1-E-Base</u>	-10.8	27.6	M
	(n=7)	-11.8±1.3	27.1±0.3	
Stockwork, Helvacibaba	89	-10.8	27.4	M
	142-A	-10.5	28.2	M
	143-A	-10.3	29.0	M(C)
	145	-10.3	27.3	M(C)
	148-A	-10.0	27.4	M
	(n=5)	-10.4±0.3	27.9±0.7	

Table 4.1.1. continued

Type and location	Sample no (**)	$\delta^{13}\text{C}$ (‰)PDB	$\delta^{18}\text{O}$ (‰)SMOW	Mineralogy (*)
Silica cap, Helvacibaba	<u>10-E</u>	n.a.	26.3	Q(Ha)
	<u>10-N</u>	n.a.	23.5	Q(Ha,D)
	<u>11-N</u>	n.a.	24.4	Q(Ha)
	<u>11-N-A</u>	n.a.	24.8	Q(Ha)
	<u>11-N-B</u>	n.a.	24.7	Q(Ha,D)
	<u>11-N-C</u>	n.a.	25.9	Q(Ha)
	<u>11-N-D</u>	n.a.	25.4	Q(Ha,D)
	<u>12-N</u>	n.a.	24.7	Q(Ha)
	<u>12-N-A</u>	n.a.	22.7	Q(Ha,D)
	<u>12-N-D</u>	n.a.	24.1	Q(Ha)
	<u>12-W-A</u>	n.a.	26.0	Q(Ha)
	143-B	n.a.	26.2	Q(Ha)
	(n=12)		24.9±1.1	
Stockwork, Kavakarasi	Kavak-A	-7.1	28.7	M
	Kavak-B	-11.5	26.8	D
	Kavak-C	-5.5	29.2	M
	Kavak-D	-8.1	27.1	M
	(n=4)	-8.1±2.5	28.0±1.2	
Stockwork, Yunak and Kozagac	Y-69-A	-8.8	27.7	M
	Y-69-B	-8.9	28.0	M
	Koz-A	-10.0	27.0	M
	(n=3)	-9.2±0.7	27.6±0.5	

Table 4.1.1. continued

Type and location	Sample no (**)	$\delta^{13}\text{C}$ (‰)PDB	$\delta^{18}\text{O}$ (‰)SMOW	Mineralogy (*)
Vein, Koyakci Tepe	52-A	-13.3	26.4	M(Q)
	58	-13.3	26.4	M
	59-B	-12.6	26.2	M(D,S)
	61-B	-13.4	26.4	M
	61-C	-12.9	27.4	M(S,C)
	62-C	-11.8	27.7	M(Q)
	63	-14.3	26.3	M(C)
	112	-13.2	26.6	M
	113-B	-13.2	27.4	M
	117	-12.8	26.8	M
	121-B	-13.3	25.9	M
	(n=13)	-13.1±0.6	26.7±0.6	
Vein, Silica Koyakci Tepe	114	n.a.	26.3	Q
	114-A	n.a.	26.3	Q
	(n=2)		26.3±0.0	
Vein, Sodur	68-A	-12.4	25.9	M
	68-B	-12.3	25.7	M
	(n=2)	-12.4±0.1	25.8±0.1	
Cretaceous limestone, Salda lake	26-A	1.6	30.9	C
	26-B	2.4	29.8	C
	(n=2)	2.0±0.6	30.4±0.8	

Table 4.1.1. continued

Type and location	Sample no (**)	$\delta^{13}\text{C}$ (‰)PDB	$\delta^{18}\text{O}$ (‰)SMOW	Mineralogy (*)
Jura- U.Cret. limestone, (olistolitic)	24	-4.6	20.7	C
	187	-3.9	20.7	C
Loras-Konya	(n=2)	-4.3±0.5	20.7±0.0	
Cretaceous limestone, Midos form. Konya	92-4	1.5	28.7	C
	92-5	1.9	29.3	C
	92-6	1.9	29.1	C
	92-7	1.1	28.7	C
	(n=4)	1.6±0.4	29.0±0.3	
Jurassic limestone, Bozkir-Konya	92-3K	3.6	24.5	C
	92-4K	3.5	25.1	C
	(n=2)	3.6±0.1	24.8±0.4	
Perm.-L.Jura limestone Ardicli-Konya	41	2.3	24.7	C
	173	1.8	23.4	C
	(n=2)	2.1±0.4	24.1±0.9	
Organic-rich limestone, Caltepe- Seydischir	9	-19.3	21.8	C
	9-B	-19.9	21.3	C
	31	-20.0	21.6	C
	32	-19.4	22.2	C
	(n=4)	-19.7±0.4	21.7±0.4	

Table 4.1.1. continued

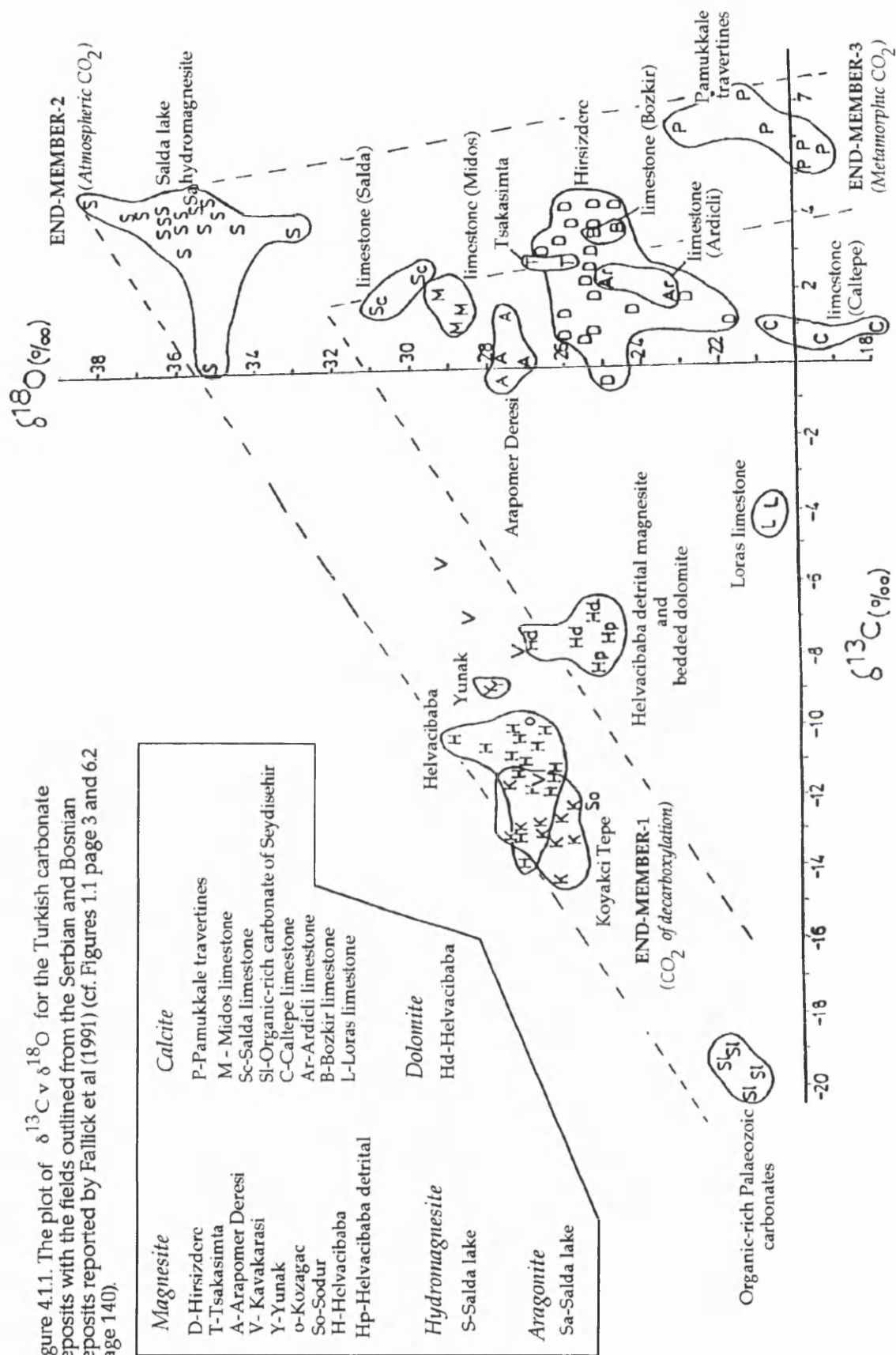
Type and location	Sample no (**)	$\delta^{13}\text{C}$ (‰)PDB	$\delta^{18}\text{O}$ (‰)SMOW	Mineralogy (*)
Camb.limes., reddish,nodular Caltepe- Seydisehir	10-A	0.5	20.8	C
	11-A	0.7	17.7	C
	11-B	0.6	19.4	C
	(n=3)	0.6±0.1	19.3±1.6	

*The predominant mineralogy is denoted by H=Hydromagnesite, C=Calcite, M=Magnesite, Q=Quartz, D=Dolomite, A=Aragonite, Cl=Clay, S=Serpentine, Ha=Haematite. Minor mineral phases are denoted within brackets.

**Underlined samples were systematically collected.

n.a. not available.

Figure 4.1.1. The plot of $\delta^{13}\text{C}_v$ $\delta^{18}\text{O}$ for the Turkish carbonate deposits with the fields outlined from the Serbian and Bosnian deposits reported by Fallick et al (1991) (cf. Figures 1.1 page 3 and 6.2 page 140).



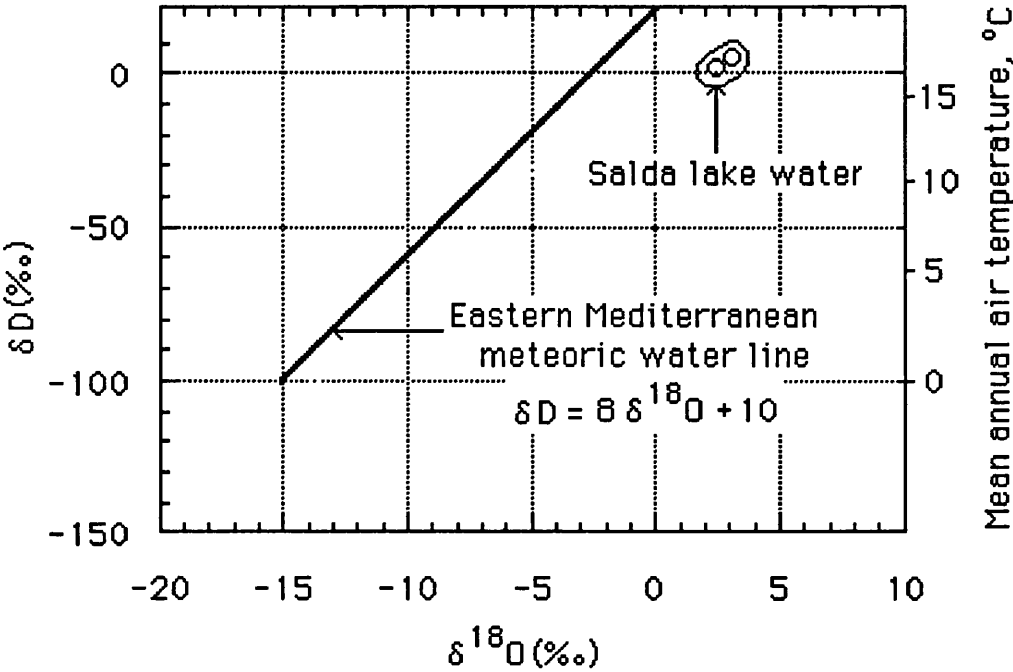


Figure 4.1.1-A. Plot of δD v $\delta^{18}\text{O}$ of two water samples from Salda lake. E Mediterranean meteoric water line and relevant equation are from Sheppard, 1986. Average meteoric water for this region is estimated on the basis of rainfall as $\delta^{18}\text{O} \sim -5\text{‰}$ and $\delta\text{D} \sim -20\text{‰}$. Salda lake values result partly from water/rock interaction and partly evaporation.

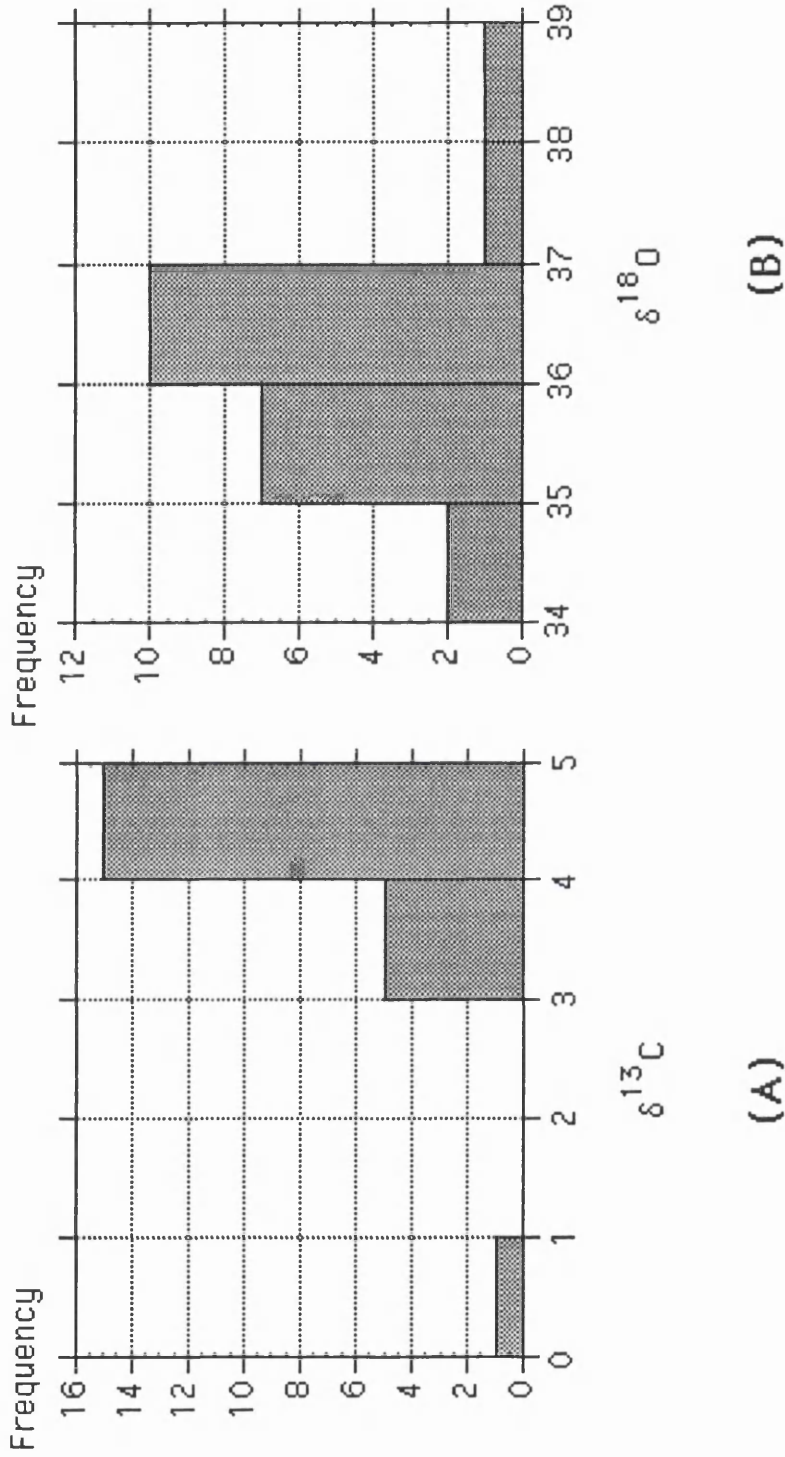


Figure 4.1.2. Frequency histogram of $\delta^{13}\text{C}$ (A) and $\delta^{18}\text{O}$ (B) values of Salda lake hydromagnesites.

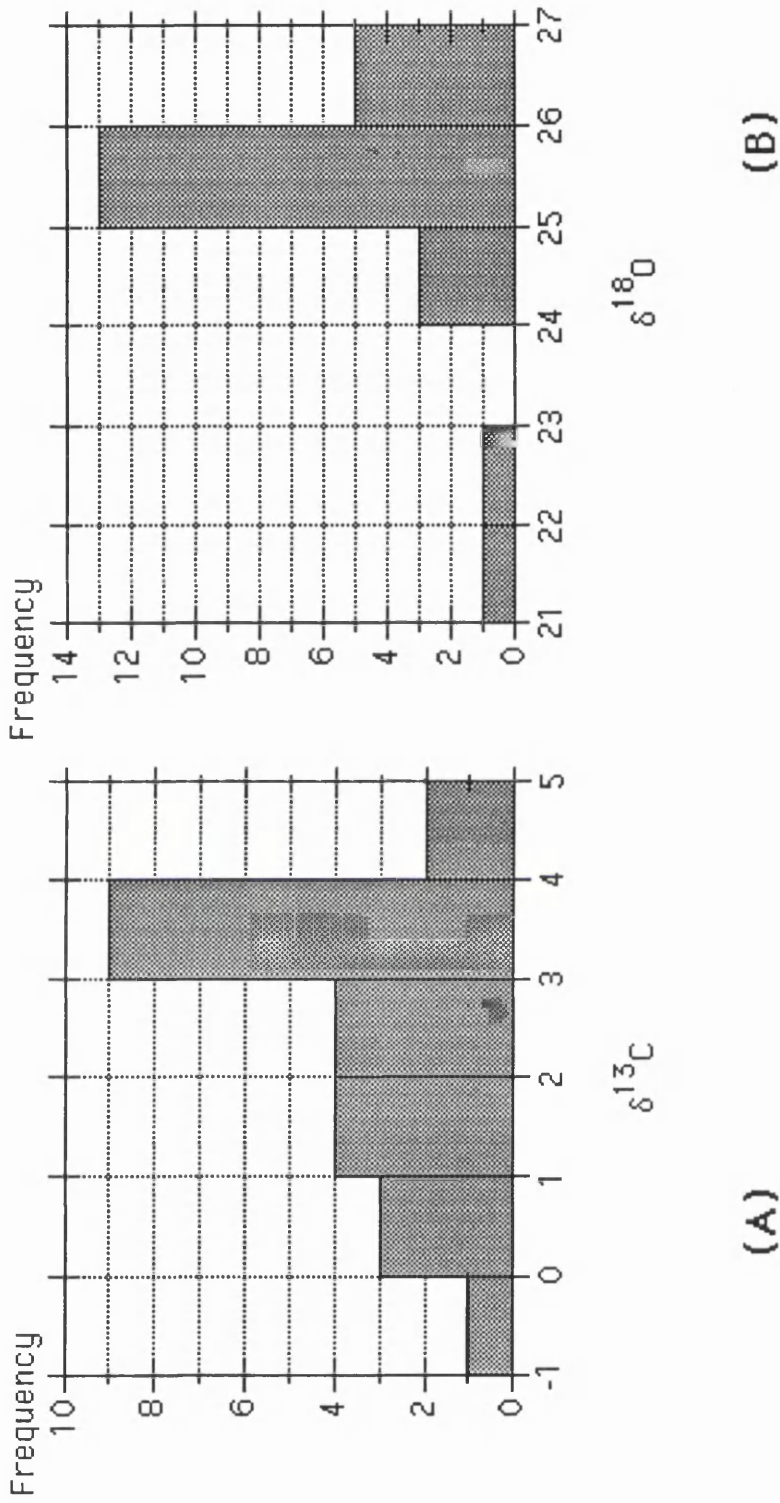


Figure 4.1.3. Frequency histograms of $\delta^{13}\text{C}$ (A) and $\delta^{18}\text{O}$ (B) values of Hirsizdere magnesite deposit.

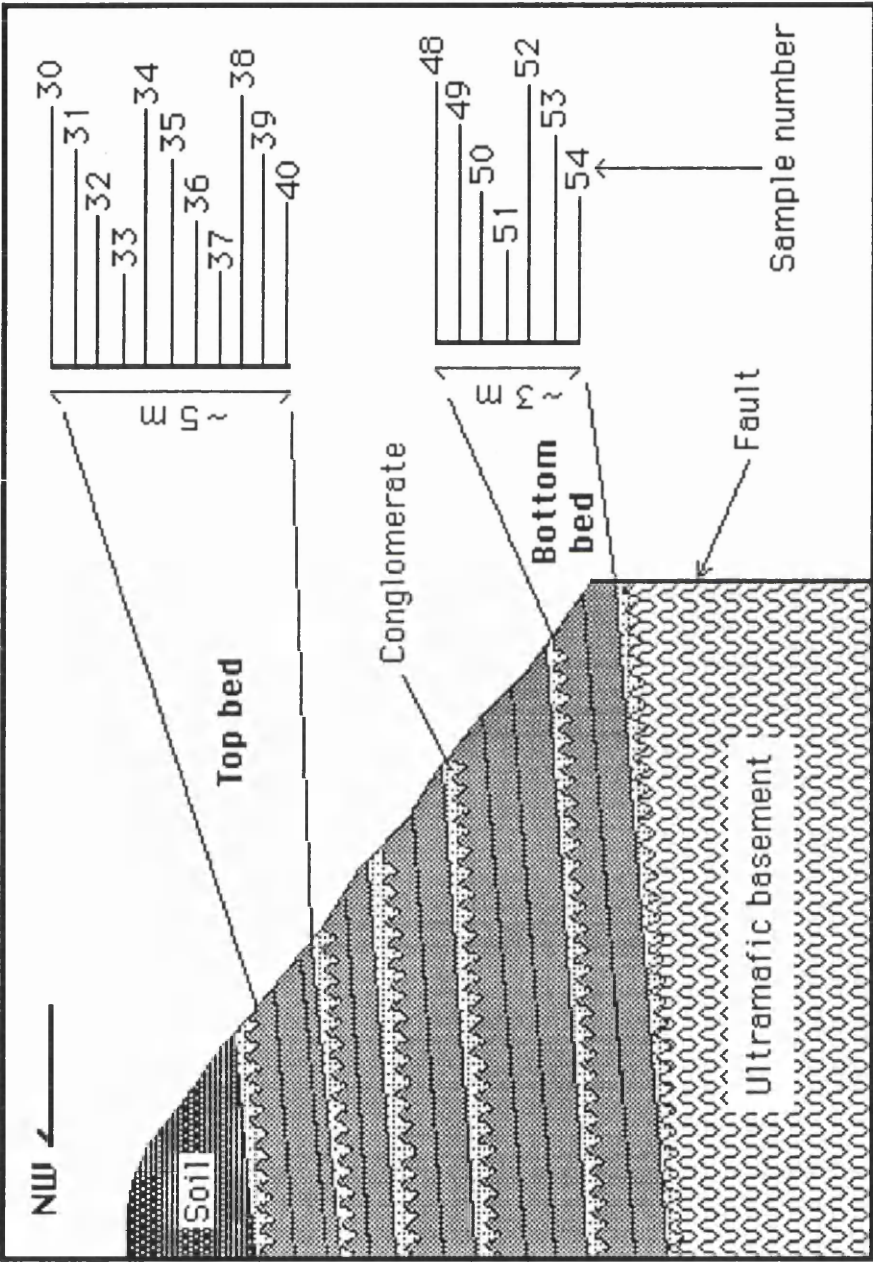


Figure 4.1.4. Systematically collected sample sites of the Hirsizdere sedimentary magnesite deposits.

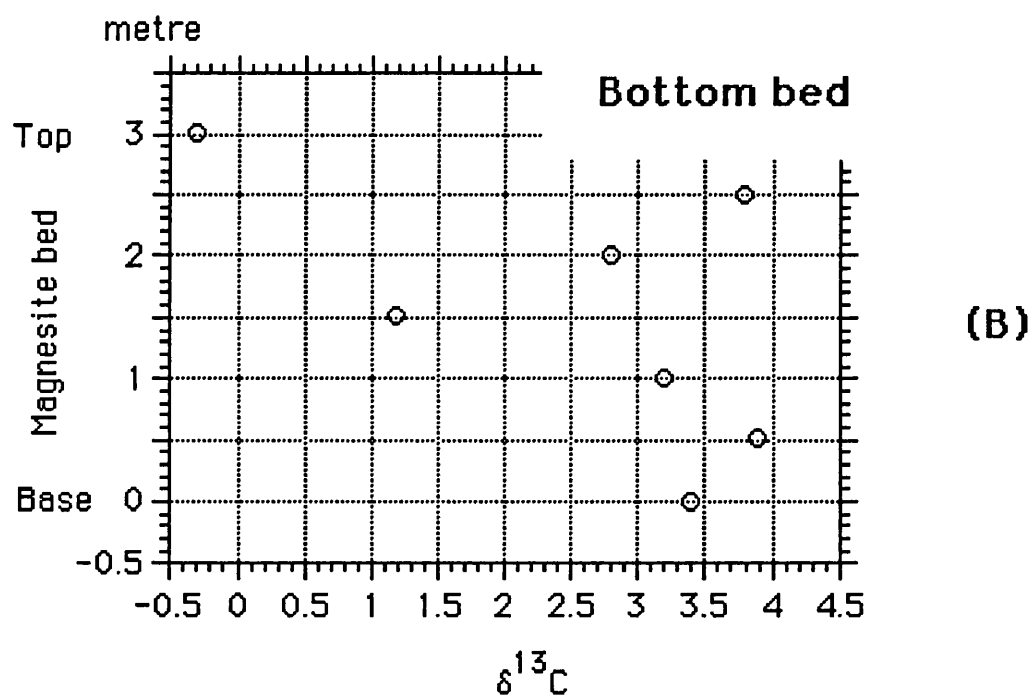
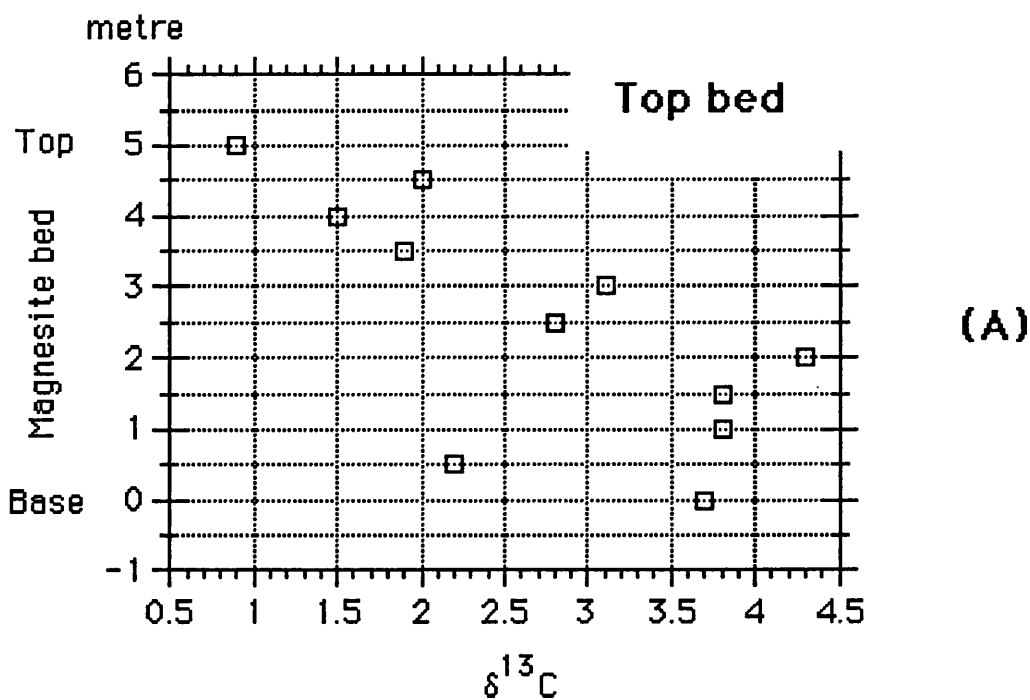


Figure 4.1.5. Relationship between $\delta^{13}\text{C}$ with depth at top (A) and bottom (B) beds in the Hirsizdere sedimentary magnesite deposits.

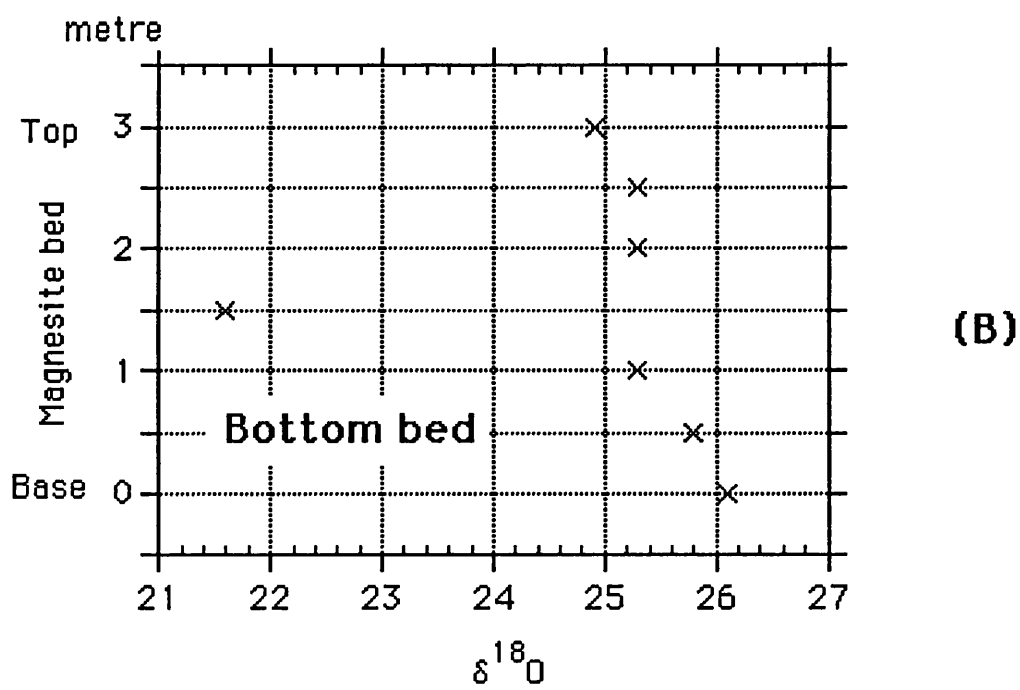
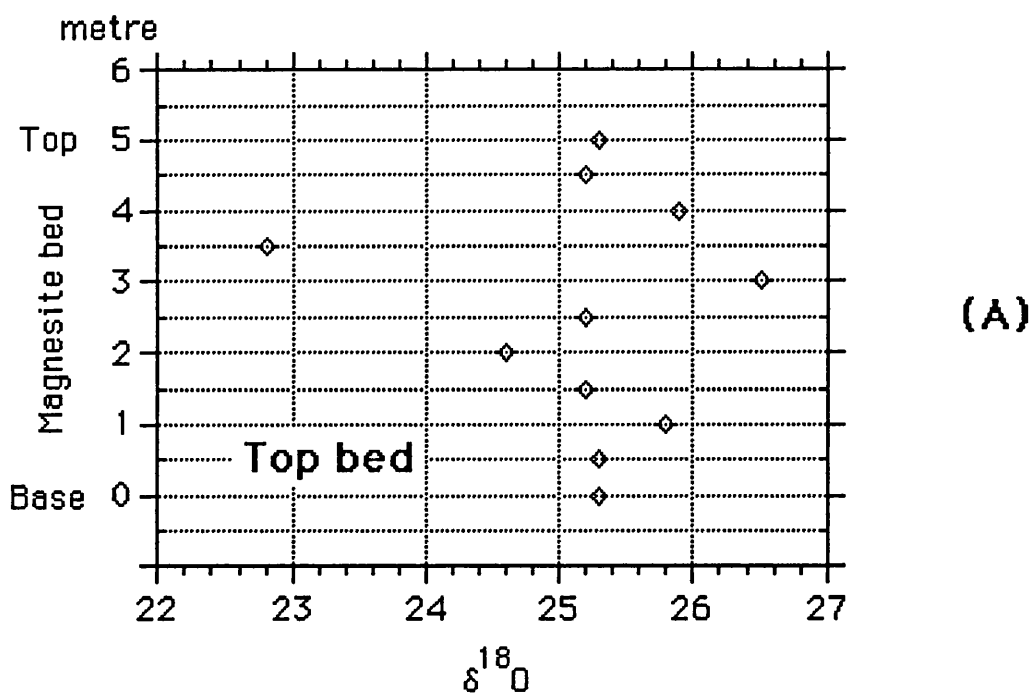


Figure 4.1.6. $\delta^{18}\text{O}$ v depth at top (A) and bottom (B) magnesite beds at Hirsizdere magnesite deposits.

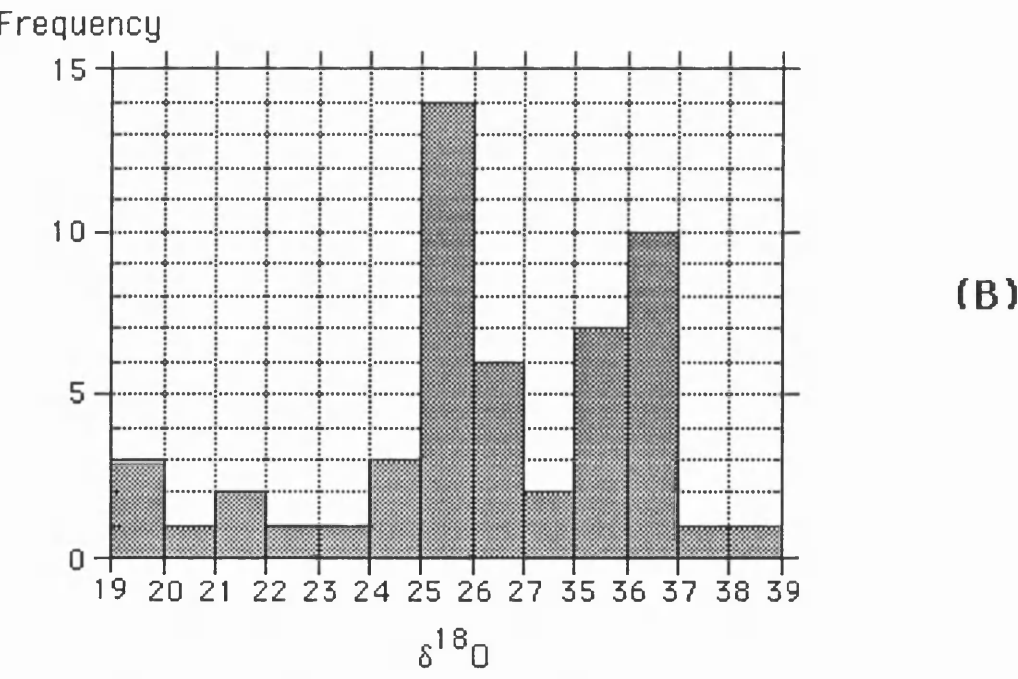
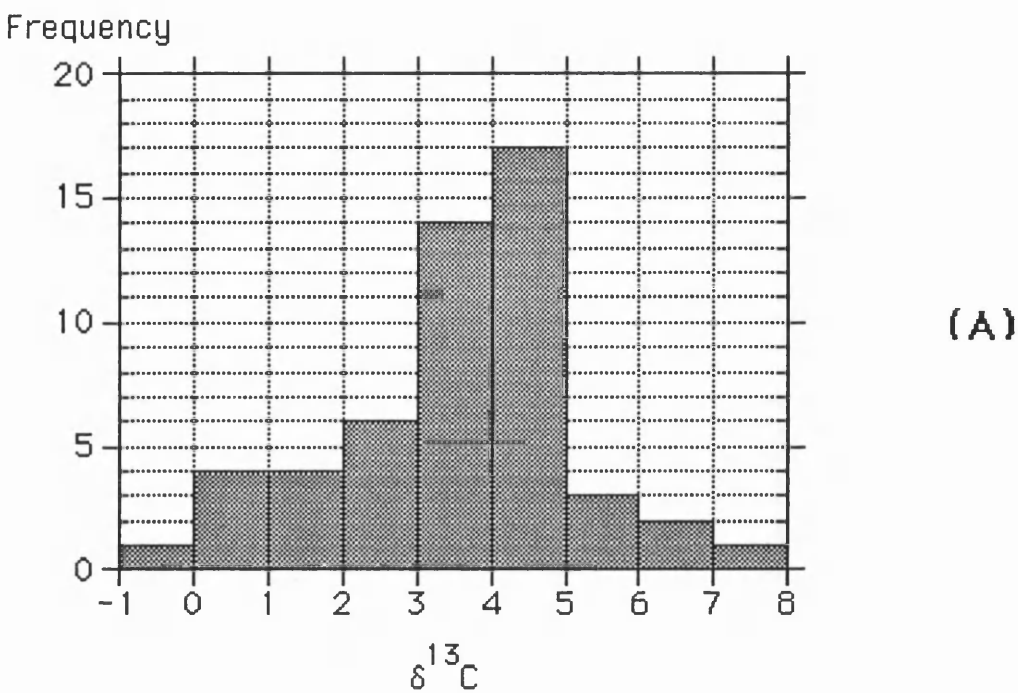


Figure 4.1.7. The histograms of frequency v $\delta^{13}\text{C}$ (A) and $\delta^{18}\text{O}$ (B) of 52 samples from sedimentary-hydrothermal (including the hot-spring Pamukkale travertine deposit) carbonates. Note that the detrital magnesite and bedded dolomites of Helvacibaba are not included.

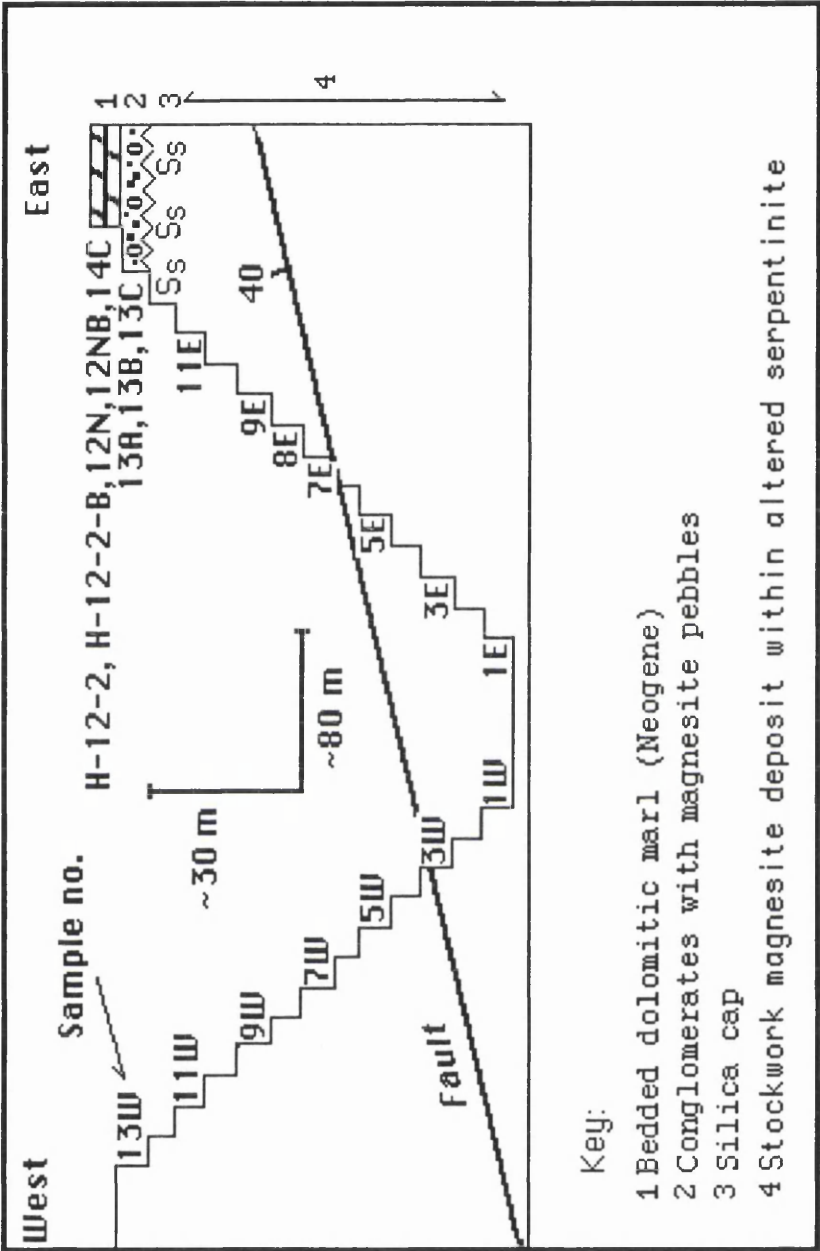


Figure 4.1.8. The sample sites and the vertical relationships between magnesite, magnesite pebbles and bedded dolomitic marl (Neogene) in the Helvaciba (Konya) open pit mine. Silica samples (except 143-B) have been taken from the silica cap (Ss).

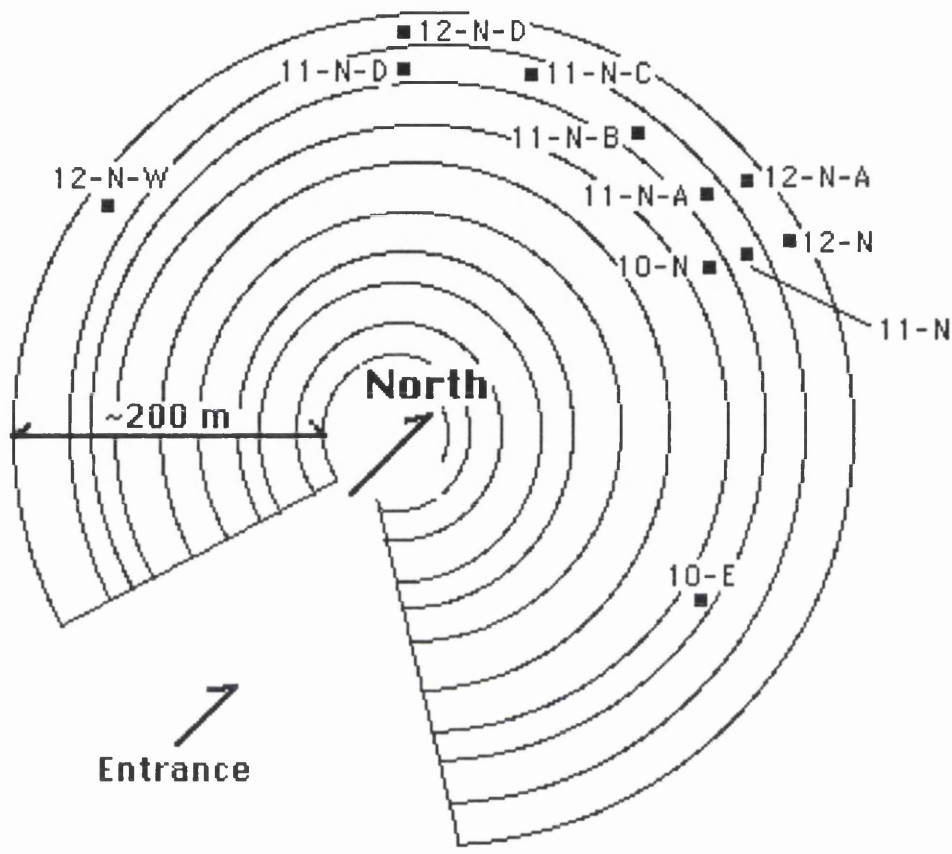


Figure 4.1.8-A. Sample sites (black spots) of silica samples from Helvacibaba silica cap.

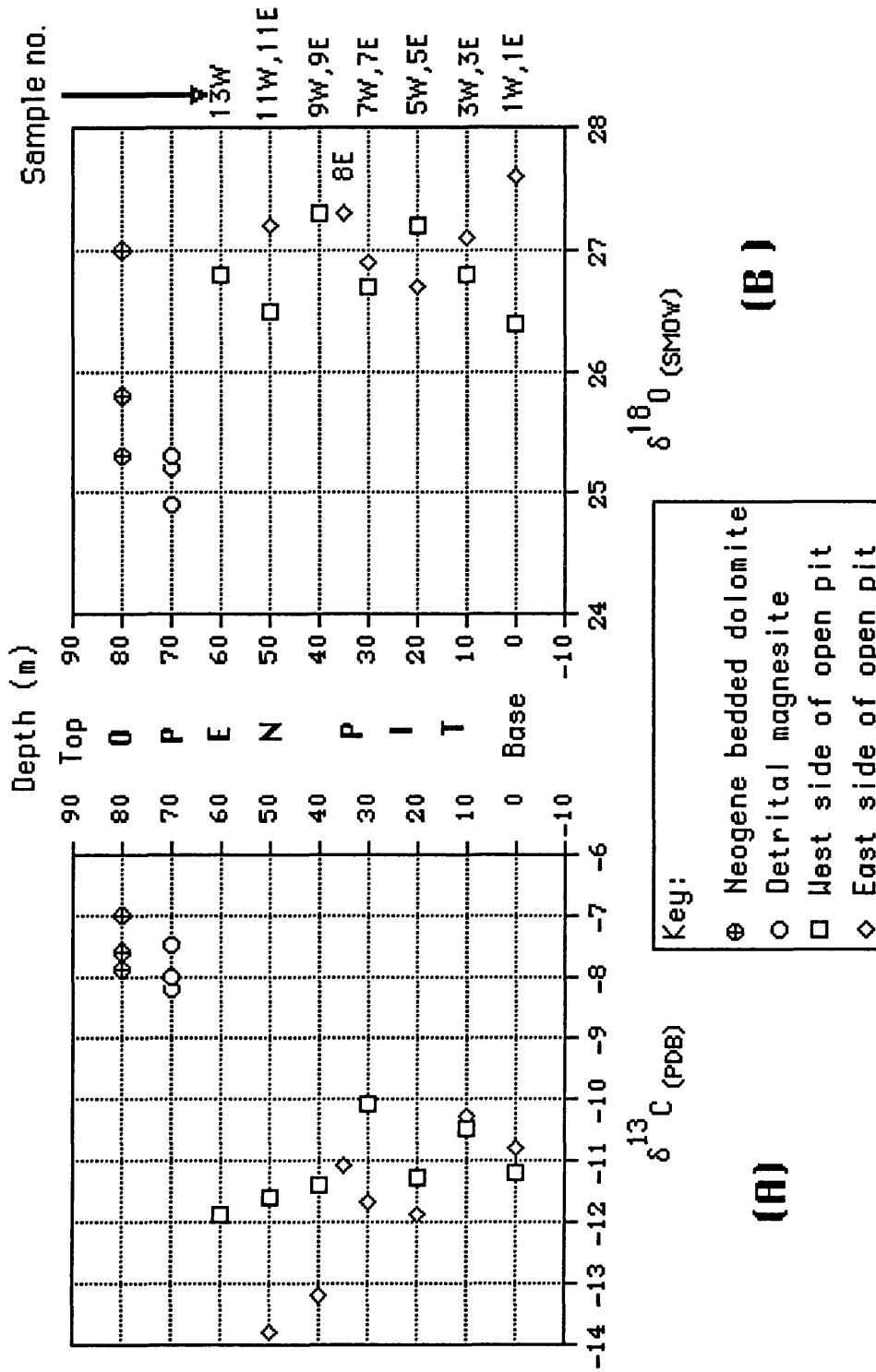


Figure 4.1.9. The plot of $\delta^{13}\text{C}$ v depth (A) and $\delta^{18}\text{O}$ v depth (B) of systematically collected samples from the Helvacibaba open pit mine (Konya).

4.2. REE RESULTS

REE concentrations were determined in magnesite and ultramafic host rocks from the Helvacibaba and Koyakci Tepe (Konya) magnesite deposits along with two hydromagnesite samples from Salda. Three water samples were also analysed, from Salda lake (Yesilova-Burdur) and a hot-spring (Pamukkale-Denizli). Full REE analyses results with chondrite-normalised values are given in Appendices 4 and 5. However, with the exception of the hydromagnesite sample 92-24^{hm}, the results for all samples are below reliability limit which is 1-2 ppb for all elements analysed.

4.3. XRD RESULTS

Most of the XRD analyses were made in order to find out the mineralogical purity of the targeted samples i.e. magnesite, hydromagnesite, quartz. In cases where the purity was below 90 % no isotopic analyses were undertaken. The results of the XRD analyses of the samples analysed by mass-spectrometer are given, with major and minor mineral phases in Table 4.1.1.

Some hydromagnesite samples were heated to various temperatures to test if the hydromagnesite would convert to magnesite. Samples were subjected to temperatures of 100°C, 200°C, 300°C and 400°C. When the hydromagnesite completely converted to periclase heating was terminated. The results of this experiment are outlined in Table 4.3.1. As seen from this table magnesite was not produced by the heating of hydromagnesite. On the basis of this table, it is possible that hydromagnesite converts to magnesite between 300°C and 400°C. Further experiments are clearly required at temperatures between 300°C and 400°C and in addition pressure must be considered.

Table 4.3.1. The mineralogical composition of hydromagnesite heated at various temperatures.

<u>Sample no</u>	<u>Pre-heated</u>	<u>100⁰C</u>	<u>200⁰C</u>	<u>300⁰C</u>	<u>400⁰C</u>
92-18	Hm (Sand)	Hm	Hm	Hm	P
92-19	Hm (Stromatolite)	Hm	Hm	Hm	P
92-22	Hm (Pebble)	Hm	Hm	Hm	P

Note Hm=Hydromagnesite, P=Periclase

4.4. AAS RESULTS

Mg, Ca, Na, Si, Fe and Ni were determined on 20 water samples from Salda lake and surrounds. Sample sites are shown in Figure 4.4.1 along with the carbonate (hydromagnesite, calcite and aragonite) sample sites. The AAS results of water samples are presented in Table 4.4.1. For easy correlation average concentrations of Mg, Ca, Na and Si in four different waters (lake, well, spring and stream) have been given in Table 4.4.2.

The lake water is apparently enriched in Mg and Na but depleted in Si with respect to the well, spring and stream waters. In general the Mg concentrations of the lake water are around 200 ppm and the Mg/Ca ratio is about 67 whilst the Mg/Si ratio is well over 200. On the other hand, the concentration of Si in the lake water is low (less than 1 ppm). The Ca content of the lake water is about 3 ppm, well below the average value (10 ppm) of twelve well waters.

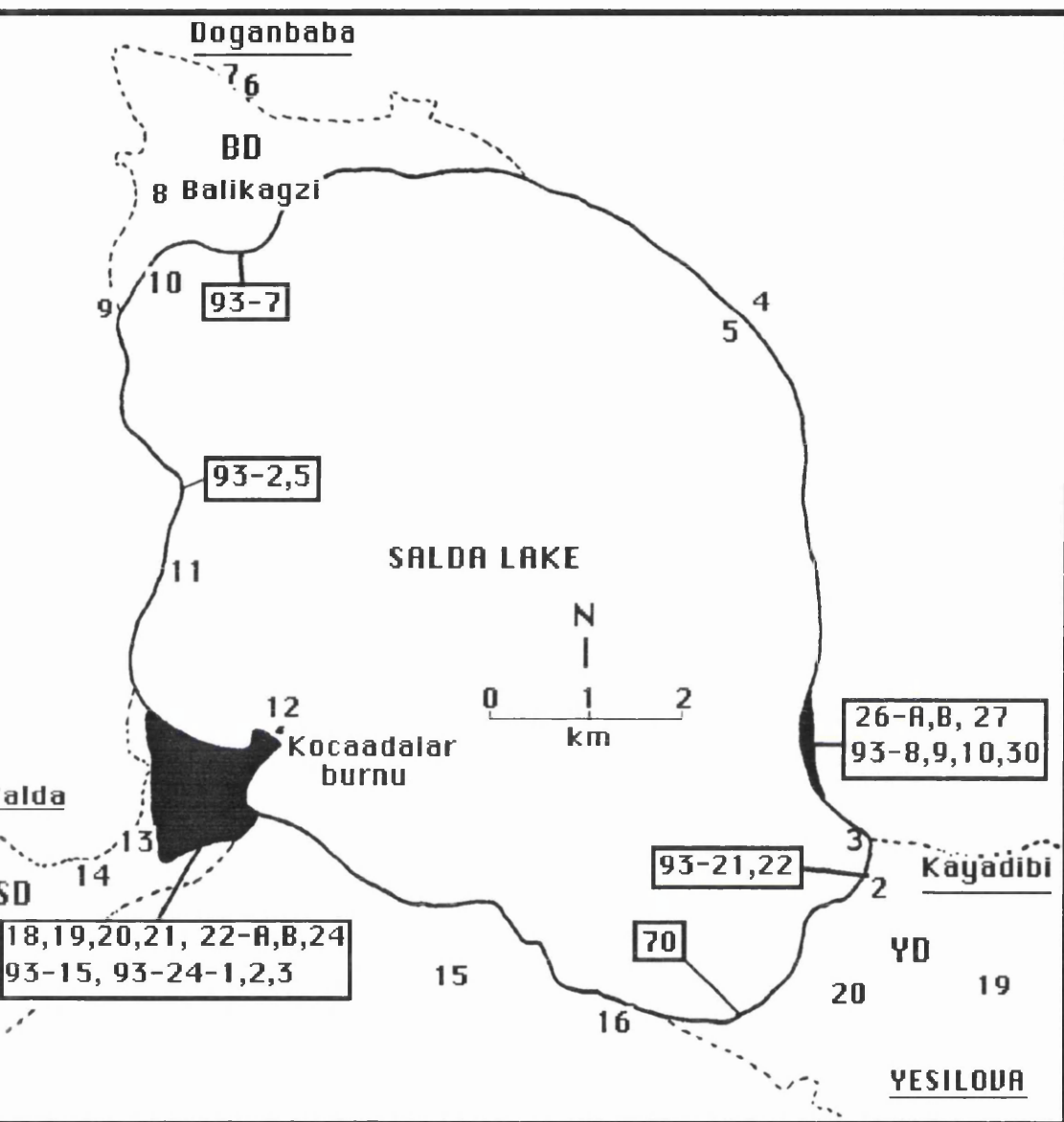


Figure 4.4.1. Sample sites at Salda lake and its surrounds. Unadorned numbers indicate the water samples (two water samples were taken ~2km south of Yesilova and are not shown on this map), numbers in boxes represent the hydromagnesite, aragonite and calcite samples. The settlements are underlined. Dotted lines indicate the delta boundary, YD:- Yesilova delta, BD:- Balikagzi delta, SD:- Salda delta. The major hydromagnesite deposits are black.

Table 4.4.1. AAS results (in ppm) of Salda lake and surrounding area waters*.

Sample no	Mg	Ca	Na	Si	pH	T °C	Deep (m)
93- 1	54	34.1	20	13.7	n.m.	n.m.	30
93- 2	60	21.4	8	12.7	n.m.	n.m.	7
93- 3	218	3.0	72	<1	8.8	25	
93- 4	49	1.3	3	<1	9.8	15	
93- 5	194	3.0	68	<1	9.7	24	
93- 6	83	9.0	7	12.6	9.0	12	80
93- 7	75	7.7	6	12.3	n.m.	n.m.	2
93- 8	82	6.6	4	16.0	7.1	26	
93- 9	93	3.3	3	8.2	8.2	24	
93-10	226	3.2	76	<1	8.8	36	
93-11	198	3.3	76	<1	9.0	26	
93-12	195	3.2	88	<1	9.2	26	
93-13	102	4.3	5	1.9	9.5	13	
93-14	78	5.5	6	14.6	8.7	22	9
93-15	41	1.8	1	5.8	n.m.	n.m.	
93-16	68	1.8	2	<1	10.0	13	
93-17	27	2.4	3	3.7	9.0	14	
93-18	44	4.2	2	11.8	8.6	17	
93-19	22	23.8	11	11.2	8.0	14	
93-20	23	5.9	5	11.3	7.9	15	

n.m. not measured.

Note: Each sample has less than 0.05 ppm Fe and Ni. pH and temperature measurements have been measured during the daytime of 9,10,11 August 1993.

*Where possible, measured pH, temperature and depth of the water are also added to the table.

Well water:-(93)1,2,4,6,7,8,9,13,15,17,19,20

Lake water:-(93)3,5,10,11,12

Spring water:-(93)16

Stream water:-(93)14,18

Table 4.4.2. Average concentrations of Mg, Ca, Na and Si (in ppm), and pH of water samples from Salda lake and its vicinity.

Water type	pH	Mg	Ca	Na	Si
Lake	9.1	206	3	76	<1
Well	8.6	59	10	6	9
Spring	10.0	68	2	2	<1
Stream	8.7	61	5	4	13

Note there is only one spring water.

4.5. AS RESULTS

Only one sample from the Salda lake stromatolites has been examined by absorbance spectrophotometry (AS). This was done in order to find out what sort of bacteria exist in the stromatolites. Figure 4.5.1 shows the diagnostic pigments of the bacteria have a peak at about 630nm on the absorbent spectrum graph. However this spectrum could also be seen for red algae, but we know Salda lake stromatolites are clearly not red algae, so with the spectrum of 630nm, we can be confident that they are cyanobacteria (Dominy, pers. commun.).

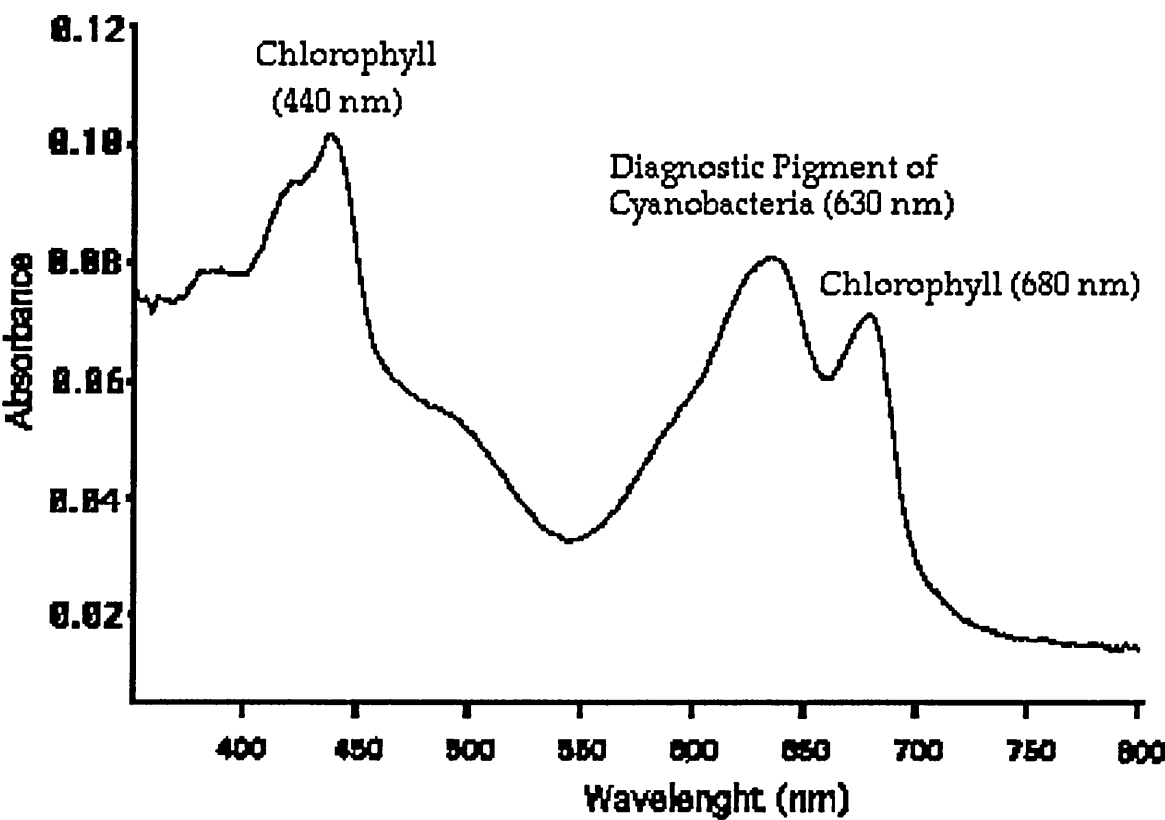


Figure 4.5.1. Absorbance spectrum of pigment from cyanobacteria of Salda lake.

4.6. SEM RESULTS

SEM studies were undertaken on stromatolites from Salda lake. Filaments of cyanobacteria, mucilage, hydromagnesite crystals and diatoms are the basic features of the newly formed (living) stromatolites (Plate 4.6.1). Well-preserved cyanobacterial filaments are the remains of *Lyngbya majuscula*(?) and *Gloeocapsa* whilst poorly preserved are *Cladophora*(?) or *Rhizoclonium*. Hydromagnesite is generally in well developed rose-like crystals resembling miniature "desert roses" (Plate 4.6.2). These are sometimes oriented they are in different size (small or large) (Plate 4.6.3). When we take a closer look to these "desert roses" individual hydromagnesite crystals are clearly blade-like and flat (Plate 4.6.4). Freeze-dried samples show that these are interlayered with diatoms and cyanobacterial filaments. This interlayering probably causes the occurrence of internal lamination in the stromatolites.

Large numbers of diatoms in different sizes have been found (Plate 4.6.5). These are *Navicula* spp., *Cymbella* spp., *Pinnularia*, *Amphora*, *Surirella* and others which are probably responsible for the colour of the stromatolites. Dissolution of these diatoms has been observed within living stromatolites under SEM (Plate 4.6.6). The high levels of pH of the lake water may have been responsible this dissolution.

In older stromatolites of Salda, we have seen no cyanobacterial filaments or diatom. Furthermore, there are no blade-like hydromagnesite rosettes. These components are probably lost during recrystallization although the internal lamination is not.

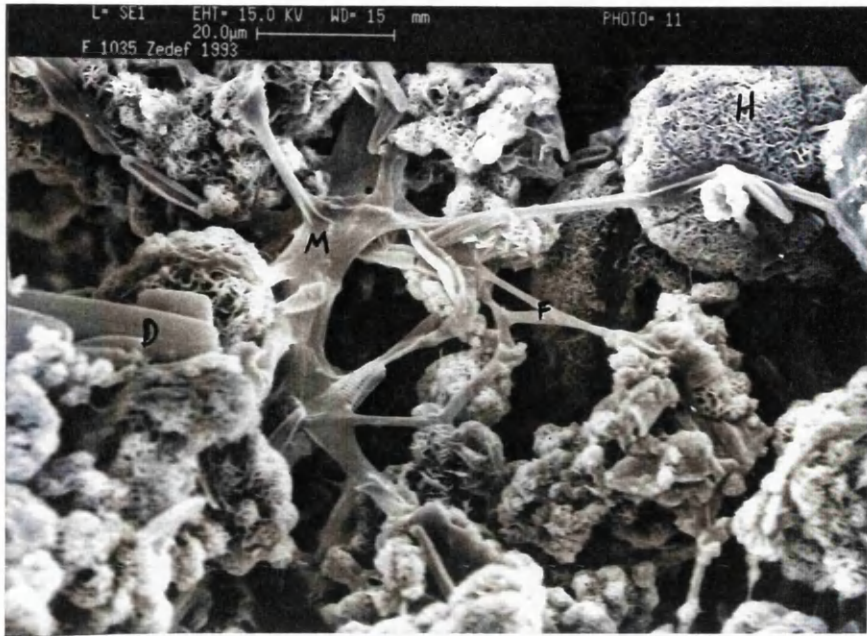


Plate 4.6.1. Cyanobacterial filaments (F), mucilage (M), hydromagnesite crystals (H) and diatoms (D) in the newly formed stromatolites from Salda lake.

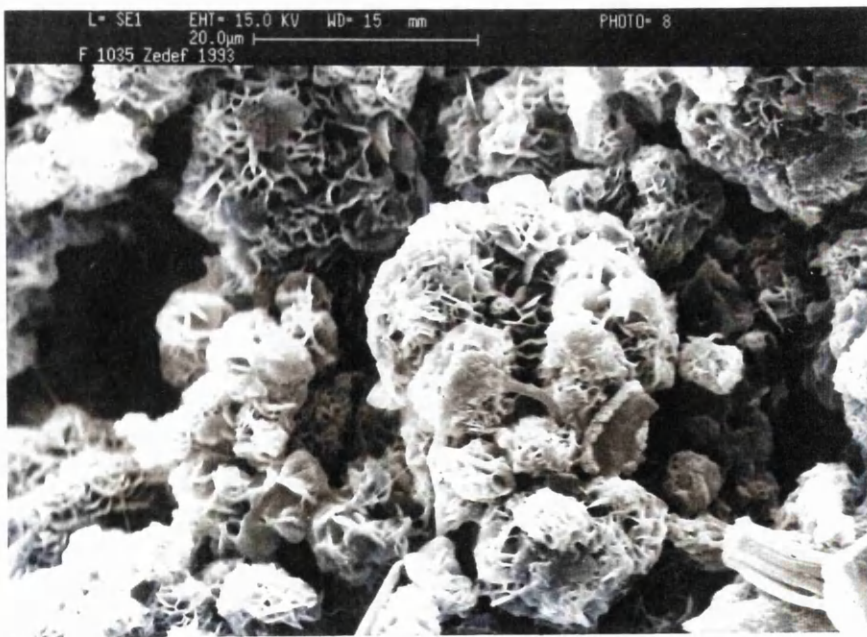


Plate 4.6.2. Perfectly developed, rose-like hydromagnesite crystals "desert roses", Salda lake.

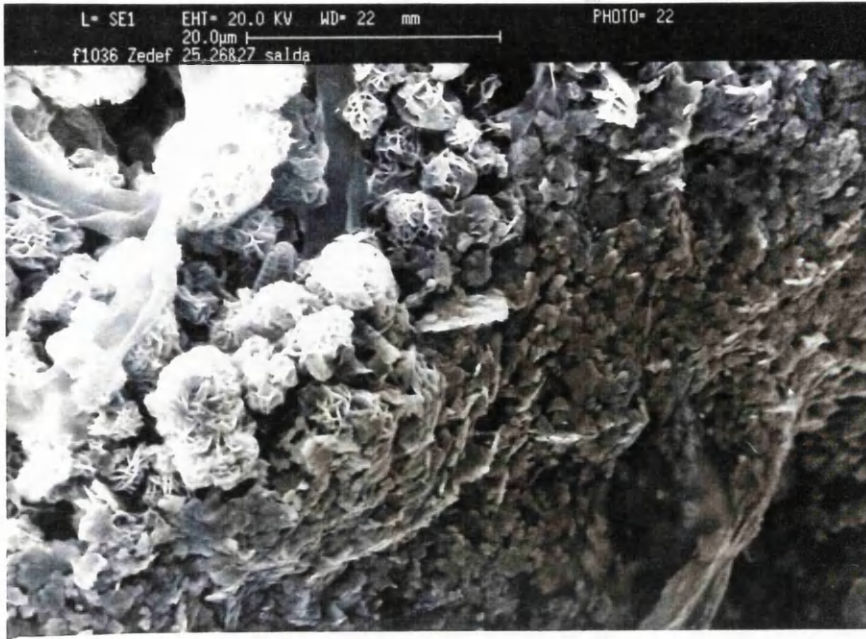


Plate 4.6.3. Orientation of hydromagnesite rosettes, Salda lake.

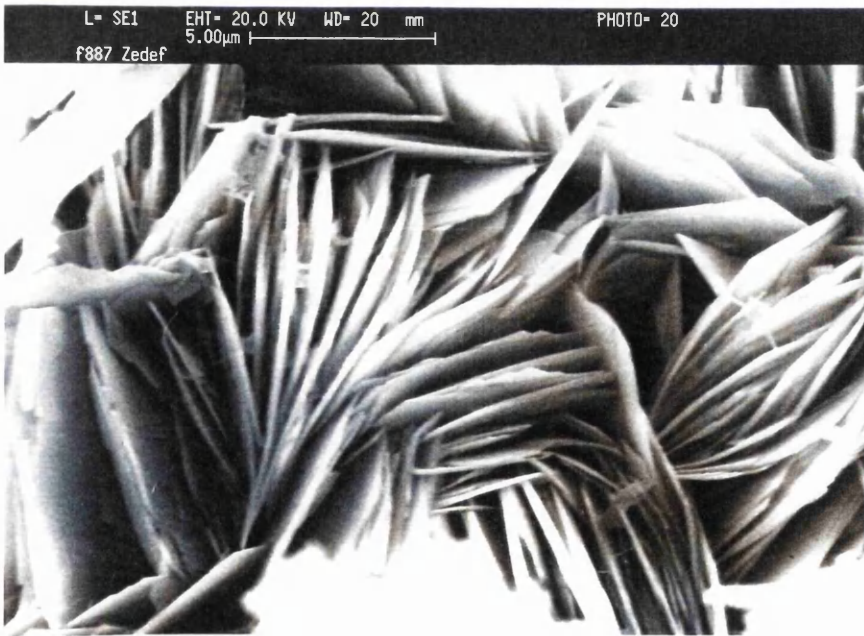


Plate 4.6.4. Blade-like, flat, individual hydromagnesite crystals of Salda lake stromatolites.

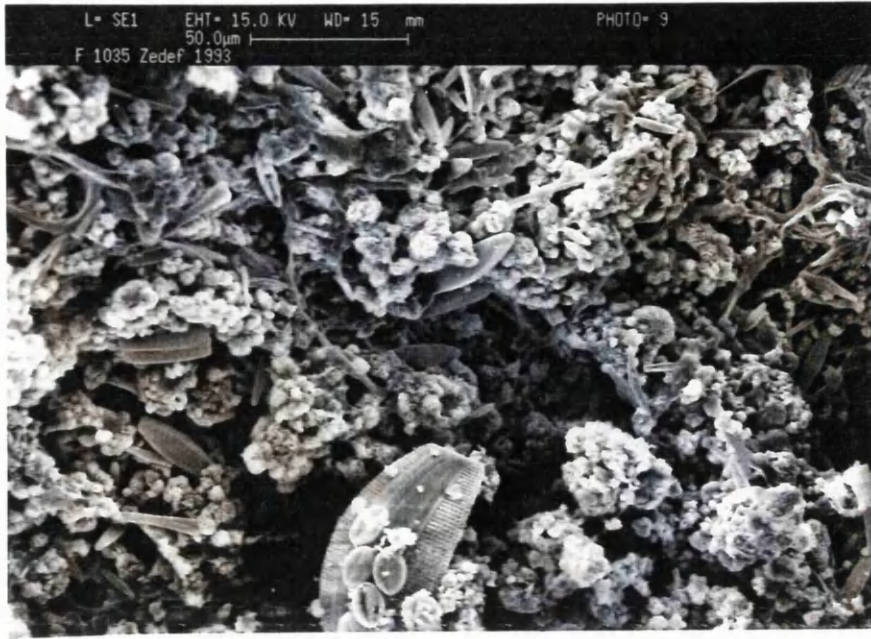


Plate 4.6.5. Scattered, different-sized diatoms with hydromagnesite, from Salda lake.

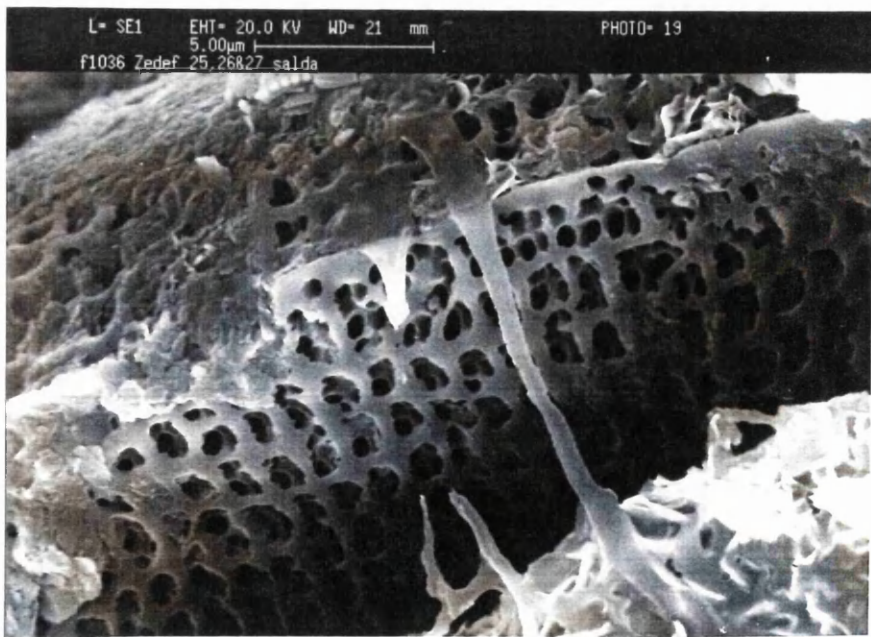


Plate 4.6.6. Surface dissolution of diatom.

CHAPTER FIVE

DISCUSSION AND GENETIC MODELS

INTRODUCTION

The origin of cryptocrystalline, fine-grained magnesite (synonymously used terms are: ultramafic-hosted, ophitic, Kraubath type, amorphous magnesite, gelmagnesite and Khalilova type magnesite) deposits within or above ultramafic rock has been extensively discussed (Ilich, 1968; Dabitzias, 1980; Kralik et al., 1989; Jedrysek and Halas, 1990; Fallick et al., 1991; Abu-Jaber and Kimberley, 1992; Brydie et al., 1993). Hydromagnesite has received less attention, perhaps because it is relatively uncommon, especially in large concentrations.

The source of carbon dioxide and magnesium, and the precipitation mechanism of the carbonate minerals, are the focus of attention. The source of carbon dioxide is especially controversial. It is widely accepted that the source of the magnesium is the ultramafic host-rocks. For the hot-spring travertine deposits, surrounding limestone and dolomite formations have been nominated as a source of calcium (Turi, 1986).

Stable isotope (^{13}C and ^{18}O) analyses of carbonates can be used to derive information regarding the probable source of the mineralising fluid. This is based on the assumption that equilibrium isotopic fractionation was established between carbon dioxide-rich fluids and the precipitating minerals during the mineralisation. The $\delta^{18}\text{O}$ value of the carbonate minerals, as well as

the silicates, is also useful to predict the mineralising temperature, since the fractionation of the isotopes is temperature dependent (O'Neil, 1986; Ohmoto, 1986). Compared to oxygen, carbon isotope fractionation is relatively insensitive to temperature so that carbon isotopes are of little use as geothermometers (Emery and Robinson, 1993). The ^{18}O and D (^2H) signatures of any water (meteoric, magmatic, hydrothermal or sea-water) are often definitive as to the source of the water (Sheppard, 1986). The chemical compositions of the water also help elucidate the hydrological history of the water.

Heavy rare earth elements (HREE) are mobile during carbonation processes (Kerrick and Watson, 1984), because these elements are fairly soluble in HCO_3^- -rich fluids compared to light rare earth elements (LREE) (Humphris, 1984). Therefore, we would expect that the carbonate deposits may show enriched HREE patterns.

The data presented in the previous chapters help in the understanding the generation of the magnesite, hydromagnesite, dolomite and hot-spring travertine deposits of western Turkey. The discussion of the possible genetic processes operating in the formation of the western Turkish carbonate deposits will continue under these headings:

1. Source of carbon dioxide
2. Isotopic composition of the fluids and their temperature
3. Variations of the REE's
4. Source of magnesium and other elements in Salda lake waters
and their surrounds
5. Genetic model
6. Further research

5.1. SOURCE OF CARBON DIOXIDE

The carbon isotope signatures of solutions from which magnesite, hydromagnesite, dolomite and calcite are deposited suggest derivations from various sources. These are: 1. Soil-derived organic CO₂ (decomposition of plant material and plant-root respiration), 2. Decarbonation of carbonate rocks, 3. decarboxylation of organic-rich sediments, 4. Atmospheric CO₂, 5. Magmatic CO₂ (including volcanogenic CO₂). Below I consider the origins of the various type of carbonate deposits.

5.1.1. Cryptocrystalline vein-stockwork magnesites

Soil-derived organic carbon has been advocated as providing carbon dioxide for cryptocrystalline magnesites by Zachmann and Johannes (1989). According to Zachmann and Johannes (*ibid.*), the source of carbon in the circulating meteoric waters is the CO₂ produced in soils by oxidative decomposition of organic matter and plant-root respiration. This CO₂ has $\delta^{13}\text{C}$ values typically ranging from -12 to -14 ‰ for the C₄-type photosynthetic cycle (grass) and -25 to -28 ‰ for the C₃-type photosynthetic cycle (trees) (Hillaire-Marcel, 1986). The mean $\delta^{13}\text{C}$ value of soil-derived CO₂ is around -26 ‰ (Ohmoto, 1986; Veizer, 1990). Because of this extremely light isotopic signature, Zachmann and Johannes (1989) suggested that soil-derived CO₂ may be considered as the primary CO₂ source for cryptocrystalline magnesites having remarkably depleted $\delta^{13}\text{C}$ (values are not specified). Zachmann and Johannes (*ibid.*) also noted the variations of $\delta^{13}\text{C}$ (-21 to -25 ‰) and $\delta^{18}\text{O}$ (-4 to -9 ‰) of soil solutions matching the isotopic variations (not specified) of cryptocrystalline magnesites. Thus they inferred that the source of CO₂ in the cryptocrystalline magnesites may have been soil-generated. If true, one would

expect at least some cryptocrystalline magnesites to have $\delta^{13}\text{C}$ between -21 and -25 ‰, but the lightest observed value, from Polish magnesite deposits is -18.7 ‰. However most values from all over the world are >-15 ‰. Moreover, western part of Turkey is predominantly tree-covered (C3-type plants). Thus, soil-derived CO_2 is unlikely to be the source of CO_2 for the western Turkish cryptocrystalline magnesite deposits, beyond some CO_2 contribution to the circulating groundwater.

Without specifying a particular metamorphic process or metamorphosed rock-type Gartzos (1990) argued for a metamorphic CO_2 source for the North Evia (Greece) magnesite deposits. Gartzos (ibid.) compared the North Evia magnesites with the Red Mountain (USA) deposits. The isotopic compositions of the local meteoric waters were similar as were wall-rock alterations, and style of mineralisation. The $\delta^{13}\text{C}$ ranges from -13.1 to -8.6 ‰, and $\delta^{18}\text{O}$ ranges from 25.4 to 29.9 ‰ so that the isotopic signatures of the deposits were also comparable and Gartzos (ibid.) concluded that the source of CO_2 might have been metamorphic as O'Neil and Barnes (1971) had suggested for the generation of the Red Mountain magnesite deposits.

Metamorphic CO_2 was also considered for the Oshve (Bosnia) magnesite deposit by Fallick et al. (1991). According to Fallick et al. (ibid.), the Oshve vein-type magnesite deposit, found adjacent to a dacite dike, has exceptionally heavy $\delta^{13}\text{C}$ (~3.1 ‰) and light $\delta^{18}\text{O}$ (~19 ‰) values, and these values are consistent with decarbonation generated CO_2 by contact metamorphism of local limestone. Similarly, the origin of the CO_2 in carbonate in the Arapomer Deresi (Burdur, Turkey) stockwork magnesite deposit may partly be from decarbonation of the adjacent carbonate rocks. Although its $\delta^{13}\text{C}$ values are within the range of atmospheric CO_2 , the $\delta^{13}\text{C}$ averages 0.3 ‰. This is

considerable higher ($>10\text{ ‰}$) than that of the other stockwork magnesites, for example, Helvacibaba and Kozagac. This enrichment may have been due to decarbonation or at least dissolution of carbonate rocks.

However, from the isotopic signatures of the magnesite, hydromagnesite and calcite deposits of western Turkey, three end-members can be recognised (Figure 4.1.1). These are: end-member-1 is dominated by decarboxylation generated carbon dioxide, end-member-2 is dominated by atmospheric carbon dioxide, and end-member-3 is dominated by decarbonation generated carbon dioxide. The carbonate veinlets within the organic-rich meta-argillites of Seydisehir formation represent end-member-1, with the lightest $\delta^{13}\text{C}$ ($\sim -19.4\text{ ‰}$) and extremely light $\delta^{18}\text{O}$ ($\sim +22.2\text{ ‰}$) values. The presently forming hydromagnesite deposits at Salda represent end-member-2, with the heaviest $\delta^{18}\text{O}$ ($\sim +35.9\text{ ‰}$) and relatively heavy $\delta^{13}\text{C}$ ($\sim +4\text{ ‰}$) values. Finally, presently forming hot-spring calcite deposits at Pamukkale represent end-member-3, with the heaviest $\delta^{13}\text{C}$ ($\sim +6.1\text{ ‰}$) and lightest $\delta^{18}\text{O}$ ($\sim +20.7\text{ ‰}$). In a broad sense, the isotopic values of all the other deposits fall between these three end-members on the $\delta^{13}\text{C}$ versus $\delta^{18}\text{O}$ plot (Figure 4.1.1).

The existence of organic-rich sediments underneath ultramafic-hosted magnesite deposits has been widely reported from all over the world. For example, on Margarita island, Venezuela (Abu-Jaber and Kimberley, 1992); in the northern part of the Bohemian massif, Poland (Jedrysek and Halas, 1990); in Serbia (Fallick et al., 1991); and in the Akamas area of Cypriot Cyprus (Brydie et al., 1993). Furthermore, the similar values are noted from fluid inclusions of quartz from the Naxos area, Greece (Kreulen, 1980) and from siderites from the North sea (Macaulay et al., 1992). This is why the hypothesis of

"decarboxylation of organic-rich sediment generated CO₂" in the cryptocrystalline magnesites must be examined with extra care.

Abu-Jaber and Kimberley (*ibid.*) worked on ultramafic-hosted vein-type magnesite deposits at Margarita island, Venezuela, and concluded that the source of the CO₂ in the magnesite may have been deep-seated metamorphic reactions. According to them, $\delta^{13}\text{C}$ signatures of the magnesite (ranging from -16 to -9‰) indicate that the organic-rich limestone and shales beneath the ultramafic host-rocks must have been metamorphosed (up to 10 km below the surface and at >300°C) to provide the extremely light ^{13}C .

The magnesite deposits within the Foresudetic Block ophiolites (Northern Bohemian massif, Poland) have large variations of $\delta^{13}\text{C}$ (-18.7 to -4.4 ‰) (Jerdysek and Halas, 1990). Jerdysek and Halas (*ibid.*) interpreted these results and suggested that most of the CO₂ must have come from the oxidation of organic-rich sediments underneath the ultramafic rocks, although they remarked that some of CO₂ may have had a mantle origin.

In a review of the $\delta^{13}\text{C}$ and $\delta^{18}\text{O}$ isotope systematics of magnesite deposits from all over the world, Kralik et al. (1989) suggested that the oxidation of organic-rich sediments below magnesite deposits could be the source of CO₂ in cryptocrystalline, vein-stockwork type magnesites. Kralik et al. (*ibid.*) also noted that most $\delta^{13}\text{C}$ values lie between -12 and -9 ‰PDB and most $\delta^{18}\text{O}$ values vary between 22 and 29 ‰SMOW.

In the Naxos area, Greece, the fluid inclusions of quartz segregations in schists have $\delta^{13}\text{C}$ values between -16 and -6 ‰, and these values have been

interpreted as resulting from the oxidation of organic carbon in nearby graphite (Kreulen, 1980).

Decarboxylation of organic-rich sediments underthrust beneath ultramafic-hosted magnesite deposits has also been suggested as the source for the extremely light $\delta^{13}\text{C}$ ($<-10\text{‰}$) values for Serbian magnesite deposits (Fallick et al., 1991). They advocated an origin by mixing of two end-member (lightest and heaviest) of both $\delta^{13}\text{C}$ and $\delta^{18}\text{O}$ for the Serbian magnesite deposits. The lightest isotopes represent the carbon dioxide in the vein-type deposits generated by decarboxylation, and the heaviest isotopes represent atmospheric carbon dioxide in the sedimentary magnesite deposits. The values between the lightest (-14 and $+25\text{‰}$ for $\delta^{13}\text{C}$ and $\delta^{18}\text{O}$ respectively) and heaviest ($\delta^{13}\text{C}=\sim+3.5\text{‰}$ and $\delta^{18}\text{O}=\sim+36\text{‰}$) have been explained by a mixing of groundwater containing atmospheric CO_2 and that containing decarboxylation-generated carbon dioxide with the exception of the Oshve vein magnesites (Bosnia) which are possibly related to thermal decarbonation (Fallick et al., *ibid.*).

Brydie et al. (1993) favour a decarboxylation generated carbon dioxide for their values of $<-8\text{‰}$ $\delta^{13}\text{C}$ for the magnesite deposits on Akamas area, Cypriot Cyprus. Similarly, Macaulay et al. (1992) have interpreted the $\delta^{13}\text{C}$ values (ranging from -14.6 to -8‰ $\delta^{13}\text{C}$) of siderites in the North Sea and concluded that organic-rich Kimmeridgian mudstones may have been decarboxylated and thus produced the carbon dioxide responsible for the light $\delta^{13}\text{C}$ in the siderites.

As indicated, the formation of cryptocrystalline vein-stockwork type magnesite deposits with extremely light $\delta^{13}\text{C}$ isotopes, generally implies

organic-rich sediment(s) as a source of their carbonate. Perhaps the crucial question is whether this isotopically light carbon dioxide is produced by metamorphic decarbonation or by decarboxylation of the organic-rich sediments underthrust beneath the ultramafic host-rocks. Because of this the isotopic composition of the carbon dioxide released by metamorphism and decarboxylation must be compared.

It is clearly not possible to generate a $\delta^{13}\text{C}$ value lower than -4‰ by decarbonation (metamorphism) of marine carbonates, unless they are particularly rich in organic matter, because marine carbonates generally have a $\delta^{13}\text{C}$ $0\pm 4\text{‰}$ (Emery and Robinson, 1993; Field and Fifarek, 1985; Salomons and Mook, 1986). Hence, carbon dioxide produced by metamorphism of limestone should have $\delta^{13}\text{C}$ values heavier than -4‰ . Thus the involvement of organic matter must be implicated to explain light $\delta^{13}\text{C}$ values (i.e. $<-5\text{‰}$) in cryptocrystalline, vein-stockwork magnesites. It may be envisaged that mixing of metamorphically generated carbon dioxide with that generated by the oxidation of organic matter within marine carbonates could explain lower values (Barnes et al., 1973; Kreulen, 1980; Hladikova et al., 1981). According to Fallick et al. (1991), such a process may give an eventual precipitation of magnesite having a higher than 0‰ $\delta^{13}\text{C}$. Fallick et al. (ibid.) also suggested that mixing may give a broader range of $\delta^{13}\text{C}$ values than in observed cryptocrystalline (especially vein-type) magnesites in Serbia which have very restricted $\delta^{13}\text{C}$.

The decarboxylation of organic-rich sediments starts at temperatures of around $70\text{-}75^\circ\text{C}$ (Curtis, 1978; Emery and Robinson, 1993), and the process gives a range of $\delta^{13}\text{C}$ values between -10 and -25‰ for carbon dioxide (as bicarbonate) (Irwin et al., 1977). However, prior to the decarboxylation

"bacterial fermentation" also produces CO_2 . This process ends before decarboxylation begins (Irwin et al., *ibid.*). The fermentation of organic matter (taking place at temperature of 0.3 to $\sim 70^\circ\text{C}$ and down to 1000 metres, Irwin et al., 1977) is inevitable before decarboxylation (taking place at $70\text{--}75^\circ\text{C}$ and ~ 1000 metres depth). However, the bacteria involved in fermentation at over 30°C are very specialised and this process appears to be extremely rare (Fallick, *pers. commun.*). Moreover, the carbon isotopic composition of fermentation-generated carbon dioxide is, according to Irwin et al. (1977), about +15 ‰. Thus, for two reasons this possibility is not considered further for the carbonate deposits of western Turkey.

So far we have seen that the best possible explanation of the $\delta^{13}\text{C}$ values lighter than -10 ‰ (perhaps < -8 ‰) in the magnesites is the decarboxylation of organic-rich rocks which underthrust beneath the ultramafic host-rocks. This could explain the carbon dioxide source for the Koyakci Tepe and Sodur vein-type magnesites of Konya. These two deposits have the lightest carbon isotope values (-13.1 and -12.4 ‰ respectively) among the Turkish magnesite deposits investigated here. There is probably less bicarbonate from meteoric sources incorporated during the formation of these deposits. The stockwork deposit at Helvacibaba has a mean $\delta^{13}\text{C}$ of -11.1 ‰ so carbon dioxide may also have been derived from decarboxylation, although the involvement of bicarbonate from meteoric water may have been greater than in the vein deposits.

There is a systematic isotope variation with depth in the east side of the Helvacibaba open pit mine. The $\delta^{13}\text{C}$ values become gradually negative towards the top. The $\delta^{13}\text{C}$ values are about 3 ‰ more negative at the top than at the bottom (Figure 4.1.9). This may be explained by (a) more than one source of CO_2 feeding the deposit, (b) more negative $\delta^{13}\text{C}$ of CO_2 is involved during

the formation of the upper part of the east-side of the deposit or (c) the isotopic variations may be merely variance since a similar trend is not observed in the west side of the open pit (Figure 4.1.9). In fact only two samples (9E and 11E) from the top of the east-side of the deposits are responsible for this apparent overall depletion through to the top. We have seen no systematic isotope exchange with depth in terms of $\delta^{18}\text{O}$ values in either the east-side or the west-side of the open pit (Figure 4.1.9). Thus it could be concluded that there was no significant temperature change during magnesite mineralisation.

The quartz samples from the silica cap of Helvacibaba have $\delta^{18}\text{O}$ values averaging 24.8 ‰ which are about 2.4 ‰ lighter than those of the associated magnesites (~27.2 ‰). If we assume that the temperature of the fluid remained unchanged, the isotopic signatures of both magnesite and quartz should be similar, since the difference in isotopic fractionation between magnesite-fluid and quartz-fluid at the same temperature is as little as 0.5 ‰. Take for example the temperature of 80°C, the isotopic fractionation between magnesite-fluid (a) and quartz-fluid (b) is as follows;

$$\delta^{18}\text{O}_{\text{magnesite}} - \delta^{18}\text{O}_{\text{fluid}} = \frac{3.53 \times 10^6}{(273+80)^2} - 3.58 = 24.75 \text{ ‰} \quad (\text{a})$$

$$\delta^{18}\text{O}_{\text{quartz}} - \delta^{18}\text{O}_{\text{fluid}} = \frac{3.38 \times 10^6}{(273+80)^2} - 2.90 = 24.22 \text{ ‰} \quad (\text{b})$$

$$\text{Thus } \delta^{18}\text{O}_{\text{magnesite}} - \delta^{18}\text{O}_{\text{quartz}} = 0.53 \text{ ‰}$$

So, we can see that there is no significant fractionation between magnesite and quartz so long as they are derived from the same fluid at about the same temperature. But, as indicated above, the $\delta^{18}\text{O}$ values of the quartz samples are about 2.4 ‰ lighter than those of the magnesites. This indicates

that at Helvacibaba the temperature during the precipitation of the quartz was at least 20°C higher than that during the precipitation of magnesite. The fractionation between quartz and fluid at temperature 100°C is as follows;

$$\delta^{18}\text{O}_{\text{quartz}} - \delta^{18}\text{O}_{\text{fluid}} = \frac{3.38 \times 10^6}{(273+100)^2} - 2.90 = 22.47 \text{ ‰}$$

The difference in fractionation between magnesite at 80°C and quartz at 100°C is: 24.75-22.47= 2.28 ‰. But this temperature difference is surprising in that the silica cap overlies the magnesite deposits, and would more probably have been precipitated at lower temperatures than the magnesite. The lower $\delta^{18}\text{O}$ values of silica resulted from precipitation of $\delta^{18}\text{O}$ depleted fluid, or from an error in the fractionation factors between magnesite-water and quartz-water, or the silica could be precipitated at depth as a colloid but transported by entrainment in the hydrothermal solution to the surface.

Two quartz samples from Koyakci Tepe have $\delta^{18}\text{O}$ values of 26.3‰. These values are similar to the mean $\delta^{18}\text{O}$ values of related magnesites (~26.7‰) at Koyakci Tepe. It is therefore probable that both magnesite and quartz precipitated at the same temperatures.

Other stockwork deposits at Yunak and Kozagac have $\delta^{13}\text{C}$ values of -8.9 and -8.1 ‰ respectively. These values are different, about 4 ‰ heavier than the vein-types and 2.5 ‰ heavier than those of the stockwork deposits. This could be explained by a mixing of extremely light CO_2 , generated by decarboxylation with relatively heavy atmospheric CO_2 (as bicarbonate) in the hydrothermal fluids.

One stockwork deposit (?) in Kavakarasi has quite scattered $\delta^{13}\text{C}$ values (-5.5 to -11 ‰). However, the samples were collected from the surface and are

of uncertain origin. It is possible the isotopic signatures of these samples may have been altered. Despite the large variations of $\delta^{13}\text{C}$, it can be said that the negative values perhaps indicate a mixing of decarboxylation generated carbon dioxide with circulating meteoric water.

With the decarboxylation of organic matter as a source of light ^{13}C (Fallick et al., 1991) in mind, carbonates from veinlets in an organic-rich meta-argillite of Cambrian-Ordovician age (within the Seydisehir formation, Figure 2.1) were analysed. These organic-rich meta-argillites were selected because they are found beneath the thrust and/or folded older Caltepe formation rocks and may well lie beneath the serpentinites hosting the Helvacibaba and associated magnesite deposits. They may have provided the carboxylic acids which were the putative source of the carbonate. If so, the calcite veinlets might be expected to be light. In the event, the calcites collected from the Seydisehir formation average -19.4‰ $\delta^{13}\text{C}$ and $+22.2\text{‰}$ $\delta^{18}\text{O}$. These values are much lower than the $\delta^{13}\text{C}$ and $\delta^{18}\text{O}$ values of either vein or stockwork magnesites but what is important is that they lie on the line drawn by Fallick et al. (1991) for Serbian magnesite deposits and could represent the light $\delta^{13}\text{C}$ and $\delta^{18}\text{O}$ end-member, i.e. the deep source. Moreover, south-western Turkish cryptocrystalline, vein-stockwork magnesite deposits (except for Arapomer Deresi), all plot on the same line. This adds further support to the hypothesis of Fallick et al. (ibid.) which favours decarboxylation-generated CO_2 as a source of carbonate in the magnesite deposits.

The limestone formations of the Konya region are unlikely to have been the source of CO_2 for the cryptocrystalline, vein-stockwork type magnesite deposits found in Koyakci Tepe, Sodur, Helvacibaba, Yunak and Kozagac (all in Konya region). The $\delta^{13}\text{C}$ values of samples from these limestones range from

-4.6 to +3.6 ‰, approximately within the range of normal marine limestones (± 4 ‰). Yet the $\delta^{18}\text{O}$ values are very variable and extend from 17.7 to 29.3 ‰ (Table 4.1.1). The $\delta^{18}\text{O}$ values of marine limestones are close to 31‰ whereas those of nonmarine carbonates are lighter because freshwater is depleted in ^{18}O (Faure, 1991). The ^{13}C and ^{18}O isotopic signatures of two calcite samples from the olistolitic limestones within the serpentinitised ultramafic rocks represent the lightest $\delta^{13}\text{C}$ (-4.6 and -3.9 ‰) and $\delta^{18}\text{O}$ (20.7 ‰ for both samples) values among the limestone formations (Figure 4.1.1). These results are interpreted as indicating that the olistolitic limestones were very probably altered during and/or following the obduction of the ultramafic rocks in Upper Cretaceous times, probably as a result of the interaction between marine limestones and meteoric ground waters, and perhaps related to the mineralising event.

5.1.2. Sedimentary-hydrothermal deposits

Atmospheric CO_2 has a $\delta^{13}\text{C}$ close to -7 ‰ (Bottinga and Craig, 1969; Keeling et al., 1979). If carbon from other sources (organic or inorganic) is absent, surface waters in equilibrium with the atmosphere should generate magnesite, hydromagnesite, calcite and dolomite with $\delta^{13}\text{C}$ values similar to those of marine carbonates (0 ± 4 ‰). Such values are recorded for the lacustrine, sedimentary-hydrothermal magnesite deposits of Hirsizdere (Denizli, Turkey), Tsakasimta (Chad Basin, Nigeria), as well as the Salda lake hydromagnesite deposits.

Hirsizdere and Tsakasimta magnesite deposits

Sedimentary-hydrothermal, strata-bound magnesite deposits at Hirsizdere (Turkey) and Tsakasimta (Chad Basin, Nigeria) have $\delta^{13}\text{C}$ values of

2.6 and 2.7 ‰ respectively (Table 4.1.1). The $\delta^{18}\text{O}$ isotopic signatures of both the Hirsizdere (25.2 ‰) and Tsakasimta (25.8 ‰) magnesite deposits are exceptionally low compared to those of other sedimentary deposits. These extremely low $\delta^{18}\text{O}$ values imply depositional temperatures of $\sim 100^\circ\text{C}$ in a lacustrine environment. Obviously the temperature of the mineralising solutions may have been higher, for example 120°C , before reaching to the lake bottom.

With the low $\delta^{18}\text{O}$ values in mind, the high $\delta^{13}\text{C}$ values (range from -0.3 to +4.4 ‰) of Hirsizdere lacustrine, stratabound-sedimentary magnesite deposits indicate that the CO_2 was a mixture of atmospheric carbon dioxide with decarbonation generated carbon dioxide. These $\delta^{13}\text{C}$ signatures are comparable with certain, well-defined sedimentary and volcanic related vein type of magnesite deposits, for example, the Serbian and Bosnian ultramafic-hosted magnesite deposits (Fallick et al., 1991). However, unusually low $\delta^{18}\text{O}$ values (between 21.6 to 26.5 ‰) are lower than the expected values of sedimentary magnesite deposits. This could be explained by precipitation temperatures between 90 and 100°C . The geological situation of Hirsizdere (See figure 2.1, in chapter-2) appears to lend itself to the decarbonation hypothesis; the deposit itself seems to be associated with Neogene andesitic rocks and occurs at the edge of a main fault and much of the CO_2 may have been derived from the decarbonation (by thermal metamorphism) or dissolution of carbonate rocks. Two calcite samples from the Cretaceous limestones of Salda lake have $\delta^{13}\text{C}$ and $\delta^{18}\text{O}$ values of 2.0 and 30.4 ‰ respectively. These values are to be expected of marine limestones. Although the sampling site is about 15 km away from Arapomer Deresi, and 50 km away from the Hirsizdere magnesite deposits, it is possible that these or similar limestone or dolomite formations in the region may have provided carbonate for the Hirsizdere sedimentary and

Arapomer Deresi stockwork magnesite deposits. Similar explanations could be made for the Tsakasimta magnesite deposit.

Systematically collected samples from the top bed of Hirsizdere show a systematic decrease in $\delta^{13}\text{C}$ values from the base of the bed through to the top (Figure 4.1.5). Similar relations are not observed in one of the bottom beds (Figure 4.1.5). A systematic decrease of $\delta^{13}\text{C}$ towards the top of the top bed could be explained by the involvement of a small amount of organic matter derived from the lake water during deposition. However, there is no significant systematic $\delta^{18}\text{O}$ isotope exchange in either top or bottom beds (Figure 4.1.6) implying that there has been no significant temperature change during the mineralisation, i.e. not more than 3 to 5 °C. Nevertheless, the vegetation around the lake may have been very much affected by small temperature changes. It is possible to imagine that if the overall temperature gradually increased during the time of the formation of the top bed, the vegetation around and in the lake may have increased and lake may have become stagnant. An excess of organic matter (representing light $\delta^{13}\text{C}$ compared to atmospheric CO_2) could have built up in the lake water. However, the carbonate in the magnesite is predominantly of metamorphic (and may be partly atmospheric) origin and the contribution of organic matter was minor.

Helvacibaba detrital magnesites and bedded dolomites

Three magnesite pebbles from the conglomeratic level overlying the Helvacibaba stockwork magnesite deposits have $\delta^{13}\text{C}$ values about 3‰ heavier whereas $\delta^{18}\text{O}$ values are 2 ‰ lighter compared to those of the underlying stockwork magnesite (Table 4.1.1). The values of samples from overlying lacustrine bedded dolomites are similar to those of the conglomerates. The $\delta^{13}\text{C}$

values of the bedded dolomites are 3.7 ‰ heavier and the $\delta^{18}\text{O}$ 1.8 ‰ lighter than those of the stockwork magnesites. The simplest explanation of the isotopic characters of the stockwork-derived magnesite pebbles is that they have been altered by atmospheric carbon dioxide and/or re-equilibrated with the lake water in which the dolomite was deposited.

Salda lake hydromagnesites

As indicated, scanning electron microscope observations and absorbance spectrometer analyses show that there are two distinct microbiotas in the stromatolites, these are cyanobacteria and diatoms. These microbial communities form thick, gelatinous coatings on rock fragments and on wood branches and even on grasses. The rosette-like clusters of bladed hydromagnesite crystals are found within these coatings. There is no indication of any direct precipitation of hydromagnesite from the surface waters of the lake itself or from warmer pools on delta margins. Presently forming hydromagnesite at Salda lake is apparently associated with the cyanobacteria comprising the microbialites, although the actual process is not understood. It may have something to do with pH changes associated with the fixation of carbon from carbon dioxide by the bacteria (Burne and Moore, 1987). Alternatively it may simply be a result of trapping of hydromagnesite precipitated at the lake surface as magnesium ions react with atmospheric carbon dioxide, the resulting particles then being trapped in the mucilaginous exterior of the mounds (Burne and Moore, *ibid*). More specifically it may be that the carboxylate groups contained in the polysaccharide sheaths of the Cyanobacteria provide the initial nucleation sites for the precipitation of the magnesium ions in the warm waters seeping through the mounds (cf. Pentecost, 1978). One process we can probably rule out is the intercellular

precipitation of carbonate for only one fresh water bacterium is known to have this propensity, namely *Achromatium oxaliferum* (Balows et al., 1991).

In terms of heavy $\delta^{13}\text{C}$ (averages 4.0 ‰) and $\delta^{18}\text{O}$ (averages 35.9 ‰) the presently forming, microbially precipitated hydromagnesites of Salda lake are representative of end-member-2 in the plot shown in Figure 4.1.1. Their $\delta^{13}\text{C}$ and $\delta^{18}\text{O}$ values are broadly comparable with those of other sedimentary magnesite, dolomite, huntite and calcite samples from elsewhere in the world. For instance, the Bela-Stena magnesite deposits of Serbia (Fallick et al., 1991), the magnesite and huntite deposits of Servia, Macedonia (Kralik et al., 1989), the evaporitic magnesite and dolomite deposits of Coorong Lagoon, South Australia (Botz and von der Borch, 1984), microbial carbonates of Sleaford and lake Felimonger, South Australia (Burne and Moore, 1987) and even one cryptocrystalline stockwork magnesite deposit at Miokovachi Beli Kamen, Serbia (Fallick et al., *ibid.*). All of these have heavy ^{13}C and ^{18}O isotopic elements indicating CO_2 of atmospheric origin. The heavy $\delta^{13}\text{C}$ and $\delta^{18}\text{O}$ values of the carbonates, particularly in the lacustrine environments may be explained either by bacterial fermentation or evaporation processes, therefore I would like to consider these processes in some detail.

According to Zachmann (1989), bacterial fermentation produces unusually ^{13}C -rich CO_2 . Fermentation has an important effect on stable isotopes, because the bacteria preferentially fix the lighter isotope (Morse and Mckenzie, 1990). Riding (1992) states, that cyanobacteria prefer alkaline conditions in freshwater, while Burne and Moore (1987) point out that the preferential use of the lighter isotope ^{12}C by cyanobacteria during photosynthesis results in an enrichment of ^{13}C in the surrounding microenvironment of the organism. In the case of Salda lake the precipitation of

hydromagnesite is apparently driven by cyanobacteria and there is no evidence of inorganic precipitation directly from the water. The predominant climate is between what can be described as 'Mediterranean' and 'intercontinental', a fraction cooler than typical Mediterranean coastal areas but warmer than continental. According to Gonfiantini (1986), the average annual temperature in the Turkish Lake District which includes Salda lake is about 12°C while the relative humidity is 60±5 %. Thus, it can easily be inferred that there is no intensive evaporation from the Salda lake. The δD content ($\sim +3.5$ ‰) and $\delta^{18}O$ content ($\sim +2.8$ ‰) of the Salda lake water contrasts strongly with that of evaporitic lakes, such as those at Guelta Gara Dibah and Sebkha el Melah in the western Sahara. These have about +130 ‰ δD and +31 ‰ $\delta^{18}O$ (Gonfiantini, 1986). I suggest that the isotopic composition of Salda lake water and of the hydromagnesite has probably not been significantly affected by evaporation. However there is no direct evidence that the carbon and oxygen isotopes of the hydromagnesite were affected by biological processes. It is possibly the lake water is in equilibrium with the atmospheric carbon dioxide since it is also possible that the lake water has a sufficient residence time (remember there is no outflow and inflow to the Salda lake) to be equilibrated with the atmospheric carbon dioxide. The $\delta^{13}C$ and $\delta^{18}O$ of the aragonitic mud, in the northern shore of the lake, are 4.7 and 35.3 ‰ respectively. These values are quite similar those of hydromagnesite which averages 4.0 and 35.9 ‰ for $\delta^{13}C$ and $\delta^{18}O$ respectively (see Table 4.1.1). This indicates that the source of carbon dioxide in the aragonitic mud is also of atmospheric origin.

Pamukkale hot-spring travertine deposits

Pamukkale calcite travertines have $\delta^{13}C$ values ranging from 5.3 to 7.2 ‰ (average 6.1 ‰, see table 4.1.1). According to Turi (1986), in general CO_2

with $\delta^{13}\text{C}$ values roughly within the range of marine limestones should be regarded conservatively as being derived from these rocks. High $\delta^{13}\text{C}$ can be produced from limestone through metamorphic reactions. It is possible that the CO_2 supplying the hot-spring calcite travertine deposits in Pamukkale, western Turkey is metamorphically generated, and that these travertines represent end-member-3 in the plot of $\delta^{13}\text{C}$ versus $\delta^{18}\text{O}$ (Figure 4.1.1). Shieh and Taylor (cited in Turi, 1986) report that CO_2 liberated by decarbonation of carbonate rocks during contact metamorphism is about 6 ‰ richer in $\delta^{13}\text{C}$ than the original carbonate. This CO_2 dissolves in groundwaters at depth and the CO_2 -charged water can, in turn, react with the carbonate rocks. A solution rich in high- ^{13}C carbon species is thus obtained, which conceivably generates travertine with heavy $\delta^{13}\text{C}$ at the surface. Assuming source marine limestone to have $\delta^{13}\text{C}$ values between -4 and +4 ‰, this process could produce carbonate having $\delta^{13}\text{C}$ between +2 and +10 ‰. On this basis, it is possible that many large scale thermal travertines derive from such sources. For example travertines at Latium and Tivoli (Italy), which have $\delta^{13}\text{C}$ values between +2 and +10 ‰, gain their CO_2 from Mesozoic limestones (Turi, *ibid.*). A similar explanation probably holds for the heavy ^{13}C isotopes of the travertines from Iran ($\delta^{13}\text{C}$ between +9 and +11 ‰) and Slovakia ($\delta^{13}\text{C}$ between 0 and +10 ‰) studied by Demovic et al. (1972).

However, travertines with extremely light $\delta^{13}\text{C}$ and $\delta^{18}\text{O}$ values have been reported from Burro Mountain, Cazadero and Red Mountain, in California. The $\delta^{13}\text{C}$ values of these travertines range from -11.0 to -23.9 ‰ and the $\delta^{18}\text{O}$ values vary between +10.5 and 26.9 ‰ (O'Neil and Barnes, 1971). According to O'Neil and Barnes (*ibid.*), the precipitation of these travertines is from waters that have a particular composition i.e. $\text{pH} > 11$, and are enriched in Ca^{2+} and OH^{-1} . O'Neil and Barnes (*ibid.*) argue that as the pH is extremely

high, the reaction between atmospheric CO_2 and water in the pools is very rapid. During this reaction, atmospheric CO_2 comprising the lighter isotope, ^{12}C dissolves more quickly than CO_2 in which the carbon is ^{13}C which confers a higher reactivity. This results in HCO_3^- bearing waters with a very low $^{13}\text{C}/^{12}\text{C}$ ratio. The same argument applies to oxygen, explaining the light $\delta^{18}\text{O}$ values in these American travertines.

5.1.3. Marine limestones

Calcite samples from limestone formations of various ages from western Turkey have rather uniform $\delta^{13}\text{C}$ values, although their $\delta^{18}\text{O}$ values are very variable (Table 5.1.1). There is a negative correlation between $\delta^{18}\text{O}$ values and the age of the marine limestones that is, the $\delta^{18}\text{O}$ of the calcite minerals progressively increases with decreasing age. This could be explained by; (1) the Palaeozoic oceans being about 70°C warmer than today's ocean waters, (Knauth and Epstein, 1976; Knauth and Lowe, 1978). In a recent study, Schwartzmann and McMenamin (1993) indicate that the earth surface was probably warmer ($60\text{-}70^\circ\text{C}$) in the Archean, (2) the original ^{18}O isotopic signatures of the marine carbonates having been altered by subsequent recrystallisation in groundwater rich in HCO_3 (Clayton and Degens, 1959; Degens and Epstein, 1962), or (3) the $\delta^{18}\text{O}$ of the ancient ocean water being 12 to 18 ‰ lighter than the modern ocean (Perry, 1967). These possibilities have been extensively discussed (Veizer, 1986; Brand and Veizer, 1981; Perry et al., 1978; Veizer, 1990; Beaty and Taylor, 1982).

Name**	$\delta^{13}\text{C}$	$\delta^{18}\text{O}$	Age
Salda lake (2)	2.0	30.4	Cretaceous
Midos (4)	1.6	29.0	Cretaceous
Loras (2)	-4.3	20.7	Jurassic-Upper Cretaceous
Bozkir (2)	3.6	24.8	Jurassic
Ardicli (2)	2.1	24.1	Permian-Lower Jurassic
Caltepe (4)	-19.7	21.7	Cambrian-Ordovician
Caltepe (3)	0.6	19.3	Cambrian

* The limestones of Salda lake (Figure 2.7) and Bozkir are not specifically named formations, The Midos and Ardicli formations have been included in the geological map (Figure 2.2). Note that the organic-rich carbonates of Seydisehir are of Cambrian-Ordovician age whilst the Caltepe limestone is nodular and of Cambrian age.

** Number of analysed samples within brackets.

However, for precise calculations, we must know either the temperature or the ^{18}O isotopic composition of the ancient ocean water, since the equation ($10^3 \ln a \cong \delta^{18}\text{O}_m - \delta^{18}\text{O}_w = A(10^6 T^{-2}) + B$, O'Neil, 1986) used includes three variables. These are, the temperature, the $\delta^{18}\text{O}$ of the water, and the mineral which precipitates from the water. In this case only the $\delta^{18}\text{O}$ value of the mineral is measurable (for further explanations see section 5.2, the "isotopic compositions of the fluids and their temperature").

It is possible that the isotopic composition of marine limestones, including western Turkish limestones, has been widely altered by local meteoric waters. It could be said that isotopic equilibrium between meteoric waters and marine limestones may be more established in older limestones than in younger ones.

5.2. ISOTOPIC COMPOSITION OF THE FLUIDS AND THEIR TEMPERATURE

In order to calculate the isotopic composition of the fluids responsible for mineralisation the equation of O'Neil is used (1986);

$$10^3 \ln \alpha \cong \delta^{18}\text{O}_m - \delta^{18}\text{O}_w = A(10^6/T^2) + B \quad (\text{a})$$

where $10^3 \ln \alpha$ is the per mil fractionation between mineral (m) and water (w); temperature (T) is in Kelvin, and A and B are special constants for every mineral (Table 5.2.1). As seen from the equation, there are three variables. These are, $\delta^{18}\text{O}_m$, $\delta^{18}\text{O}_w$ and temperature. In most cases, only $\delta^{18}\text{O}_m$ is measurable. This is why either the temperature (T) or the isotopic composition of the mineralising fluid ($\delta^{18}\text{O}_w$) must be estimated. In the study of the presently forming hydromagnesite in Salda lake, all three variables could be measured since mineralisation is still taking place.

A temperature of 80°C has been suggested for the deposition of cryptocrystalline vein-stockwork type magnesites because of their monomineralic nature and the very fine-grained nature of the magnesites (Fallick et al., 1991; Brydie et al., 1993). I also assume this temperature for the generation of the cryptocrystalline, vein-stockwork type magnesite deposits at Koyakci Tepe, Sodur, Helvacibaba, Yunak, Kozagac (Konya), Kavakarasi (Mugla) and Arap Omer Deresi (Burdur).

The Hirsizdere sedimentary magnesite deposit, considering its extremely low $\delta^{18}\text{O}$ values, could have been formed in a boiling solution, although a lower temperature is possible if the fluid had an extremely low ^{18}O .

Tsakasimta (Nigeria) sedimentary magnesite deposits could also bear similar interpretations.

The Helvacibaba magnesite pebbles within the conglomerates (derived from the stockwork magnesites), as well as the immediately overlying lacustrine bedded dolomites, have little heavier isotopic compositions to those of stockwork magnesites. There are at least two possible explanations (1) lacustrine, bedded dolomites have been formed from hydrothermal exhalative fluids at a temperature at about 80°C, the isotopic composition of the magnesite pebbles having been re-equilibrated with this fluid or (2) the temperature of the lake water was around 20°C but the water has a low $\delta^{18}\text{O}$. If temperature of the lake water was around 80°C (possibility 1), the $\delta^{18}\text{O}$ values of this water should lie between 0 and 3.5 ‰ (Table 5.2.2). If the temperature of the lake water was around 20°C (possibility 2), this implies that the lake water had a low $\delta^{18}\text{O}$ (as low as -12.5 ‰). I suggest that the former alternative (possibility 1) is more likely since the water from the Salda lake, which can be considered a similar environment, has $\delta^{18}\text{O}$ values of 2.8 ‰. Furthermore, Fallick et al. (1991) report such a hydrothermal-sedimentary dolomite from Braneschi, Serbia.

Table 5.2.1. Values of constants A and B used to calculate the isotopic composition of the fluids responsible for mineralisation for the equation

$$10^3 \ln a \equiv \delta^{18}\text{O}_m - \delta^{18}\text{O}_w = A(10^6 T^{-2}) + B$$

Mineral	A	B	Reference
Hydromagnesite	2.74	0.83	Aharon, 1988
Magnesite	3.53	-3.58	Aharon, 1988
Dolomite	3.23	-3.29	Sheppard and Schwarz, 1970
Quartz	3.38	-2.90	Friedmann and O'Neil, 1977

The Salda lake hydromagnesites are considered to be exhalative-sedimentary (SEDEX) although surface mineralisation is taking place at around 20°C or so. If our assumptions for temperatures are reasonable, the average $\delta^{18}\text{O}$ values of the mineralising fluids should lie between 0 and +3 ‰. Two water samples from Salda lake were analysed for their $\delta^{18}\text{O}$ values. They have $\delta^{18}\text{O}$ values of 3.1 and 2.5 ‰, which are within the predicted $\delta^{18}\text{O}$ values of the fluids responsible for western Turkish magnesite, hydromagnesite and dolomite mineralisations.

On the basis of these findings, probable temperatures and $\delta^{18}\text{O}$ compositions of the fluids responsible for mineralisation in western Turkish carbonate deposits are outlined in Table 5.2.2. We must keep in mind that all of these temperatures are only "best guesses" (except for the Salda lake hydromagnesites). Further investigation is needed on this subject, for example fluid inclusions but unfortunately they have not been discovered because of the cryptocrystalline nature of the magnesite.

5.3. VARIATIONS OF THE REE's

Although there are a few studies on REE contents of cryptocrystalline magnesites (Morteani, 1982; Abu-Jaber and Kimberley, 1992), extremely low REE concentrations are almost general features of the ultramafic-hosted magnesite deposits.

Table 5.2.2. The isotopic composition of the fluids responsible for the mineralisation of western Turkish carbonate deposits.

Type and location*	Measured $\delta^{18}\text{O}_{\text{mineral}}$ (‰,SMOW)	Assumed Temperature (°C)	Calculated $\delta^{18}\text{O}_{\text{fluid}}$ (‰,SMOW)
Sedimentary			
Salda (h)	35.9	20	0.9
Hirsizdere (m)	25.2	90	2.0
Tsakasimta (m)	26.3	90	3.1
Helvacibaba			
detrital (m)	25.1	80	0.4
bedded dolomite	25.8	80	3.2
Stockwork			
Helvacibaba (m)	27.2	80	2.5
Helvacibaba (q)	24.8	60	3.15
Arapomer D. (m)	27.5	80	2.8
Kavakarasi (m)	28.0	80	3.3
Yunak-Kozagac (m)	27.6	80	2.9
Vein			
Koyakci Tepe (m)	26.7	80	2.0
Koyakci Tepe (q)	26.3	80	2.1
Sodur (m)	25.8	80	1.1

* Note that the letters within brackets are: h=hydromagnesite, m=magnesite, q=quartz

Why are the REE concentrations exceedingly low in the cryptocrystalline magnesites? It is generally accepted that the ionic sizes (as well as charge) of the elements have a major role in substitution of the elements in the crystal lattice (McKay, 1989). The ionic radii of the REE from La to Lu range from 1.16 to 0.97 Å (Henderson, 1984). The assumed sources for Mg^{2+} ions are ultramafic rocks in the cryptocrystalline magnesite deposits. The Mg^{2+} ion has an ionic radii 0.89 Å (Henderson, 1986). Because of these large differences in ionic sizes of REE and Mg^{2+} , the REE's are rejected during the crystallisation of olivine and orthopyroxenes, which are the main constituents of the ultramafic rocks. The serpentinisation probably causes further depletion of REE (Frey, 1984; Menzies, 1976). The extremely low REE concentrations in Turkish cryptocrystalline magnesite deposits and their host ultramafic (many of them serpentinised) are therefore not unexpected.

Moller and Bau (1993) have suggested that waters in the highly alkaline (pH=9.6) Lake Van (Eastern Turkey) with a positive Ce anomaly and pronounced heavy REE enrichment are characteristic of alkaline, carbonate-rich, aerobic lakes. Data from the Salda lake waters (which have pH between 8.8 and 10.5, and have extremely low REE contents) do not lead us to such a conclusion.

5.4. SOURCE OF MAGNESIUM and OTHER ELEMENTS IN THE SALDA LAKE WATERS and ITS SURROUNDS

Clearly magnesium is the predominant cation in Salda lake waters and those in surrounding wells, springs and streams (Table 4.4.1 and 4.4.2). However, the lake water is about five times richer in magnesium than these others. Thus the magnesium is apparently concentrated in the lake. Although at

lower concentrations, sodium behaves in a similar way. The source of Mg, Na and Si is very probably the ultramafic rocks found all round the lake. The maximum Ca concentrations are found in wells 1, 2 and 19, which are nearest to the Cretaceous limestones. Thus the predominant source of Ca in the lake water is probably these limestones which occur south-east of the lake. Why then is Mg in the lake water enriched compared to these other elements? There are two possible explanations; the first is that it is supplied by some hydrothermal input to the lake; the second is that it is concentrated by evaporation, or a combination of both. However, there is some evidence which clarifies the nature of these processes of Mg-enrichment. We have already explained (in chapter-2) how Salda lake and its surrounds are likely to be the focus of hydrothermal exhalations. Also the Salda lake water is not on the meteoric water line (Figure 4.1.1-A), and this indicates that there is a water-rock interaction (Criss and Taylor, 1986). On the other hand, around Salda lake evaporation outweighs annual precipitation by more than one metre (Figure 2.8 and 2.9). So evaporation also had an effect on Mg-enrichment.

The Si in the water is apparently used by diatoms, during their skeletal construction, but diatoms are very probably short-lived and observations suggest almost immediate dissolution of the skeletons in the alkaline lake water.

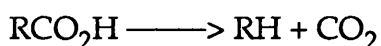
5.5. GENETIC MODEL

Ultramafic rocks found in western Turkey, where unexposed are always covered by Upper Cretaceous sediments (Ketin, 1983). These ultramafic rocks were extensively disturbed by Alpine orogenic movements (Gedik, 1988). The obduction of ultramafic rocks probably took place during closure of the Tethys

Ocean (the precursor of the Mediterranean Sea). Serpentinisation of the ultramafic rocks in fault zones and along contacts with country rocks may have taken place before, during or following emplacement by thrusting over the Palaeozoic and Mesozoic formations. As indicated previously, extensional stresses have been operative in western Turkey since the Oligocene. These resulted in the development of several grabens, such as the Menderes and Gediz examples, and led to volcanic eruptions (Seyitoglu and Scott, 1991). Kissel et al. (1993) report that part of western Turkey (the Isparta region) has been rotated up to 40° clockwise since the Palaeocene. In addition, western Turkey is still a seismically active area (Livermore and Smith, 1985; Jackson and McKenzie, 1984; Udias, 1985).

This helps to explain why the whole of western Turkey was and is a very suitable place for the development of hydrothermal activity. Percolating water in a continent will generally have a meteoric origin. Moreover, large hydrothermal carbonate deposits clearly require a meteoric water recharge (Fallick et al., 1991). Heating of meteoric water takes place by interaction with hot rocks at depth, by exothermic reactions and/or magmatic intrusion. In such a tectonically active area as western Turkey, the geothermal gradient would be expected to be 35 to 40°C/km which is higher than the usual 25 to 30°C/km. At this high gradient, temperatures between two or three kilometre depths (75°C or higher) are probably enough to cause decarboxylation of organic-rich sediments trapped beneath overthrust ultramafic sheets.

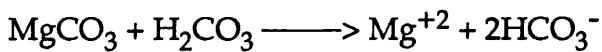
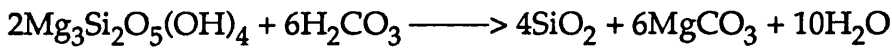
The decarboxylation of organic-rich material has been formulated by Irwin et al. (1977) as;



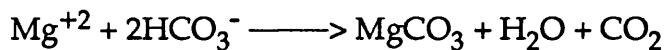
When this carbon dioxide meets hydrothermal water, carbonic acid (H_2CO_3) is generated (Fournier, 1985) as;



The carbonic acid may dissolve magnesium as the bicarbonate from serpentinite, leaving silica (SiO_2) behind (Henderson and Fortey, 1982):-

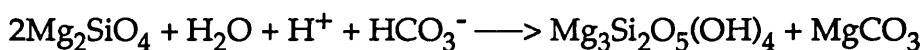


And as this fluid rises up along the suitable channelways (faults and fractures) pressure loss leads to the sudden release of carbon dioxide from bicarbonate (HCO_3^-) causing rapid magnesite precipitation at shallow depths or on lake bottoms;



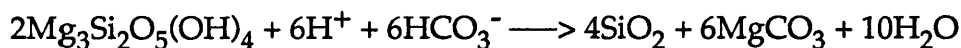
If the precipitation is along the faults then vein-type magnesites would be expected; in the case of fluid flow along fractures then stockwork-type magnesites are generated (Fallick et al., 1991).

On the other hand if serpentinisation of the ultramafic rocks had not already been established the bicarbonate-rich fluids (dissociates of carbonic acid : $\text{H}_2\text{CO}_3 \longrightarrow \text{H}^+ + \text{HCO}_3^-$, see Fournier, 1985) can serpentinise them (Abu-Jaber and Kimberley, 1992);



It is important to note that the buffering of H^+ from the fluid during this reaction causes an increase of pH of the fluid up to 12 (Neal and Stanger, 1984). When serpentinisation is completed, according to Barnes et al. (1973) and

Stanger (1985), silica may also be dissolved by the reaction of highly alkaline solutions with serpentinite;



As the reaction progresses the pH of the fluid is probably high enough to dissolve silica. So hydrothermal solutions would be initially rich in dissolved silica. When these first fluids rise along channelways, precipitation of silica would be expected followed by magnesite.

All these genetical aspects are geologically and isotopically realistic. As mentioned before, the occurrence of large magnesite deposits clearly requires meteoric-water recharge. Therefore, the $\delta^{18}\text{O}$ of the fluids should be within the range of $\delta^{18}\text{O}$ values of local meteoric water of that age. The fluids responsible for the western Turkish magnesite deposits have indeed limited $\delta^{18}\text{O}$ values (varying between 0 and 3 ‰) within the predicted temperatures (see table 5.2.2).

Why some magnesite deposits have silica caps and why some others have silica beds in the footwall is yet to be explained. The answer is probably embedded in the local geological conditions and in the behaviour of silica in the hydrothermal system. When the hydrothermal fluid (rich in both magnesium and silica) rises up in the crust the precipitation of silica may initially take place as a result of mixing with groundwaters in the fractured ultramafic rocks thus generating magnesium-rich fluids. If the hydraulic channelways were not sealed by silica magnesite would precipitate, overlying silica. If the channelways were sealed by silica precipitation, the pressure might increase and hydraulic fracturing and even hydrothermal explosions would result. Thus the rock would be brecciated and porous, vuggy silica produced either at the

surface or on the lake bottom. Equally, a sudden drop of pressure of the fluid would result in magnesite precipitation in the remaining fluid beneath the silica (cap) level. If the hydrothermal fluids reached a lake bottom, magnesite would be precipitated as well as silica. If the precipitation in the lake was rapid, the $\delta^{18}\text{O}$ of the magnesite would not have time to be equilibrated with the bicarbonate of lake waters. This is the situation seen at Hirsizdere, where precipitation was slow equilibration between mineral and water would take place, as in Salda lake and other lacustrine deposits such as Bela-Stena and Miokovachi Beli-Kamen, Serbia (Fallick et al., 1991).

A remaining problem is why sedimentary/hydrothermal magnesites are often interbedded with other lake sediments. I suggest that each pulse of hydrothermal activity is relatively short-lived but perhaps because of changing groundwater conditions and tectonic activity, it is repeated at intervals. Such repeated events would cause the alternation of magnesite beds with lake sediments such as dolomite, limestone and marl. As hydrothermal activity slows down or stops, the magnesite becomes less dominant or even absent such as in Hirsizdere, Turkey. In Salda lake, the microbial communities of the lake probably drive hydromagnesite precipitation from Mg-rich lake water. If the hydrothermal fluids comprising the lake water were Ca-rich, then calcite precipitation would be expected as in the stromatolite produced by a microbial community in lake Van, eastern Turkey (Kempe et al., 1991).

In Salda lake we may imagine that the hydromagnesites will be converted into magnesite during diagenesis or low pressure, low temperature metamorphism since very few hydromagnesite occurrences have been reported in comparison to those of magnesite. According to Syles and Fyfe (1973), hydromagnesite can convert into magnesite at temperatures of 55°C and carbon

dioxide partial pressures of about 1 kb. The stable isotopic compositions of the Salda lake hydromagnesites are comparable with the well-defined sedimentary magnesites.

The suggested genetic model for all of the different types of carbonate deposits of western Turkey is outlined in figure 5.1. I suggest that Mg-rich (for magnesite and hydromagnesite deposits), Ca-rich (for calcite deposits) and Ca-Mg-rich (for dolomite deposits), artesian-drive hydrothermal fluids have been operative during the formation of western Turkish carbonate deposits.

5.6. FURTHER RESEARCH

Cryptocrystalline, fine-grained vein-stockwork and hydrothermal/sedimentary magnesite deposits are sometimes related with the mercury anomalies (Ilich, 1968). It may be useful to investigate the existence (if any) of mercury anomalies related to Turkish magnesite deposits.

The isotopic variations (especially $\delta^{13}\text{C}$) within individual magnesite deposits needs to be further investigated for improved interpretations, since a small excess of organic matter into the system (especially in the lacustrine environments) may affect $\delta^{13}\text{C}$ variations, since the differences in $\delta^{13}\text{C}$ of organic matter and lake water are very large.

Dabitzas (1980) has reported a close similarity of $^{87}\text{Sr}/^{86}\text{Sr}$ ratios of limestones beneath ultramafic hosted magnesites and the magnesites themselves. According to Dabitzas, the similar $^{87}\text{Sr}/^{86}\text{Sr}$ ratios of calcite and magnesite from the Vavdos Area (Greece) indicate a transmission of metamorphically generated carbon dioxide from the limestones to the

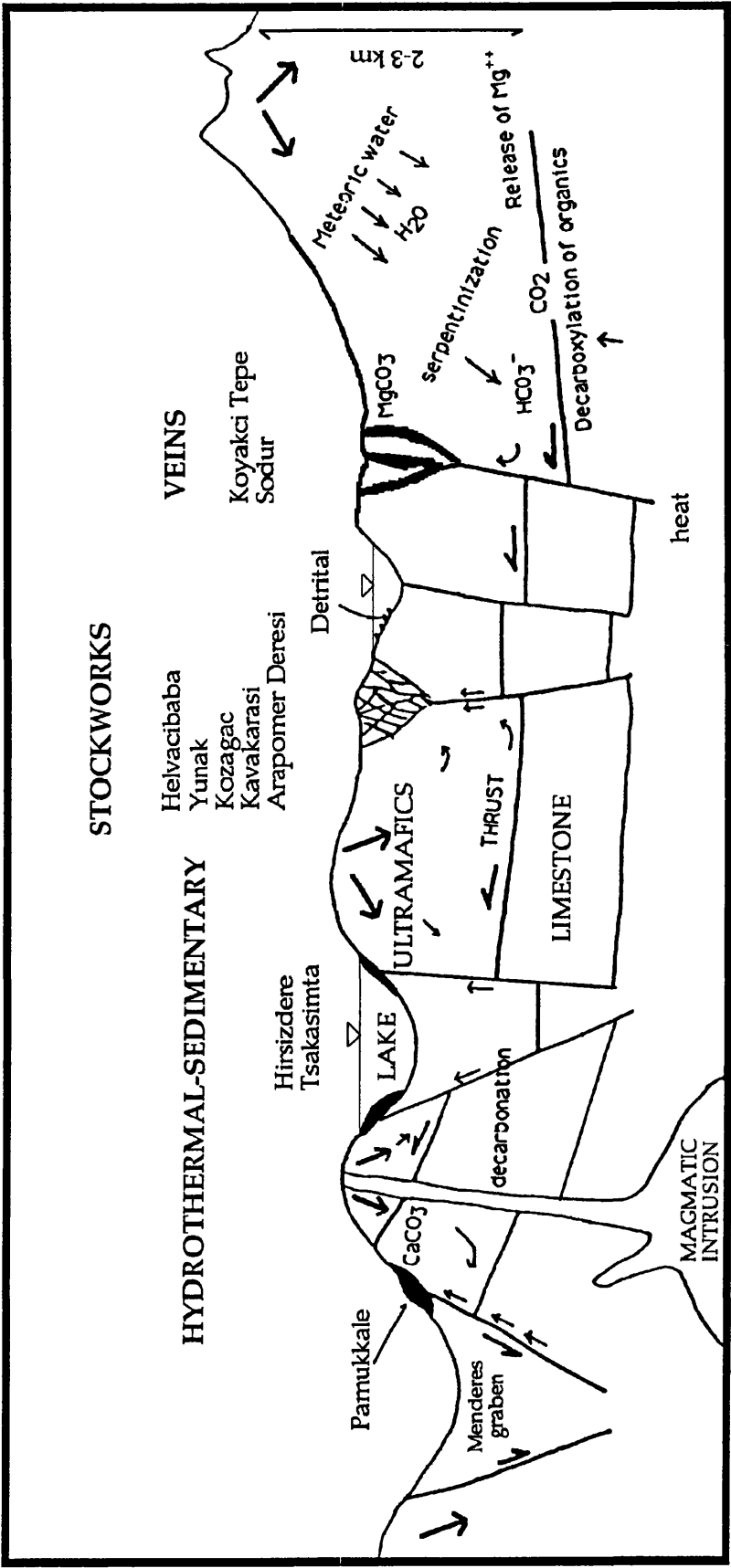


Figure 5.1. Proposed genetic model for western Turkish carbonate deposits. Note that this sketch is not geographically located cross-section and Tsakasmıta is in Nigeria (cf. Fallick et al., 1991).

magnesites. A comparative study of the $^{87}\text{Sr}/^{86}\text{Sr}$ ratio of the western Turkish magnesite deposits and the limestones beneath should be undertaken to test for a similar relationships.

Finally, apart from the relatively well known deposits at Helvacibaba, Kozagac and Koyakci Tepe (all in Konya), detailed mapping would certainly be useful for a better understanding of the relationships between carbonate deposits and country rocks.

CHAPTER SIX

6. CONCLUSIONS

Western Turkey features a variety of magnesite, hydromagnesite, dolomite and calcite deposits. These are: (1) cryptocrystalline vein-type magnesites at Koyakci Tepe (Figure 3.1, location 14b), and Sodur (Figure 3.1, 14f), (2) cryptocrystalline stockwork-type magnesite deposits at Helvacibaba (Figure 3.1, location 14a), Kozagac (Figure 3.1, 14c), Yunak (Figure 3.1, 14d), Kavakarasi (Figure 3.1, 17), and Arapomer Deresi (Figure 3.1, (Figure 3.1, 6b), (3) cryptocrystalline, sedimentary-hydrothermal magnesite and dolomite deposits at Hirsizdere (Figure 3.1, 9a) and Helvacibaba (Figure 3.1, 14a) (the later also includes detrital magnesite), (4) Presently forming hydromagnesite deposits at Salda (Figure 3.1, 6a) as well as hot-spring travertines (calcite) at Pamukkale (Figure 3.1, 9b). Thus, western Turkey offers a very good opportunity to solve the magnesite deposition problem, both past and present, in the surface, at shallow depth and, furthermore, in the lacustrine environment. Apart from the Pamukkale hot-spring travertines, the deposits are associated with ultramafic rocks.

If the decarboxylation of organic-rich sediments is the dominant carbon dioxide source for the light $\delta^{13}\text{C}$ and $\delta^{18}\text{O}$ in the cryptocrystalline vein-type magnesite deposits as Fallick et al. (1991) first suggested, we should find such a source rock for carbon dioxide which has lighter $\delta^{13}\text{C}$ and $\delta^{18}\text{O}$ beneath magnesite deposits. In fact, we have found carbonate veinlets within an outcrop of the organic-rich meta-argillites of Seydisehir formation (which presumably underlie the cryptocrystalline, vein-stockwork type magnesite

deposits at Konya). This outcrop of the Seydisehir formation is about 80 km southwest of Konya. The $\delta^{13}\text{C}$ and $\delta^{18}\text{O}$ values of these organic-rich limestones average -19.7 and +21.7 ‰ for $\delta^{13}\text{C}$ and $\delta^{18}\text{O}$ respectively (Table 4.4.1). Oxidation of organic matter takes place at higher temperatures (>100°C) than decarboxylation (>75°C) but also produces carbon dioxide. This is reflected in the carbonate by lighter $\delta^{13}\text{C}$ (<-25 ‰) and $\delta^{18}\text{O}$ (<24 ‰) than the decarboxylation. It is notable that the $\delta^{13}\text{C}$ and $\delta^{18}\text{O}$ values of cryptocrystalline, vein-stockwork magnesite never drop to such levels in Turkish magnesite deposits. So we may conclude that, although the organic-rich meta-argillites of Seydisehir formation may have been the source of carbon dioxide for the magnesite deposits at Konya, this would have been by decarboxylation rather than oxidation.

With the exception of Kavakarasi magnesites, all other deposits have limited fields on the $\delta^{13}\text{C}$ versus $\delta^{18}\text{O}$ plot (Figure 4.1.1). Two vein deposits (Koyakci Tepe and Sodur) have the lightest $\delta^{13}\text{C}$ (-13.1 and -12.4 ‰ respectively) and $\delta^{18}\text{O}$ (26.6 and 25.8 ‰) values among the vein-stockwork type magnesite deposits. This carbon dioxide was probably also derived from the decarboxylation of organic-rich sedimentary rocks.

The stockwork deposits (Helvacibaba, Yunak and Kozagac) have quite narrow $\delta^{13}\text{C}$ values (-11.1, -8.9 and -10.0 ‰ respectively). Their $\delta^{18}\text{O}$ values average 27.2, 27.9 and 27.0 ‰ for Helvacibaba, Yunak and Kozagac respectively. These values (both $\delta^{13}\text{C}$ and $\delta^{18}\text{O}$) are slightly heavier than the veins. Decarboxylation generated carbon dioxide may still have dominated in the precipitation of the magnesite but with an addition of bicarbonate contributed from the meteoric water.

One stockwork deposit, at Arapomer Deresi [the supposed (Schmid, 1987), but now disproven source of the Salda lake hydromagnesites], has an anomalous $\delta^{13}\text{C}$ value of $\sim +0.3\text{ ‰}$. Decarbonation and/or dissolution of limestone generated carbon dioxide or carbonate (which are characterised by heavy $\delta^{13}\text{C}$) mixing with the relatively light $\delta^{13}\text{C}$ characteristic of CO_2 meteoric water, could explain this unusually heavy $\delta^{13}\text{C}$. The $\delta^{18}\text{O}$ value of this deposit (27.5 ‰) is very similar to those of other stockworks, which, from fractionation calculations, computes to a $\sim 80^\circ\text{C}$ depositional temperature. In contrast, at Kavakarasi mixing was between decarboxylation generated carbon dioxide and the bicarbonate in meteoric water, but the depositional temperature was also around 80°C .

Hirsizdere sedimentary/hydrothermal magnesite deposits have $\delta^{13}\text{C}$ ($\sim +2.6\text{ ‰}$) isotopic signatures comparable with sedimentary/hydrothermal deposits in other parts of the world, for example Bela Stena, Serbia (Fallick et al., 1991). This carbonate may have comprised a mixture of carbon dioxide released during contact metamorphism and that supplied to the lake water from the atmosphere. That the generation of magnesites at Hirsizdere was probably at high temperatures ($\sim 100^\circ\text{C}$) in a lacustrine environment is also supported by the low $\delta^{18}\text{O}$ values ($\sim +25.2\text{ ‰}$) which indicate a high precipitation temperature. Similar interpretations could hold for the magnesite deposit at Tsakasimta (Chad Basin, Nigeria) since its isotopic signatures are quite similar to those of Hirsizdere.

Although the actual process is not understood, presently forming hydromagnesite at Salda lake is apparently associated with the cyanobacteria comprising the microbialites. It may have something to do with pH changes (Burne and Moore, 1987). Alternatively it may simply be a result of trapping of

hydromagnesite precipitated at the lake surface as magnesium ions react with atmospheric carbon dioxide (Burne and Moore, *ibid*). More specifically it may be that the carboxylate groups contained in the polysaccharide sheaths of the Cyanobacteria provide the initial nucleation sites for the precipitation of the magnesium ions in the warm waters seeping through the mounds (cf. Pentecost, 1978). One process we can probably rule out is the intercellular precipitation of carbonate for only one fresh water bacterium is known to have this propensity. Hydromagnesites have $\delta^{13}\text{C}$ ($\sim +4.0$ ‰) and $\delta^{18}\text{O}$ (~ 35.9 ‰) values indicating an atmospheric origin for carbon dioxide. There is good evidence that the Salda lake hydromagnesites may represent a precursor for the hydrothermal/sedimentary type of magnesite deposit. There are several arguments for this. Particularly the isotopic signatures of Salda lake's hydromagnesites are similar to the well-defined sedimentary-hydrothermal magnesite deposit at Bela-Stena, Serbia (Fallick et al., 1991). Also physical features, for example shape and the relationship with surrounding sediments of Salda lake's hydromagnesite deposits match not only the Bela-Stena deposit but other sedimentary-hydrothermal magnesite deposits such as the nearby Raska (Ilich, 1970) and Servia in Macedonia (Zachmann, 1989). For instance, if we imagine Salda's hydromagnesite deposits to be buried by sediments the relationship between massive carbonate and the fringing carbonate beds is comparable to Bela-Stena when one considers the effect of further epigenetic mineralisation and replacement in the microbialite (Figure 6.1). Conversion of hydromagnesite into the magnesite is likely during diagenesis and low grade metamorphism (Sayles and Fyfe, 1973), which explains why sedimentary-hydrothermal magnesite deposits are very common whereas the hydromagnesite deposits are not. Very few hydromagnesite occurrences have been reported; these are in Servia, Greece (Kralik et al., 1989), in New Idria and

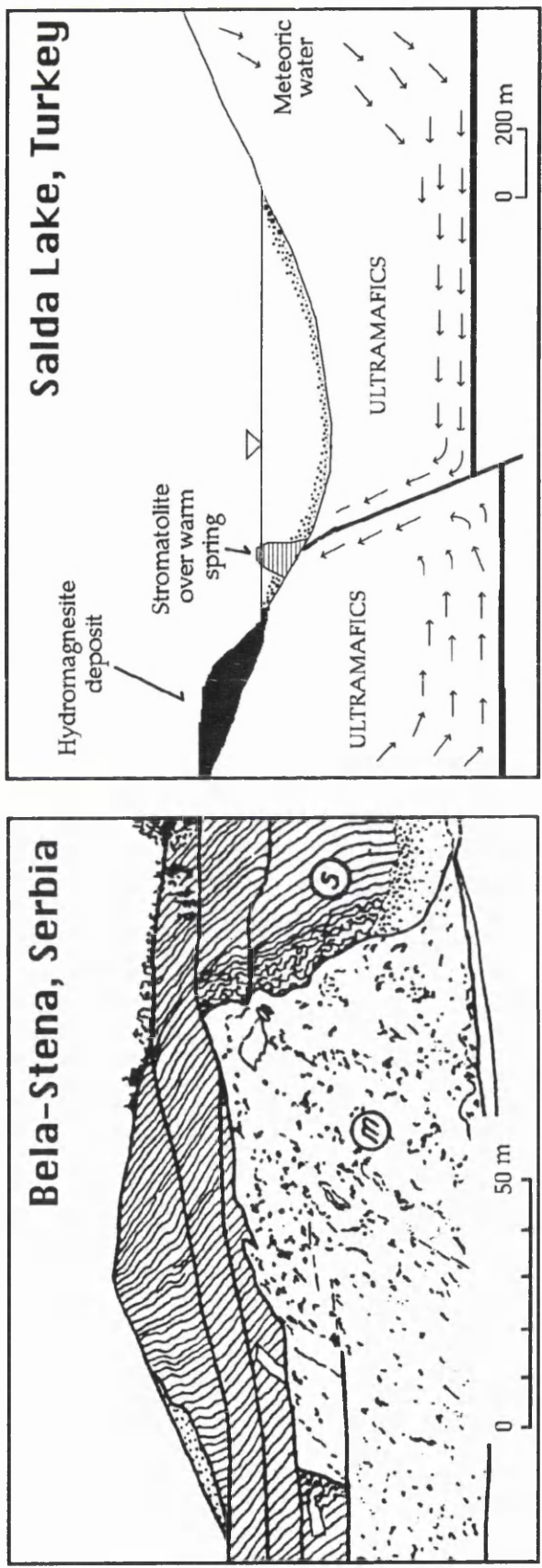


Figure 6.1. A comparison of the Bela-Stena (Serbia) Miocene magnesite deposits with the presently forming Salda lake (Burdur, Turkey) hydromagnesite deposit, supporting the speculation of a comparable genesis. The Bela-Stena's figure is modified from Ilich (1970).
 Note: m:-magnesite, s:-magnesite-rich muds and magnesite beds.

Red Mountain, California (O'Neil and Barnes, 1971) and in the eastern Andes of Bolivia (Redwood, 1993).

With its extremely heavy $\delta^{13}\text{C}$ values (ranging from +5.3 to 7.2 ‰) the Pamukkale hot-spring travertine (calcite) deposits may be expected to have their carbonates derived from decarbonation (thermal metamorphism and/or dissolution) of marine limestones and or dolomites. Palaeozoic marbles and Pliocene limestones have been reported underneath these hot-spring travertines (Gokgoz and Filiz, 1994).

The variations of $\delta^{13}\text{C}$ in the lacustrine magnesite deposit are probably caused by the increase and/or decrease of organic matter being brought into the lake in response gradual temperature change. The vegetation in and around the lake may have increased as temperature increased and *vice versa*. The $\delta^{13}\text{C}$ values of the Hirsizdere top magnesite bed gradually decrease through to the top, indicating that the organic matter brought into the lake increased with time.

The REE concentrations in the magnesites and their host-rocks ultramafics are exceedingly low, an indication that the magnesium was gained from the ultramafic rocks, as to be expected by the geological affiliation.

Finally, the overall isotopic signatures of western Turkish carbonate deposits indicate three distinct carbon dioxide sources. End-member-1 is explained by decarboxylation of organic-rich sediments with extremely light $\delta^{13}\text{C}$ (<-8.0 ‰), end-member-2 results from atmospheric carbon dioxide ($\delta^{13}\text{C}$ is between 0 and 4 ‰), and end-member-3 reflects thermal metamorphism and/or dissolution of marine carbonates (>0 ‰ of $\delta^{13}\text{C}$) (Figure 6.2). Depositional temperatures have an effect on the $\delta^{18}\text{O}$ in the deposits as isotopic

fractionation of the oxygen is temperature dependent. The main oxygen source was meteoric water circulating in the crust, not unsurprising considering that the formation of 50 million tones of magnesite requires 200 billion tons of water (assuming a Mg^{2+} concentration of 400 ppm in solution); a mass so great that it can only be satisfied by rainwater recharge.

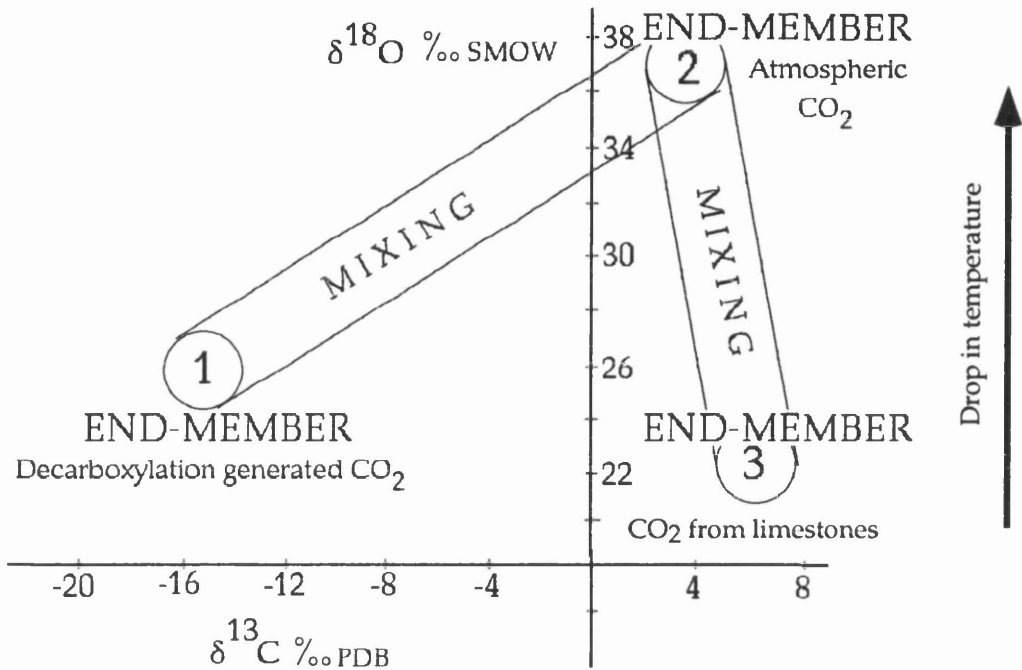


Figure 6.2. Idealised three end-member model of the Turkish carbonate deposits, based on their $\delta^{13}\text{C}$ and $\delta^{18}\text{O}$ values and relation with the source of carbon dioxide; compare with figures 1.1 and 4.1.1. Note that end-member-2 is represented by Salda lake (Burdur, Turkey), Bela-Stena (Serbia) and Servia (Macedonia) sedimentary-hydrothermal (hydro)magnesite deposits and that end-member-3 may derive its carbon dioxide either from contact (thermal) metamorphism of limestone or dissolution.

REFERENCES

- Abu-Jaber, N.S. and Kimberley, M.M., 1992, Origin of ultramafic-hosted vein magnesite deposits: *Ore Geology Reviews*, v. 7, p. 155-191.
- Aharon, P., 1988, A stable-isotope study of magnesites from the Rum Jungle uranium field, Australia: Implications for the origin of strata-bound massive magnesites: *Chemical Geology*, v. 69, p. 127-145.
- Ayhan, A., Pers. Commun., S. U. Muh.-Mim. Fak. Jeoloji Bl., Konya, Turkey.
- Balows, A., Truper, H. G., Dworkin, M., Harder, W. and Schleifer, K.H., 1991, *The Prokaryotes* (2nd ed.): Springer Verlag, New York.
- Barnes, I. and O'Neil, J.R., 1969, The relationship between fluids in some fresh Alpine-type ultramafics and possible modern serpentinitisation, Western United States: *Geological Society of America Bulletin*, v. 80, p. 1947-1960.
- Barnes, I., O'Neil, J.R., Rapp, J.B. and White, D.E., 1973, Silica-carbonate alteration of serpentine: wall rock alteration in mercury deposits of the California Coast Ranges: *Economic Geology*, v. 68, p. 388-398.
- Bayhan, H. and Tolluoglu, U., 1987, The mineralogical-petrographical and geochemical characteristics of Cayagazi syenitoid (Northwest of Kirshir province): *Yerbilimleri*, v. 14, p. 109-120.
- Beatty, D.W. and Taylor, H.P., 1982, Some petrologic and oxygen isotopic relationships in the Amulet Mone, Noranda, Quebec, and their bearing on the origin of Archean massive sulfide deposits: *Economic Geology*, v. 77, p. 95-108.
- Bingol, E., Akyurek, B. and Korkmazer, B., 1975, Biga yarimadasinin jeolojisi ve Karakaya serisinin bazi ozellikleri In: *Conference proceedings of Cumhuriyetin 50. yili Yerbilimleri Kongresi*, Ankara, Turkey, p 71-77. Maden Tetkik ve Arama Enstitusu.
- Bolt, B.A., 1993, *Earthquakes, Newly Revised and Expanded* : W. H. Freeman and Co., New York, 320 p.

- Boray, A., 1975, Bitlis dolayinin yapisi ve metamorfizmasi: *Turkiye Jeoloji Kurumu Bulteni*, v. 18, p. 81-84.
- Borthwick, J. and Harmon, R.J., 1982, A note regarding ClF_3 as an alternative to BrF_5 for oxygen isotope analysis: *Geochimica et Cosmochimica Acta*, v. 46, p. 1665-1668.
- Bottinga, Y. and Craig, H., 1969, Oxygen isotopic fractionation between CO_2 and water and the isotopic composition of marine atmospheric CO_2 : *Earth and Planetary Science Letters*, v. 5, p. 285-295.
- Botz, R.W. and von der Borch, C.C., 1984, Stable isotope study of carbonate sediments from the Corong Area, South Australia: *Sedimentology*, v. 31, p. 837-849.
- Boynton, W.V., 1984, Geochemistry of the rare earth elements: meteorite studies In: *Rare earth element geochemistry* (Ed. by P. Henderson), p. 63-114. Elsevier, Amsterdam.
- Brand, U. and Veizer, J., 1981, Chemical diagenesis of a multicomponent carbonate system: *Journal of Sedimentary Petrology* (Stable isotopes-2), v. 51, p. 987-998.
- Brennich, G., 1959, Denizli-Cambasi manyezit yataklari Maden Tetkik ve Arama Enstitusu (Unpublished report, report no secret), Ankara, Turkey.
- Brydie, J.R., Fallick, A.E., Ilich, M., Maliotis, G. and Russell, M.J., 1993, A stable isotopic study of magnesite deposits in the Akamas Area, N. W. Cyprus: *Trans. Instn Min. Metall. (Sect. B: Appl. earth sci.)*, v. 102, p. B50-B53.
- Burne, R.V. and Moore, L.S., 1987, Microbialites: Organosedimentary deposits of benthic microbial communities: *The Society of Economic Paleontologists and Mineralogists*, v. 2, p. 241-254.
- Cayirli, H. and Yavas, N., 1975, Yesilova (Burdur) cevresinin asbest ve magnezit genel prospeksiyonu raporu Maden Tetkik ve Arama Enstitusu (Unpublished report, report no secret), Ankara, Turkey.

- Clayton, R.N. and Degens, E.T., 1959, Use of C isotope analyses for differentiatin fresh-water and marine sediments: American Association of Petroleum Geologists Bulletin, v. 43, p. 890-897.
- Clayton, R.N. and Mayeda, T.K., 1963, The use of bromine pentafluoride in the extraction of oxygen from oxides and silicates for isotopic analysis: *Geochimica et Cosmochimica Acta*, v. 27, p. 43-53.
- Costa, U.R., Fyfe, W.S., Kerrich, R. and Nesbitt, H.W., 1980, Archean hydrothermal talc evidence for high ocean temperatures: *Chemical geology*, v. 30, p. 341-349.
- Costa, U.R., Barnett, R.L. and Kerrich, R., 1983, The Mattagami lake mine Archean Zn-Cu sulfide deposit, Quebec: Hydrothermal coprecipitation of talc and sulfides in a sea-floor brine pool-evidence from geochemistry, $^{18}\text{O}/^{16}\text{O}$, and mineral chemistry: *Economic Geology*, v. 78, p. 1144-1203.
- Criss, R. E. and Taylor, H. P. 1986, Meteoric-hydrothermal systems In: *Stable isotopes in high temperature geological processes* (Ed. by J. W. Valley, H. P. Taylor and J. R. O'Neil), p. 165-185. Mineralogical Society of America, Washington.
- Curtis, C.D., 1978, Possible links between sandstone diagenesis and depth-related geochemical reactions occurring in enclosing mudstones: *Journal of the Geological Society of London*, v. 135, p. 107-117.
- Dabitizas, S.G., 1980, Additional evidence and a synopsis on the origin of the magnesite deposits in the Vavdos District, Northen Greece In: *Conference proceedings of An international symposium on metallogeny of mafic and ultramafic complexes: The Eastern Mediterranean-Western Asia Area, and its comparison with similar metallogenic environments in the world*, Athens (Greece), p 269-283. UNESCO.
- Dean, W.T., 1971, The Trilobites of the Seydisehir Formation (Lower Ordovician): *Brit. Mus. (Nat. Hist.) Geology*, v. 20, p. 1-24.

- Degens, E.T. and Epstein, S., 1962, Relationship between O^{18}/O^{16} ratios in coexisting carbonates, cherts and diatomites: American Association of Petroleum Geologists Bulletin, v. 46, p. 534-542.
- Demirhan, M., 1986, Manyezit : Maden Tetkik ve Arama (MTA) Enstitusu Genel Mudurlugu Maden Etud ve Arama Dairesi Refrakter Hammaddeler Servisi, Ankara, 27 p.
- Demovic, R., Hoefs, J. and Wedepohl, K.H., 1972, Geochemische untersuchungen an travertinen der Slowakei: Contributions to Mineralogy and Petrology, v. 37, p. 15-28.
- Dominy, P., Pers. Commun., Botany department, Glasgow Univ., Glasgow, U.K.
- Doyen, A., Pers. Commun., S.U. Muh.-Mim. Fak. Jeoloji Bl. Konya, Turkey.
- Emery, D. and Robinson, A., 1993, Inorganic geochemistry: Applications to petroleum geology : Blackwell, London, 254 p.
- Erdem, N.P., 1974, Turkiyedeki ofiyolitik seriler: Maden Tetkik ve Arama (MTA) Enstitusu Dergisi (Turkey), v. 83, p. 131-144.
- Ergun, O.N., 1988, Sereflikochisar yoresi Tuz Golu guncel evaporit cokellerinin sedimantolojik incelemesi : Ondokuz Mayis Universitesi, Turkey, Samsun, 73 p.
- Fallick, A.E., Ilich, M. and Russell, M.J., 1991, A stable isotopic study of the magnesite deposits associated with the Alpine-type ultramafic rocks of Yugoslavia: Economic Geology, v. 86, p. 847-861.
- Fallick, A.T., Pers. Commun., Scottish Universities Research and Reactor Centre (SURRC), Eastkilbride, U.K.
- Faure, G., 1991, Inorganic geochemistry : Macmillan, New York, 626 p.
- Field, C.W. and Fifarek, R.H., 1985, Light stable-isotope systematics in the epithermal environment In: Gology and geochemistry of epithermal

- systems (Ed. by B. R. Berger and P. M. Bethke), p. 99-128. Society of economic geologists, El Paso, Texas.
- Fisekci, A., 1989, Yesilova (Burdur) ve civari magnesit zuhurlarinin prospeksiyon raporu Maden Tetkik ve Arama Enstitusu (Unpublished report, report no secret), Ankara, Turkey.
- Folk, R.L., 1962, Spectral subdivision of limestone types: Classification of carbonate rocks: American Association of Petroleum Geologists Bulletin, v. 1, p. 62-84.
- Fournier, R.O., 1985, Carbonate transport and deposition in the epithermal environment In: Geology and geochemistry of epithermal systems (Ed. by B. R. Berger and P. M. Bethke), p. 63-72. Society of economic geologists, El Paso, Texas.
- Frey, F.A., 1984, Rare earth element abundances in upper mantle rocks In: Rare earth element geochemistry (Ed. by P. Henderson), p. 153-203. Elsevier, Amsterdam.
- Friedman, I. and O'Neil, J.R., 1977, Compilation of stable isotope fractionation factors of geochemical interest : U. S. Geol. Survey., Prof. Pap., 440-KK p.
- Gartzos, E., 1990, Carbon and oxygen isotope constraints on the origin of magnesite deposits, North Evia (Greece): Schweiz. Mineral. Petrogr. Mitt., v. 70, p. 67-72.
- Gedik, I., 1988, A paleogeographic approach to the Devonian of Turkey In: Devonian of the World (Ed. by N. J. McMillan, A. F. Embry and D. J. Glass), p. 557-567. D. W. Friesen and Sons, Calgary-Alberta, Canada.
- Gokgoz, A. and Filiz, S., 1994, Pamukkale-Karahayit-Golemezli hidrotermal karstinin hidrojeolojisi : TMMOB Jeoloji Muhendisleri Odasi, Ankara, 175 p.
- Gonfiantini, R., 1986, Environmental isotopes in lake studies In: Handbook of environmental isotope geochemistry (Ed. by P. Fritz and J. C. Fontes), p. 113-168. Elsevier, Amsterdam.

- Gormus, M., 1984, Kiziloren dolayinin jeolojisi : Unpublished MSc thesis, Selcuk Univ., Konya, Turkey.
- Gray, G.J., 1986, Lithogeochemical aureoles to Irish mineralisation : Unpublished PhD thesis, Strathclyde Univ., Glasgow, U.K.
- Griffis, R., 1972, Genesis of a magnesite deposit: Deloro Twp, Ontario: *Economic Geology*, v. 67, p. 63-71.
- Gulec, N., 1991, Crust-mantle interaction in western Turkey: Implications from Sr and Nd isotope geochemistry of Tertiary and Quaternary volcanics: *Geological Magazine*, v. 128 (5), p. 417-485.
- Gundogdu, N. and Ataman, G., 1976, Tavsanlı (Kütahya) çevresinde sedimanter manyezit oluşumu: Hacettepe Üniversitesi Yerbilimleri Enstitüsü Yayın Organı, v. 2, p. 134-140.
- Hall, R., 1976, Ophiolite emplacement and evolution of the Taurus suture zone, southeast Turkey: *Geological Society of America Bulletin*, v. 87, p. 1078-1088.
- Henderson, W.G. and Fortey, N.J., 1982, Highland Border rocks at Loch Lomond and Aberfoyle: *Scottish Jour. Geology*, v. 18, p. 227-245.
- Henderson, P., 1984, General geochemical properties and abundances of the rare earth elements In: *Rare earth element geochemistry* (Ed. by P. Henderson), p. 1-32. Elsevier, Amsterdam.
- Henderson, P., 1986, *Inorganic geochemistry* : Pergamon Press, Oxford, 353 p.
- Hillarie-Marcel, C., 1986, Isotopes and food In: *Handbook of environmental isotope geochemistry* (Ed. by P. Fritz and J. C. Fontes), p. 507-548. Elsevier, Amsterdam.
- Hladikova, J., Rajlich, P. and Smejkal, V., 1981, Isotopic composition of carbonates from the Devonian of the Jeseník Mountains, the Drahanská-

- Vrchovina Upland and from the sulphide deposit Zlate Hory: *Casopis pro mineralogii a geologii*, v. 26, p. 225-240.
- Humphris, S.E., 1984, The mobility of rare earth elements in the crust In: *Rare earth element geochemistry* (Ed. by P. Henderson), p. 317-342. Elsevier, Amsterdam.
- Ilich, M., 1968, Problems of the genesis and genetic classification of magnesite deposits: *Geologicky Zbornik-Geologica Carpathica XIX*, Bratislava, v. 1, p. 149-160.
- Ilich, M., 1970, Results of recent studies of magnesite deposits in the neighbourhood of Raska: *Transactions of the mining and geological fakulties* (Separate offprint), University of Beograd, v. Sv. 11-12, p. 89-217.
- Irwin, H., Curtis, C. and Coleman, M., 1977, Isotopic evidence for source of diagenetic carbonates during burial of organic-rich sediments: *Nature*, v. 269, p. 209-213.
- Jackson, J. and McKenzie, D., 1984, Active tectonics of the Alpine-Himalayan Belt between western Turkey and Pakistan: *Geophys. J. R. astr. Soc.*, v. 77, p. 185-264.
- Jedrysek, M.O. and Halas, S., 1990, The origin of magnesite deposits from the Polish Foresudetic Block ophiolites: preliminary $\delta^{13}\text{C}$ and $\delta^{18}\text{O}$ investigations: *Terra Nova*, v. 2, p. 154-159.
- Kaaden, G., 1965., Sumerbank manyezit yataklari (Konya-Meram) Maden Tetkik ve Arama Enstitusu (Unpublished report, report no secret), Ankara, Turkey.
- Karaman, T., 1987, Yesilovo ve Tefenni (Burdur) batisinda kalan alanin jeolojisi ve petrografisi : Unpublished MSc thesis, Selcuk Univ., Konya, Turkey.
- Kastens, K.A., 1991 Responses to impending continent-continent collision in the Mediterranean Lamont-Doherty Geological observatory (Report).

- Keeling, C.D., Mook, W.G. and Tans, P.P., 1979, Recent trends in the $^{13}\text{C}/^{12}\text{C}$ ratio of atmospheric carbon dioxide: *Nature*, v. 277, p. 121-122.
- Kempe, S., Kazmierczak, J., Landmann, G., Konuk, T., Reimer, A. and Lipp, A., 1991, Largest known microbialites discovered in Lake Van, Turkey: *Nature*, v. 349, p. 605-608.
- Kendall, T., 1993, Turkey's industrial minerals So much more than boron: *Industrial Minerals*, November, v. p. 51-70.
- Kerrick, R. and Watson, G.P., 1984, The Macassa mine Archean lode gold deposit, Kirkland Lake, Ontario: Geology, patterns of alteration and hydrothermal regimes: *Economic Geology*, v. p. 1104-1130.
- Ketin, I., 1966, Anadolunun tektonik birlikleri: *Maden Tetkik ve Arama Enstitüsü Dergisi*, v. 66, p. 37-67.
- Ketin, I., 1983, *Türkiye jeolojisine genel bir bakış* : İstanbul Teknik Üniversitesi, İstanbul, 595 p.
- Kissel, C., Averbuch, O., de Lamotte, D.F., Monod, O. and Allerton, S., 1993, First paleomagnetic evidence for a post-Eocene clockwise rotation of the Western Taurides thrust belt east of the Isparta reentrant (Southwestern Turkey): *Earth and Planetary Science Letters*, v. 117, p. 1-14.
- Knauth, L.P. and Epstein, S., 1976, Hydrogen and oxygen isotope ratios in nodular and bedded cherts: *Geochimica et Cosmochimica Acta*, v. 40, p. 1095-1108.
- Knauth, L.P. and Lowe, D.R., 1978, Oxygen isotope geochemistry of cherts from the Onverwacht Group (3.4 billion years), Transvaal, South Africa, with implications for secular variations in the isotopic composition of cherts: *Earth and Planetary Science Letters*, v. 41, p. 209-222.

- Kocyigit, A., 1991, An example of accretionary forearc basin from northern Central Anatolia and its implications for the history of subduction of Neo-Tethys in Turkey: Geological Society of America Bulletin, v. 103, p. 22-36.
- Kralik, M., Aharon, P., Schroll, E. and Zachmann, D., 1989, Carbon and oxygen isotope systematics of magnesites: a review In: Magnesite. Geology, Mineralogy, Geochemistry and Formation of Mg-Carbonates (Monography series on mineral deposits, 28) (Ed. by P. Moller), p. 197-223. Gebruder Borntraeger, Berlin.
- Krauskopf, K.B., 1979, Introduction to geochemistry : Mc-Crawhill, New York, 617 p.
- Kreulen, R., 1980, CO₂-rich fluids during regional metamorphism on Naxos (Greece): Carbon isotopes and fluid inclusions: American Journal of Science, v. 280, p. 745-771.
- Langmuir, D., 1965, Stability of carbonates in the system MgO-CO₂-H₂O: Journal of Geology, v. 73, p. 730-754.
- Livermore, R.A. and Smith, A.G., 1985, Some boundary conditions for the evolution of the Mediterranean Region In: Geological evolution of the Mediterranean Basin (Ed. by D. J. Stanley and F. C. Wezel), p. 83-100. Springer-Verlag, Berlin.
- Macaulay, C.I., Haszeldine, R.S. and Fallick, A.E., 1992, Distribution, chemistry, isotopic composition and origin of diagenetic carbonates: Magnus Sandstone, North Sea: Journal of Sedimentary Petrology, v. 63, p. 33-43.
- McCrea, J.M., 1950, The isotopic chemistry of carbonates and paleotemperature scale: Journal of Chemical Physics, v. 18, p. 849-857.
- McKay, G.A., 1989, Partitioning of rare earth elements between major silicate minerals and basaltic melts In: Geochemistry and mineralogy of rare earth elements (Ed. by B. R. Lipin and G. A. McKay), p. 45-78. Mineralogical Society of America, Washington.

- Menzies, M., 1976, Rare earth element geochemistry of fused ophiolitic and alpine lherzolites: Othris, Lanzo and Troodos: *Geochimica et Cosmochimica Acta*, v. 40, p. 645-656.
- Moller, P., 1989, Nucleation processes of magnesite In: *Magnesite. Geology, Mineralogy, Geochemistry and Formation of Mg-Carbonates* (Monography series on mineral deposits, 28) (Ed. by P. Moller), p. 287-292. Gebruder Borntraeger, Berlin.
- Moller, P. and Bau, M., 1993, Rare-earth patterns with positive cerium anomaly in alkaline waters from Lake Van, Turkey: *Earth and Planetary Science Letters*, v. 117, p. 671-676.
- Morse, J.W. and Mackenzie, F.T., 1990, *Geochemistry of sedimentary carbonates* : Elsevier, Amsterdam, 707 p.
- Morteani, G., Moller, P. and Schley, F., 1982, The rare earth element contents and the origin of sparry magnesite mineralizations of Tux-Lanersbach, Entachen Alm, Spiessnagel and Hochfilzen, Austria, and the lacustrine magnesite deposits of Aiani Kozani, Greece and Bela Stena, Yugoslavia: *Economic Geology*, v. 77, p. 617-631.
- Neal, C. and Stanger, G., 1984, Calcium and magnesium hydroxide precipitation from alkaline groundwater in Oman, and their significance to the process of serpentinization: *Mineralogical Magazine*, v. 48, p. 237-241.
- O'Neil, J.R. and Barnes, I., 1971, C^{13} and O^{18} composition in some fresh-water carbonate associated with ultramafic rocks: Western United States: *Geochimica et Cosmochimica Acta*, v. 35, p. 687-697.
- O'Neil, J.R., 1986, Theoretical and experimental aspects of isotopic fractionation In: *Stable isotopes in high temperature geological processes* (Ed. by J. W. Valley, H. P. Taylor and J. R. O'Neil), p. 1-40. Mineralogical Society of America, Washington.

- Ohmoto, H., 1986, Stable isotope geochemistry of ore deposits In: Stable isotopes in high temperature geological processes (Ed. by J. W. Valley, H. P. Taylor and J. R. O'Neil), p. 491-561. Mineralogical Society of America, Washington.
- Okay, A.I., 1986, High-pressure/low-temperature metamorphic rocks of Turkey: Geological Society of America Memoir, v. 164, p. 333-347.
- Ozcan, A., Goncuoglu, M.C., Turan, N., Uysal, S., Senturk, K. and Isik, A., 1988, Late Paleozoic evolution of the Kutahya-Bolkardag Belt: Journal of Pure and Applied Sciences (METU, Middle-East Tecnic Univ., Turkey), v. 21, p. 211-220.
- Ozgul, N., 1976, Toroslarin bazi temel jeoloji ozellikleri: Turkiye Jeoloji Kurumu Bulteni, v. 19, p. 66-78.
- Ozgul, N., 1984, Stratigraphy and tectonic evolution of the Central Taurides In: Geology of the Taurus Belt, Proceedings (Ed. by O. Tekeli and M. C. Goncuoglu), p. 77-90. Maden Tetkik ve Arama Enstitusu, Ankara.
- Pentecost, A., 1978, Association of cyanobacteria with tufa deposits: Identity, enumeration, and a nature of the sheat material revealed by histochemistry: Geomicrobiology Journal, v. 4, p. 285-298.
- Perry, E.A., 1967, The oxygen isotope chemistry of ancient cherts: Earth and Planetary Science Letters, v. 3, p. 62-66.
- Perry, E.C., Ahmad, S.N. and Swulius, T.M., 1978, The oxygen isotope composition of 3,800 M.Y. old metamorphosed chert and iron formation from Isakusia, West Greenland: Journal of Geology, v. 86, p. 223-239.
- Petraschek, W.E., 1971, Der kristaline magnesit im serpantin von snamum: Radex rdsch., v. 3, p. 487-491.
- Pohl, W., 1989, Comparative geology of magnesite deposits and occurrences In: Magnesite. Geology, Mineralogy, Geochemistry and Formation of Mg-Carbonates (Monography series on mineral deposits, 28) (Ed. by P. Moller), p. 1-13. Gebruder Borntraeger, Berlin.

- Redwood, S.D., 1993, Crocidolite and magnesite associated with Lake Superior-type banded iron formation in Chapare Group of eastern Andes, Bolivia: *Trans. Instn Min. Metall. (Sect. B: Appl. earth sci.)*, v. 102, p. B114-B121.
- Riding, R., 1992, Temporal variation in calcification in marine cyanobacteria: *Journal of the Geological Society of London*, v. 149, p. 979-989.
- Robertson, A.H.F. and Woodcock, N.H., 1981, Alakir cay group, Antalya complex, SW Turkey: A deformed Mesozoic carbonate margin: *Sedimentary Geology*, v. 30, p. 95-131.
- Rosenbaum, J. and Sheppard, S.M.F., 1986, An isotopic study of siderites, dolomites and ankerites at high temperatures: *Geochimica et Cosmochimica Acta*, v. 50, p. 1147-1150.
- Salomons, W. and Mook, W.G., 1986, Isotope geochemistry of carbonates in the weathering zone In: *Handbook of environmental isotope geochemistry* (Ed. by P. Fritz and J. C. Fontes), p. 239-270. Elsevier, Amsterdam.
- Sancar, M.S., 1982, *Turkiye manyezit envanteri : Maden Tetkik ve Arama Enstitusu*, Ankara, Turkey, Ankara, 78 p.
- Sariiz, K., 1990, Turkmentokat-Karatepe (Eskisehir) manyezit yataklarinin olusumu: *MTA Dergisi*, v. 110, p. 77-96.
- Sayles, W. and Fyfe, W.S., 1973, The crystallisation of magnesite aqueous solution: *Geochimica et Cosmochimica Acta*, v. 37, p. 87-99.
- Schmid, I.H., 1987, Turkey's Salda lake, a genetic model for Australia's newly discovered magnesite deposits: *Industrial Minerals*, v. p. 19-31.
- Schwartzman, D.W. and McMenamin, M., 1993, A much warmer Earth surface for most of geologic time: Implications to biotic weathering: *Chemical Geology*, v. 107, p. 221-223.
- Sengor, A.M.C. and Kidd, W.S.F., 1979, Post-collisional tectonics of the Turkish-Iranian plateau and comparison with Tibet: *Tectonophysics*, v. 55, p. 361-376.

- Sengor, A.M.C., 1979, Mid-Mesozoic closure of Permo-Triassic Tethys and its implications: *Nature*, v. 279, p. 590-593.
- Sengor, A.M.C. and Yilmaz, Y., 1981, Tethyan evolution of Turkey: a plate tectonics approach: *Tectonophysics*, v. 75, p. 181-241.
- Sengor, A.M.C. and Yilmaz, Y., 1983, The evolution of Tethys in Turkey: An implication of plate tectonic : *Geological survey of Turkey, Ankara*, 75 p.
- Sengor, A.M.C., Satir, M. and Akkok, R., 1984, Timing of tectonic events in the Menderes Massif, Western Turkey: Implications for tectonic evolution and evidence for Pan-African basement in Turkey: *Tectonics*, v. 3/7, p. 693-707.
- Seyitoglu, G. and Scott, B., 1991, Late Cenozoic crustal extension and basin formation in west Turkey: *Geological Magazine*, v. 128(2), p. 155-166.
- Sheppard, S.M.F. and Schwarcz, H.P., 1970, Fractionation of carbon and oxygen isotopes and magnesium between co-existing metamorphic calcite and dolomite: *Contr. Mineralogy Petrology*, v. 26, p. 161-198.
- Sheppard, S.M.F., 1986, Characterization and isotopic variations in natural waters In: *Stable isotopes in high temperature geological processes* (Ed. by J. W. Valley, H. P. Taylor and J. R. O'Neil), p. 165-185. Mineralogical Society of America, Washington.
- Shieh, Y.N. and Taylor, H.P., 1969, Oxygen and carbon isotope studies of contact metamorphism of carbonate rocks: *Journal of Petrology*, v. 10, p. 307-331.
- Stanger, G., 1985, Silicified serpentinite in the Semail nappe of Oman: *Lithos*, v. 18, p. 13-22.
- Termier, G. and Monod, O., 1978, Inarticulate Brachiopods from Cambro-Ordovician Formations in the Western Taurus (Turkey): *Bulletin of the Geological Society of Turkey*, v. 21, p. 145-152.

- Tolluoglu, U., 1989, Mesoscopical tectonic features of the Kirsehir metamorphites: *Yerbilimleri*, v. 15, p. 89-103.
- Turi, B., 1986, Stable isotope geochemistry of travertines In: *Handbook of environmental isotope geochemistry* (Ed. by P. Fritz and J. C. Fontes), p. 207-238. Elsevier, Amsterdam.
- Udias, A., 1985, Seismicity of the Mediterranean Basin In: *Geological evolution of the Mediterranean Basin* (Ed. by D. J. Stanley and F. C. Wezel), p. 55-64. Springer-Verlag, Berlin.
- Veizer, J., 1990, Trace elements and isotopes in sedimentary carbonates In: *Carbonates: Mineralogy and chemistry* (Ed. by R. J. Reeder), p. 265-300. Mineralogical Society of America, Washington.
- Yeniyol, M., 1982, Yunak (Konya) magnezitlerinin olusum sorunlari, degerlendirilmeleri ve yore kayaclarinin petrojenezi: *Istanbul Universitesi Yerbilimleri Fakultesi Dergisi*, v. 3, p. 21-51.
- Zachmann, D.W., 1989, Mg-carbonate deposits in freshwater environment In: *Magnesite. Geology, Mineralogy, Geochemistry, and Formation of Mg-Carbonates* (Monography series on mineral deposits, 28) (Ed. by P. Moller), p. 61-94. Gebruder Borntraeger, Berlin.
- Zachmann, D.W. and Johannes, W., 1989, Cryptocrystalline magnesite In: *Magnesite. Geology, Mineralogy, Geochemistry and Formation of Mg-Carbonates* (Monography series on mineral deposits, 28) (Ed. by P. Moller), p. 15-28. Gebruder Borntraeger, Berlin.

Appendix-1. The evaporation rates (mm) of the Salda lake area*.

		M	O	N	T	H	S	
Years	April	May	June	July	Aug.	Sept.	Oct.	Total
1971	81.3	132.9	188.4	225.9	209.3	153.5	101.2	1093
1972	138.7	164.5	179.6	231.6	223.5	163.6	81.8	1183
1973	111.1	182.3	210.4	263.3	239.0	185.3	93.6	1285
1974	100.1	168.9	228.3	274.2	230.1	150.1	105.8	1258
1975	42.8	121.4	172.1	240.0	207.8	166.1	94.3	1045
1976	106.5	135.3	177.1	215.4	198.5	146.5	95.1	1074
1977	91.3	182.5	216.0	238.6	245.8	144.6	49.9	1169
1978	52.6	179.7	198.7	256.0	219.9	149.0	95.5	1151
1979	131.6	137.3	182.7	222.8	280.4	162.1	93.0	1210
1980	76.6	168.6	206.4	263.3	226.7	252.4	97.4	1191
1981	113.1	130.6	186.3	239.7	176.6	nda	nda	846
1982	43.1	152.8	179.1	220.1	221.1	174.5	93.7	1084
1983	nda	71.4	174.8	213.1	204.3	153.5	94.9	912
1984	nda	156.7	195.8	244.8	187.6	157.8	104.5	1047
1985	111.5	157.0	194.8	237.0	238.3	166.4	84.1	1189
1986	138.4	158.3	186.9	235.7	217.8	138.6	96.2	1172
1987	85.8	151.2	181.5	247.4	218.6	158.9	82.7	1126
1988	85.9	151.2	181.5	247.4	218.6	158.6	82.7	1126
Total	1510	2703	3410	4316	3964	2782	1546	
Average	94	150	190	240	220	164	91	

nda: No data available

* Meteorologic station: Burdur

Latitude : 37°40'

Longitude : 30°20'

Altitude : 967m

Source: The meteorology office of Turkey.

Appendix-2. The rainfall (mm) of around Salda Lake (Yesilova-Burdur)*.

Years	January	February	March	April	May	June	July	August	Septem.	October	Novem.	Decem.	Total
1971	43.8	70.4	70.6	37.7	55.7	12.6	15.5	28.4	5.1	9.1	33.4	51.7	434.0
1972	22.8	66.1	23.8	30.1	27.0	42.8	47.2	32.0	3.1	50.9	20.8	nda	367.2
1973	37.7	93.3	10.5	43.6	12.2	15.3	20.6	nda	nda	41.5	10.0	22.9	307.6
1974	65.5	52.3	42.3	27.5	26.1	4.9	nda	19.4	13.0	20.9	20.5	44.9	337.3
1975	48.0	72.5	24.5	27.4	65.4	37.0	9.8	21.0	nda	24.1	67.3	42.6	439.6
1976	67.4	35.3	43.1	91.8	58.1	32.6	13.0	0.0	1.3	40.5	42.9	96.9	522.9
1977	40.7	22.3	23.5	78.0	16.5	11.0	8.6	nda	45.4	18.0	5.3	56.1	325.4
1978	107.1	127.4	65.5	41.6	9.5	19.0	1.5	nda	19.2	82.8	13.8	76.1	563.5
1981	175.0	39.8	84.5	15.8	48.8	16.7	nda	nda	nda	nda	31.2	86.3	498.1
1982	40.9	32.7	35.0	41.8	11.8	36.2	27.2	7.1	25.1	37.3	8.7	28.8	332.6
1983	68.0	78.0	59.5	53.4	51.8	39.5	26.1	14.2	30.6	4.8	92.5	88.3	606.7
1984	61.3	18.4	63.0	69.9	11.4	0.2	49.8	6.2	5.8	nda	68.3	14.2	368.5
1985	117.1	68.9	51.6	8.4	73.5	5.2	0.6	1.3	7.1	45.9	nda	44.0	423.6
1986	70.2	73.9	14.3	29.7	nda	nda	nda	nda	32.2	28.4	24.9	81.9	355.5
1987	52.6	35.2	38.9	24.7	26.7	18.2	3.8	1.7	0.0	21.2	34.7	56.8	314.5
1988	10.6	69.6	85.9	28.0	32.9	0.1	2.0	22.8	6.0	37.8	nda	nda	295.7
Total	1029	956	737	650	527	291	226	154	194	463	476	792	
Average	64	60	46	41	35	19	17	14	15	33	34	57	

* Source:-The meteorological office of Turkey, nda:-no data available. Also there is no data for the years1979 and 1980.

Meteorologic station; Burdur:

Latitude : 37°40'

Longitude : 30°20'

Altitude : 967m

Appendix-3. Chemical composition of culture BG-11+

<u>Chemical</u>	<u>g/l</u>
1. Citric acid	0.012
2. $\text{FeSO}_4 \cdot 7\text{H}_2\text{O}$	0.006
3. EDTA-disodium salt	0.001
4. NaNO_3	3.000
5. K_2HPO_4	0.04
6. $\text{MgSO}_4 \cdot 7\text{H}_2\text{O}$	0.075
7. $\text{CaCl}_2 \cdot 2\text{H}_2\text{O}$	0.036
8. NaCO_3	0.02
9. Trace elements	
H_3BO_3	
$\text{MnCl}_2 \cdot 4\text{H}_2\text{O}$	
$\text{ZnSO}_4 \cdot 7\text{H}_2\text{O}$	
$\text{Na}_2\text{MoO}_4 \cdot 2\text{H}_2\text{O}$	
$\text{CuSO}_4 \cdot 5\text{H}_2\text{O}$	
$\text{Co}(\text{NO}_3)_2 \cdot 6\text{H}_2\text{O}$	

Note: 500 mls of distilled water was added the above solution in numerical order, then made up to one litre with distilled water.

Appendix-4 . Rare earth element analyses (in ppb) of magnesite and host-rock of Konya, hydromagnesite and water (Salda and Pamukkale) from western Turkey.

Sample no*	La	Ce	Pr	Nd	Sm	Eu	Gd
52-Am	0.210	0.270	0.000	0.040	0.000	0.000	0.000
58m	0.260	0.250	0.140	0.160	0.110	0.000	0.000
61-A ^{ss}	0.600	0.690	0.080	0.280	0.100	0.040	0.010
89m	0.110	0.260	0.030	0.060	0.020	0.000	0.000
114 ^{ss}	0.580	1.090	0.150	0.440	0.130	0.020	0.010
141 ^{ss}	0.720	0.460	0.080	0.190	0.110	0.050	0.000
143-Am	0.310	0.190	0.020	0.050	0.010	0.000	0.000
143-B ^{ss}	0.180	0.280	0.030	0.110	0.020	0.000	0.000
145m	0.710	0.250	0.100	0.320	0.060	0.010	0.000
155 ^{sp}	0.150	0.220	0.010	0.030	0.020	0.000	0.000
156 ^{sp}	0.150	0.030	0.010	0.020	0.010	0.000	0.000
92-23 ^{sw}	0.100	0.030	0.030	0.030	0.010	0.010	0.010
92-25 ^{sw}	0.140	0.030	0.020	0.080	0.050	0.020	0.040
92-57 ^{pw}	0.090	0.050	0.090	0.080	0.080	0.030	0.030
92-24 ^{hm}	2.378	3.910	0.454	1.675	0.335	0.234	0.367
92-27 ^{hm}	0.502	0.910	0.099	0.431	0.092	0.027	0.130

* Where m magnesite, ^{ss} altered serpentinite, ^{ss} silicified serpentinite,

^{sp} serpentinitised peridotite, ^{sw} Salda lake water, ^{pw} Pamukkale hot-spring water,

hm Salda hydromagnesite.

Appendix-5. Chondrite-normalised values of the REE results of the samples from Turkey.

Sample no*	La	Ce	Pr	Nd	Sm	Eu	Gd
52-A ^m	6.77e-4	3.34e-4	0e+0	6.70e-5	0e+0	0e+0	0e+0
58 ^m	8.39e-4	3.09e-4	1.15e-3	2.67e-4	5.64e-4	0e+0	0e+0
61-A ^{ss}	1.94e-3	8.54e-4	6.56e-4	4.67e-4	5.13e-4	5.44e-4	3.90e-5
89 ^m	3.55e-4	3.22e-4	2.46e-4	1e-4	1.03e-4	0e+0	0e+0
114 ^{ss}	1.87e-3	1.35e-3	1.23e-3	7.33e-4	6.67e-4	2.72e-4	3.90e-5
141 ^{ss}	2.32e-3	5.69e-4	6.56e-4	3.17e-4	5.64e-4	6.80e-4	0e+0
143-A ^m	1e-3	2.35e-4	1.64e-4	8.30e-5	5.10e-5	0e+0	0e+0
143-B ^{ss}	5.81e-4	3.47e-4	2.46e-4	1.83e-4	1.03e-4	0e+0	0e+0
145 ^m	2.29e-3	3.09e-4	8.20e-4	5.33e-4	3.08e-4	1.36e-4	0e+0
155 ^{sp}	4.84e-4	2.72e-4	8.20e-5	5.00e-5	1.03e-4	0e+0	0e+0
156 ^{sp}	4.84e-4	3.70e-5	8.20e-5	3.30e-5	5.10e-5	0e+0	0e+0
92-23 ^{sw}	3.23e-4	3.70e-5	2.46e-4	5.00e-5	5.10e-5	1.36e-4	3.90e-5
92-25 ^{sw}	4.52e-4	3.70e-5	1.64e-4	1.33e-4	2.56e-4	2.72e-4	1.54e-4
92-57 ^{pw}	2.90e-4	6.20e-5	7.38e-4	1.33e-4	4.10e-4	4.08e-4	1.16e-4
92-24 ^{hm}	7.67e-3	4.84e-3	3.72e-3	2.79e-3	1.72e-3	3.18e-3	1.42e-3
92-27 ^{hm}	1.62e-3	1.13e-3	8.11e-4	7.18e-4	4.72e-4	3.67e-4	5.02e-4

* Indices are the same as Appendix-4.

Note calculations are converted to ppm. Chondrite values are from Boynton, (1984).

